Imaging the Proton: experimental study of Generalised Parton Distributions

Daria Sokhan

University of Glasgow, UK

EINN: 13th European Research Conference on Electromagnetic Interactions with Nucleons and Nuclei

Paphos, Cyprus — 30th October 2019

Introduction

A constructivist view of the nucleon

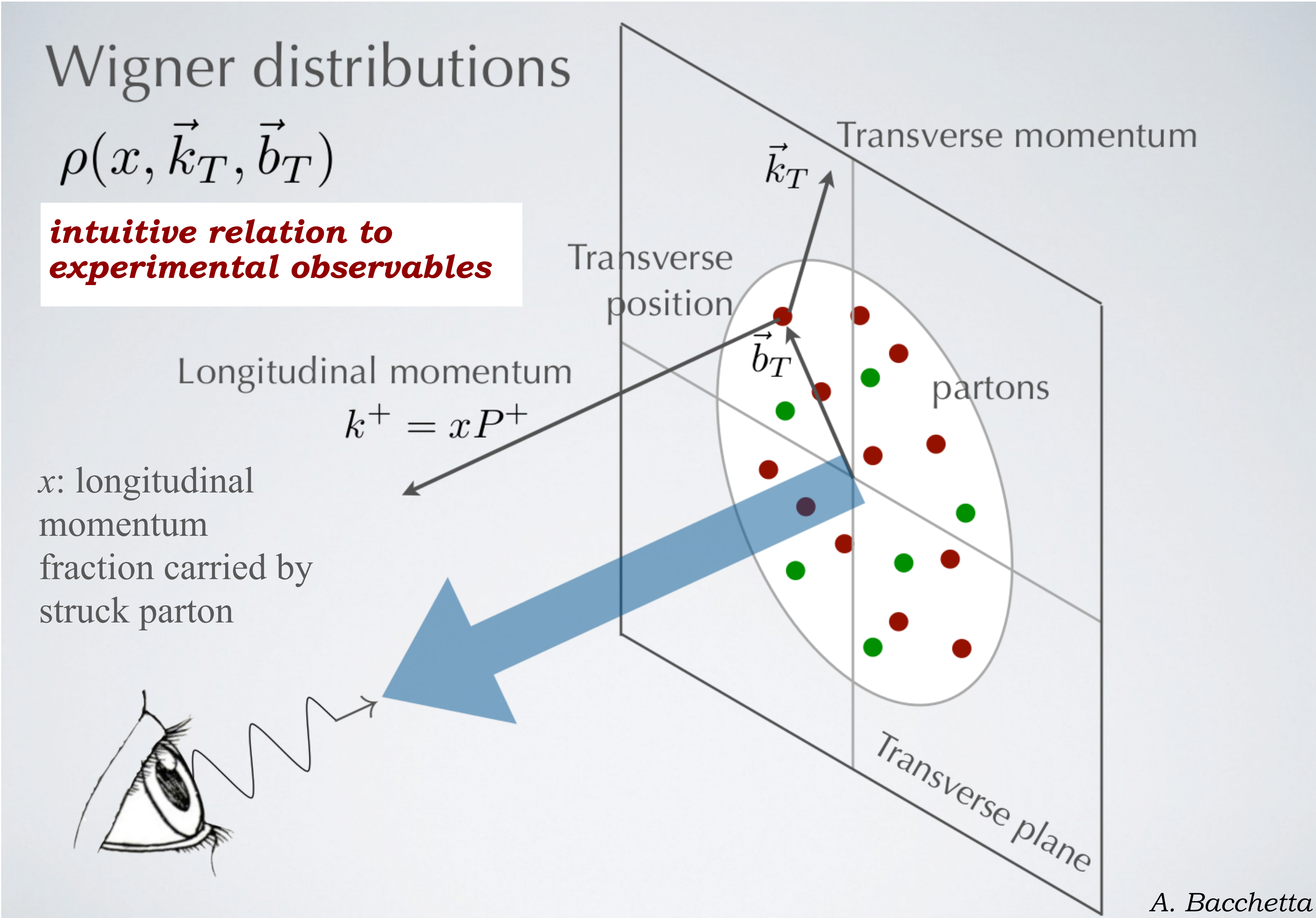

A. Bacchetta

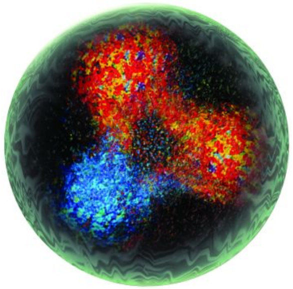

Wigner function:
full phase space parton distribution of the nucleon

Generalised Transverse Momentum Distributions (GTMDs)

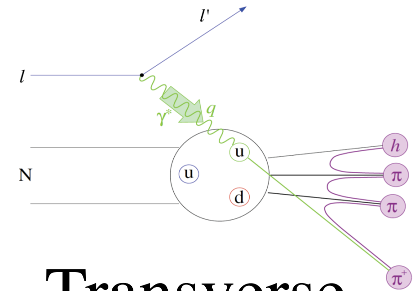

$\int d^2k_T$

$\int d^2b_T$

Transverse Momentum Distributions (TMDs)

Generalised Parton Distributions (GPDs)

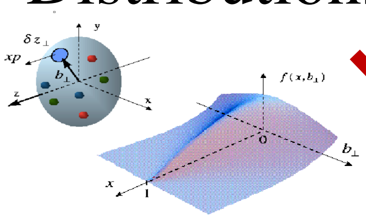

$\int dx$

$\int d^2b_T$

$\int d^2k_T$

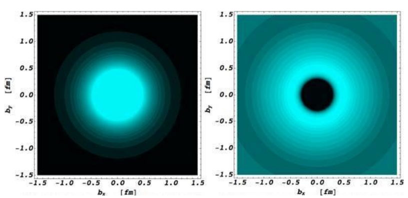

Form Factors
eg: G_E, G_M

Parton Distribution Functions (PDFs)

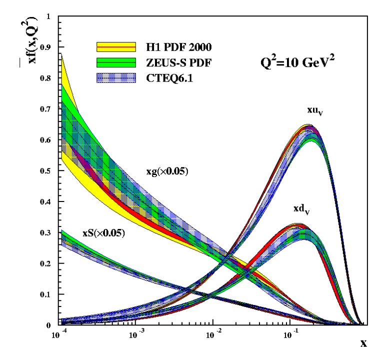

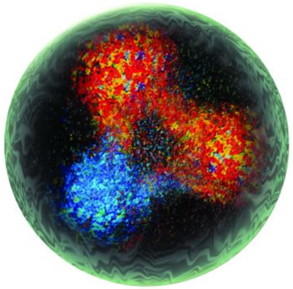

Wigner function: full phase space parton distribution of the nucleon

Generalised Transverse Momentum Distributions (GTMDs)

$\int d^2 k_T$

$\int d^2 b_T$

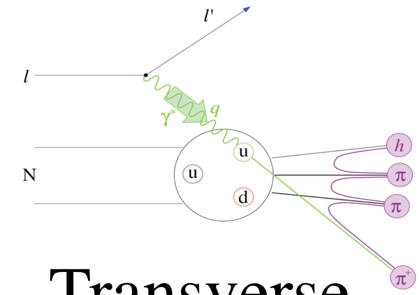

Transverse Momentum Distributions (TMDs)

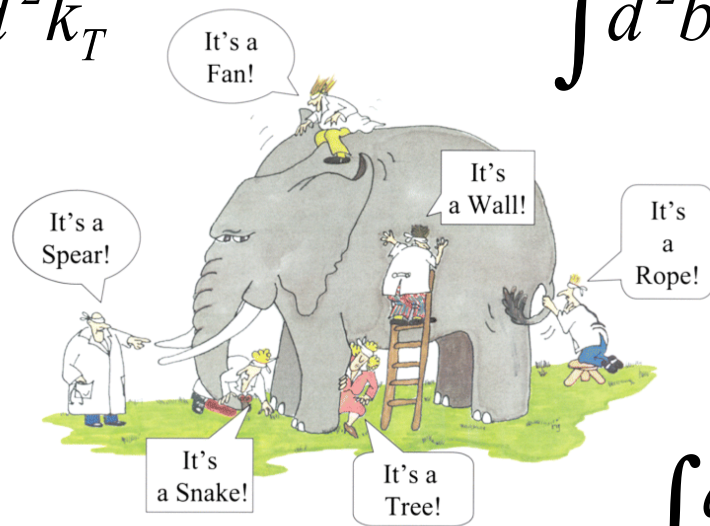

G. Renee Guzlas, artist.

Generalised Parton Distributions (GPDs)

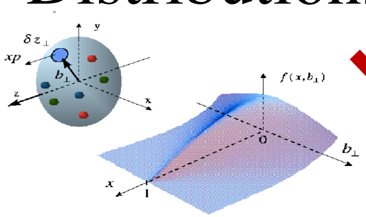

$\int dx$

$\int d^2 k_T$

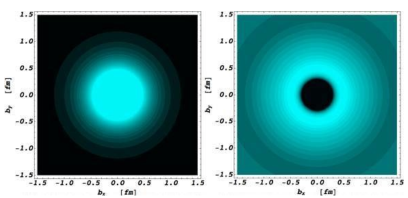

Form Factors *eg*: G_{E}, G_{M}

Parton Distribution Functions (PDFs)

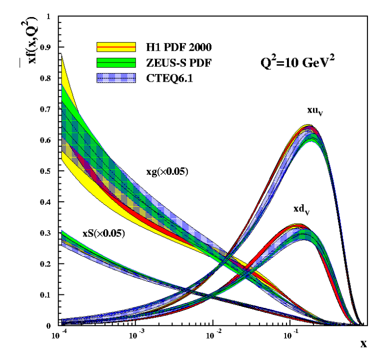

Generalised Parton Distributions

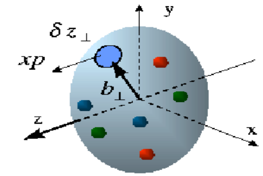

- proposed by Müller (1994), Radyushkin, Ji (1997).
- can be interpreted as relating, in the infinite momentum frame, transverse position of partons (impact parameter $b_\perp$) to longitudinal momentum fraction (x).

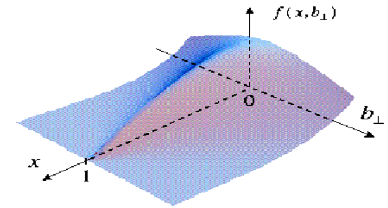

* **Tomography** of the nucleon: transverse spatial distributions of quarks and gluons in longitudinal momentum space.

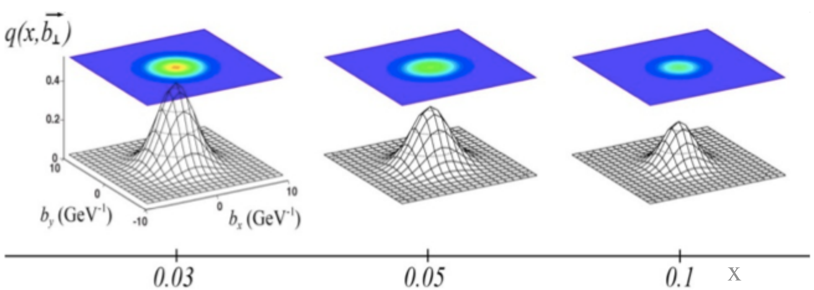

* Information on the orbital angular momentum contribution to nucleon spin: **the spin puzzle**.

$$J_N = \frac{1}{2} = \frac{1}{2}\Sigma_q + L_q + J_g$$

Ji's relation:

$$J^q = \frac{1}{2} - J^g$$

$$= \frac{1}{2}\int_{-1}^{1} x dx \left\{ H^q(x,\xi,0) + E^q(x,\xi,0) \right\}$$

* Indirect access to mechanical properties of the nucleon: possibilities of extracting **pressure distributions** within the nucleon.

* Combine with TMDs to access **spin-orbit correlations** of quarks and gluons, study non-perturbative interactions of partons.

Experimental processes for accessing GPDs

Accessible in *exclusive* processes, where all final state particles are determined:

- Deeply Virtual Compton Scattering (DVCS)
- Deeply Virtual Meson Production (DVMP) / Hard Exclusive Meson Production (HEMP)
- Time-like Compton Scattering (TCS)
- Double DVCS
- Production of a meson-photon pair, …

Relies on *factorisation* of the process amplitude into a hard, perturbative part and the soft non-perturbative part containing GPD information.

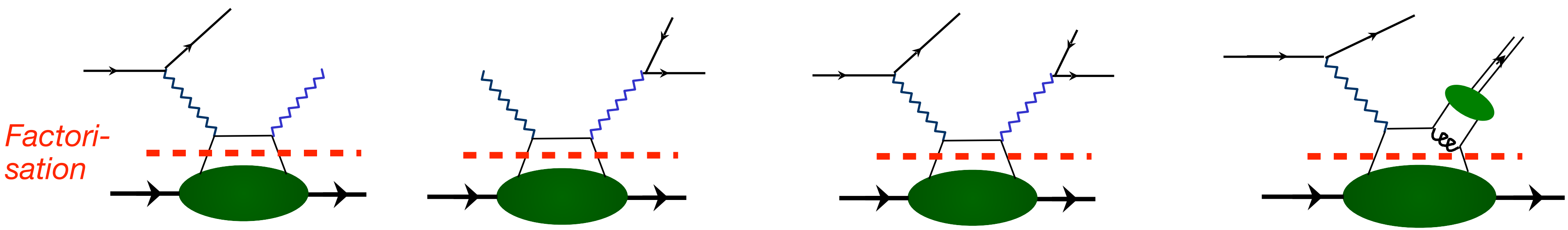

DVCS — *Virtual photon space-like*

TCS — *Virtual photon time-like*

DDVCS — *One time-like, one space-like virtual photon*

DVMP — *Virtual photon space-like*

Deeply Virtual Compton Scattering

the "golden channel" for GPD extraction

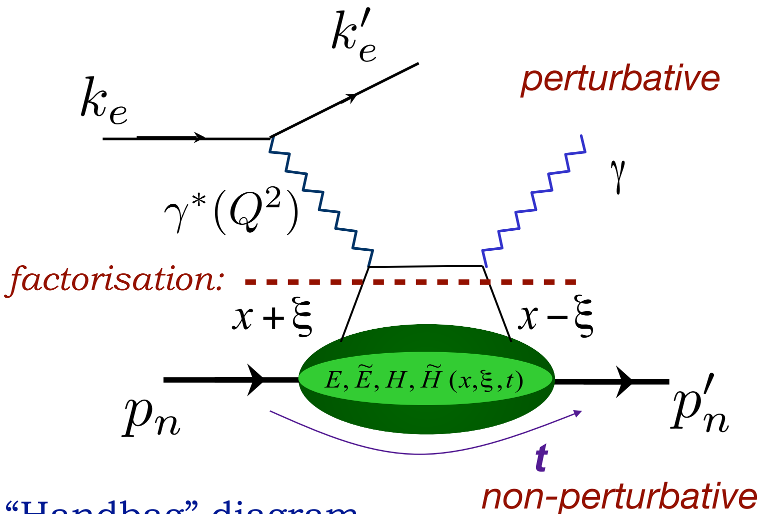

"Handbag" diagram

$$Q^2 = -(\mathbf{k} - \mathbf{k}')^2 \qquad t = (\mathbf{p'_n} - \mathbf{p_n})^2$$

Bjorken variable: $x_B = \dfrac{Q^2}{2\mathbf{p_n}\cdot\mathbf{q}}$

$x \pm \xi$ *longitudinal momentum fractions of the struck parton*

Skewness: $\xi \cong \dfrac{x_B}{2 - x_B}$

- At high exchanged Q^2 and low t access to four parton helicity-conserving, chiral-even GPDs:

$$E^q, \tilde{E}^q, H^q, \tilde{H}^q(x, \xi, t)$$

- Can be related to PDFs:

$$H(x,0,0) = q(x) \quad \tilde{H}(x,0,0) = \Delta q(x)$$

and form factors:

$$\int_{-1}^{+1} H dx = F_1 \qquad \int_{-1}^{+1} \tilde{H}\, dx = G_A$$

$$\int_{-1}^{+1} E\, dx = F_2 \qquad \int_{-1}^{+1} \tilde{E}\, dx = G_P$$

(Dirac and Pauli) *(axial and pseudo-scalar)*

- Small changes in nucleon transverse momentum allows mapping of transverse structure at large distances.

Measuring DVCS

✳ Process measured in experiment:

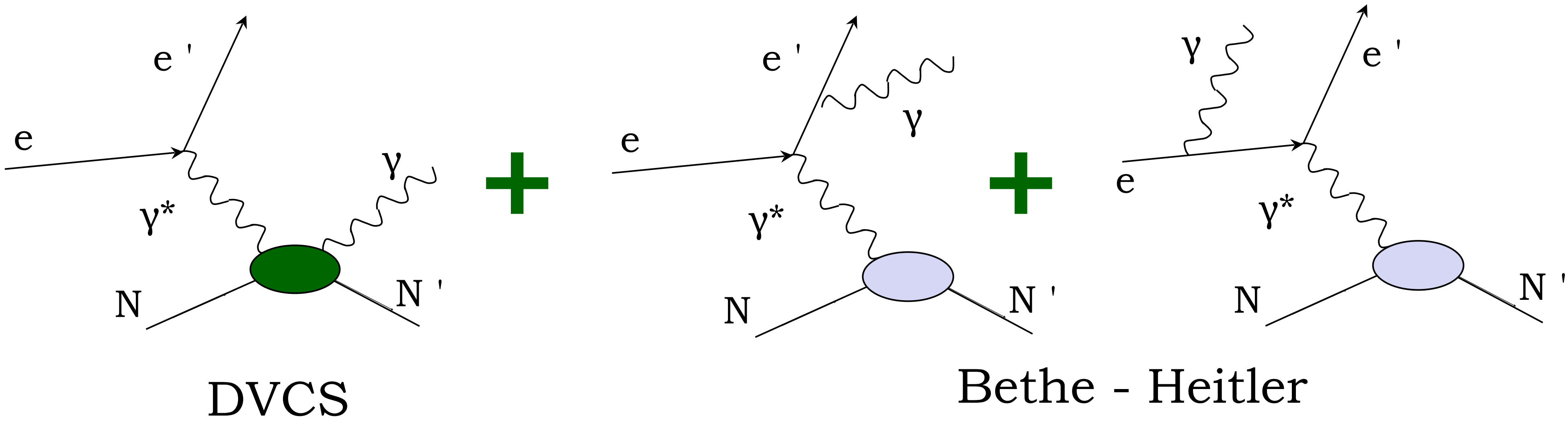

$$d\sigma \propto |T_{DVCS}|^2 + |T_{BH}|^2 + T_{BH}T^*_{DVCS} + T_{DVCS}T^*_{BH}$$

Amplitude parameterised in terms of Compton Form Factors

Amplitude calculable from elastic Form Factors and QED

Interference term

$$|T_{DVCS}|^2 << |T_{BH}|^2$$

Compton Form Factors in DVCS

Experimentally accessible in DVCS cross-sections and spin asymmetries, eg:

$$A_{LU} = \frac{d\vec{\sigma} - d\overleftarrow{\sigma}}{d\vec{\sigma} + d\overleftarrow{\sigma}} = \frac{\Delta\sigma_{LU}}{d\vec{\sigma} + d\overleftarrow{\sigma}}$$

cross-sections, beam-charge and double polarisation asymmetries

single-spin asymmetries

At leading twist, leading order:

$$T^{DVCS} \sim \int_{-1}^{+1} \frac{GPDs\,(x,\xi,t)}{x \pm \xi + i\varepsilon} dx \; + \ldots \sim \quad P\int_{-1}^{+1} \frac{GPDs\,(x,\xi,t)}{x \pm \xi} dx \pm i\pi GPDs\,(\pm\xi,\xi,t) + \ldots$$

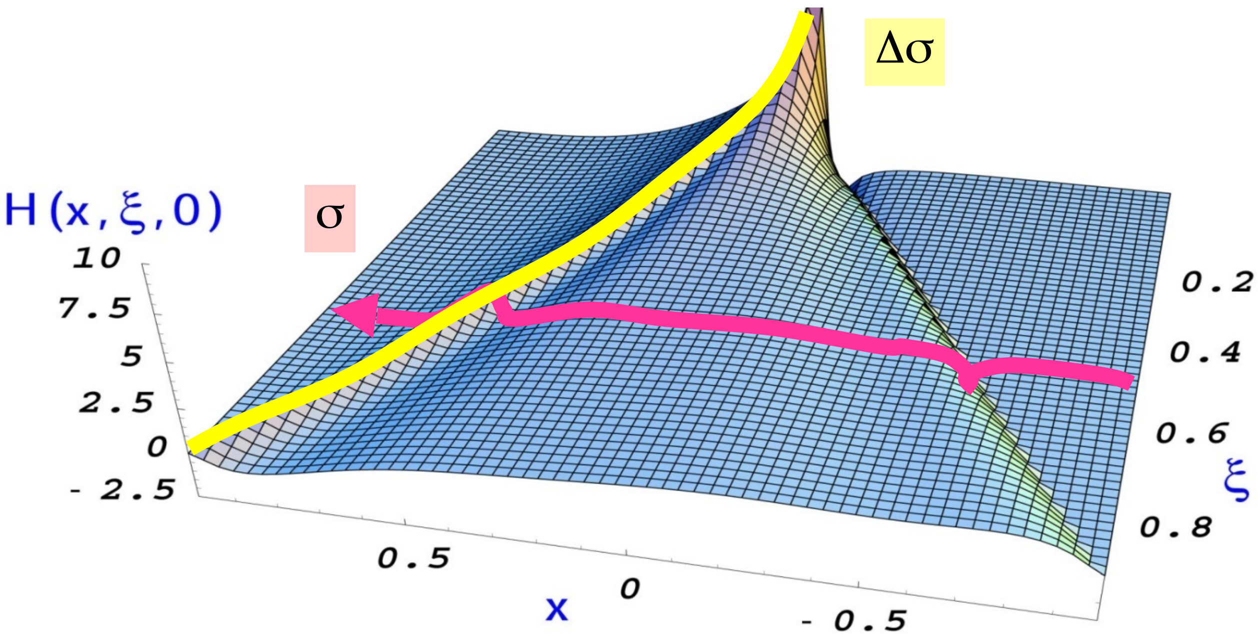

Only ξ and t are accessible experimentally!

To get information on x need extensive measurements in Q^2.

Need measurements off proton and neutron to get flavour separation of CFFs in DVCS.

John Bercow, Speaker of the House
(*BT.com*)

Order and Twist

Leading order (LO)

Next-to-leading order (NLO)

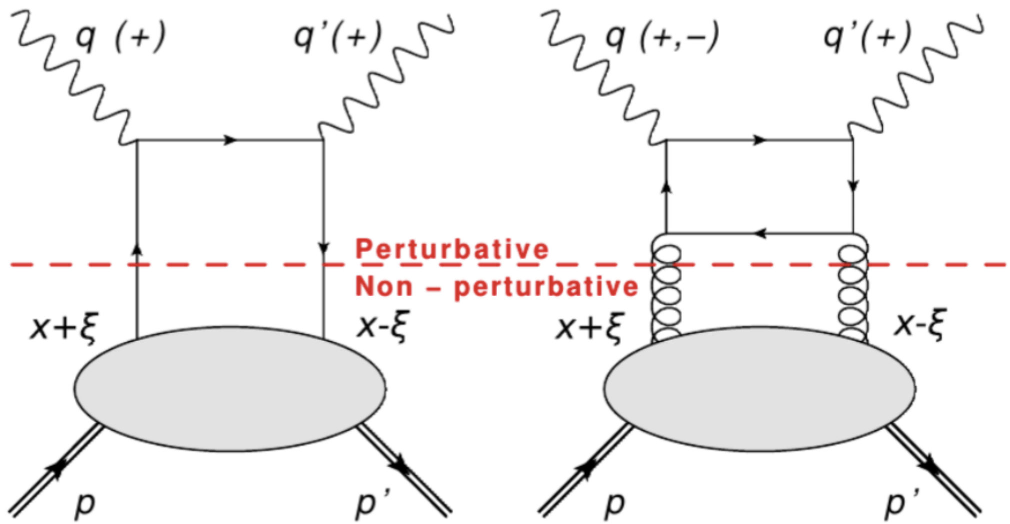

- Twist: powers of $\frac{1}{\sqrt{Q^2}}$ in the DVCS amplitude. Leading-twist (LT) is twist-2.

- Order: introduces powers of α_s

- Leading Order (LO) requires $Q^2 >> M^2$ (M: target mass)

Nucleon Tomography from GPDs

* At a fixed Q^2, x_B, slope of GPD with t is related, via a Fourier Transform, to the transverse spatial spread.

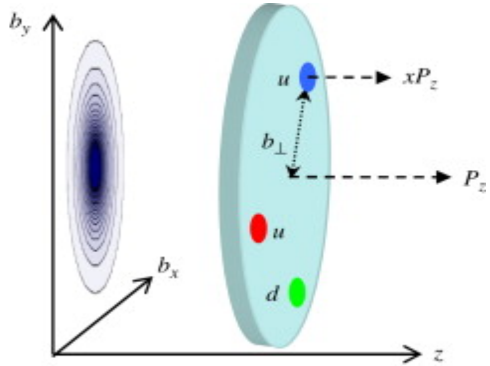

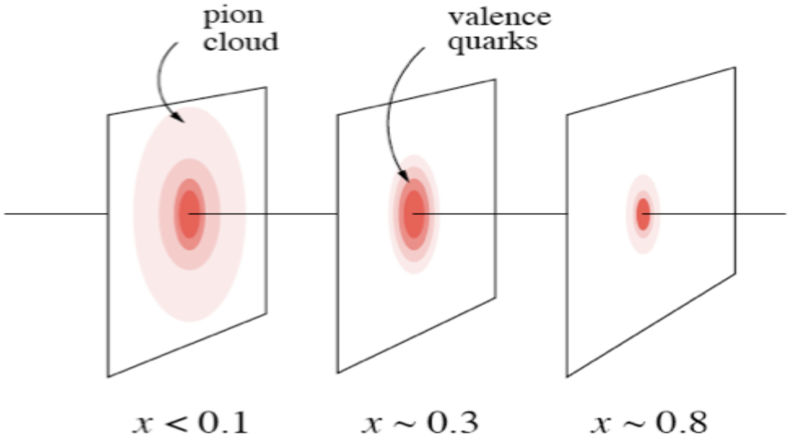

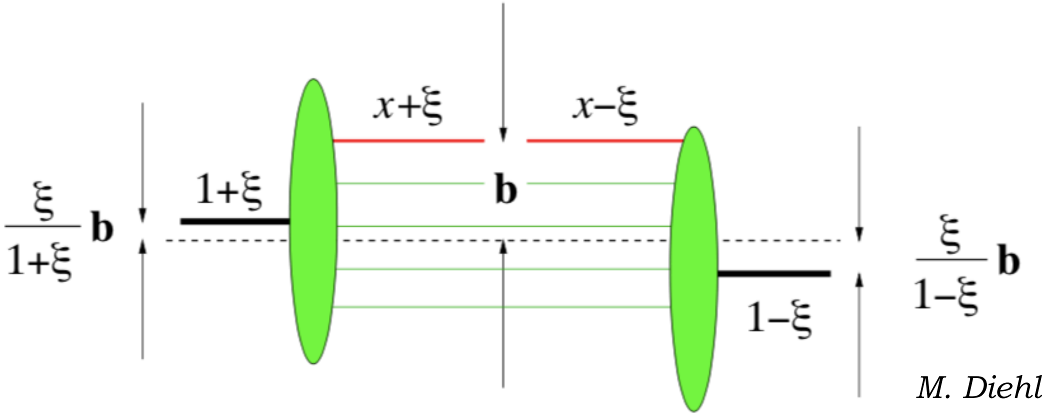

Formally, the radial separation, **b**, *between the struck parton and the centre of momentum of the remaining spectators.*

* Experimentally, fit the t-dependence of CFFs or structure functions (from HEMP) with an exponential.

eg: $$\frac{d\sigma_U}{dt} = Ae^{Bt}$$

Nucleon at different scales

Valence quarks

Jefferson Lab: fixed-target electron scattering

$$0.1 < x_B < 0.7$$

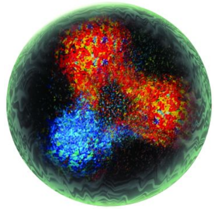

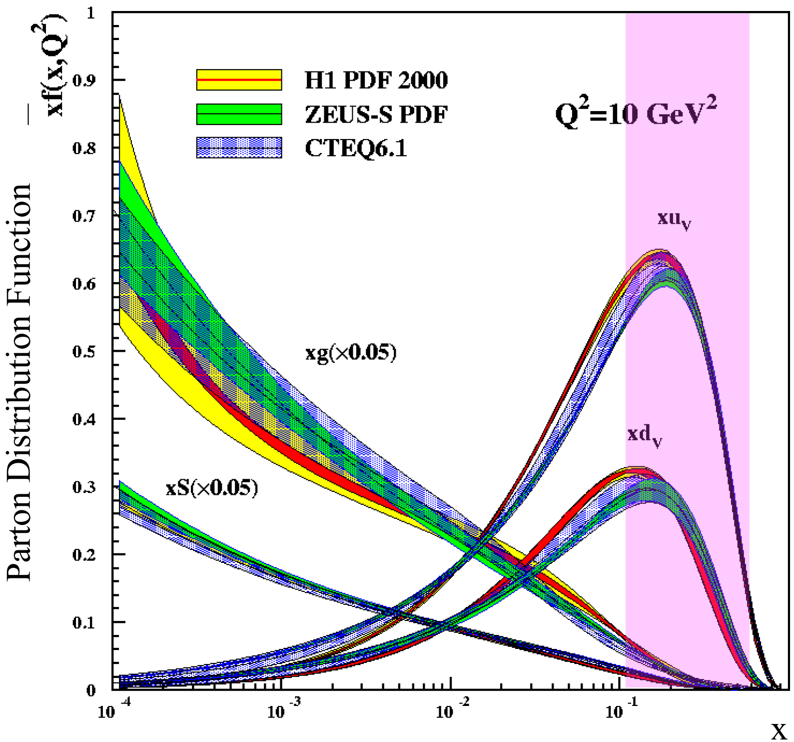

Nucleon at different scales

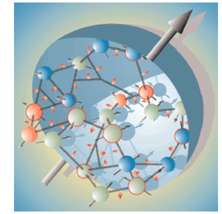

Valence quarks

Jefferson Lab: fixed-target electron scattering

$0.1 < x_B < 0.7$

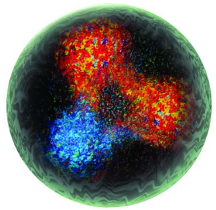

Sea quarks

HERMES: fixed gas-target electron/positron scattering

$0.02 < x_B < 0.3$

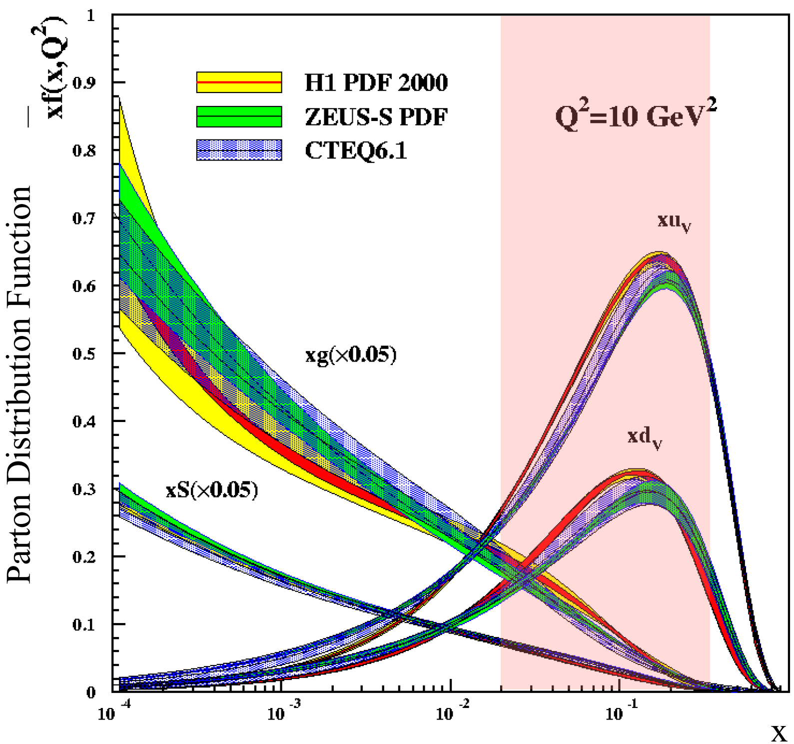

Nucleon at different scales

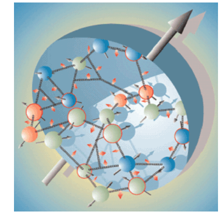

Valence quarks

Jefferson Lab: fixed-target electron scattering

$0.1 < x_B < 0.7$

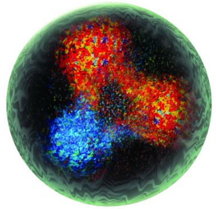

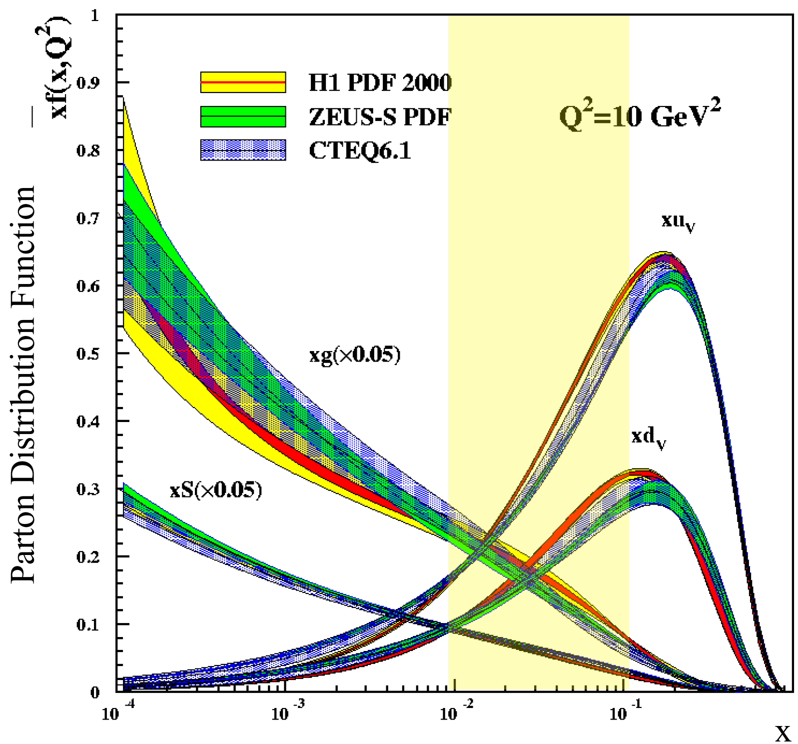

Sea quarks

HERMES: fixed gas-target electron/positron scattering

$0.02 < x_B < 0.3$

COMPASS: fixed-target muon scattering

$0.01 < x_B < 0.1$

Nucleon at different scales

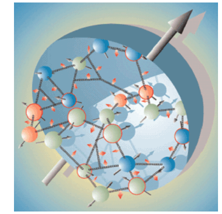

Valence quarks

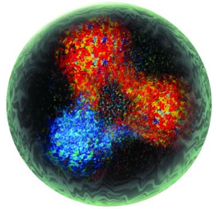

Jefferson Lab: fixed-target electron scattering

$0.1 < x_B < 0.7$

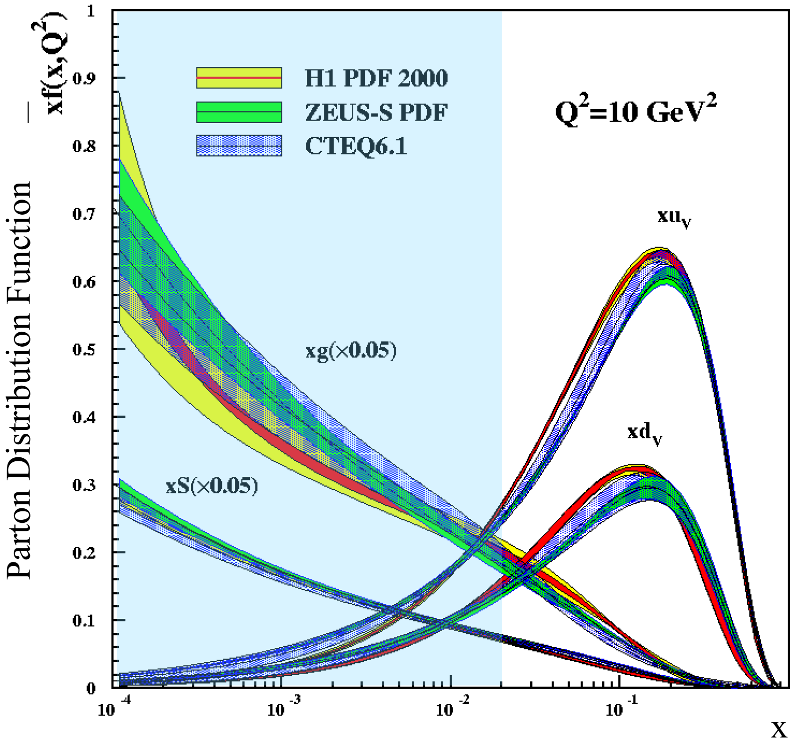

Sea quarks

HERMES: fixed gas-target electron/positron scattering

$0.02 < x_B < 0.3$

COMPASS: fixed-target muon scattering

$0.01 < x_B < 0.1$

The glue

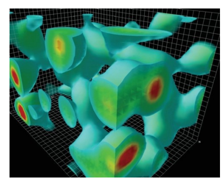

Derek Leinweber

ZEUS/H1: electron/positron-proton collider

$10^{-4} < x_B < 0.02$

Nucleon at different scales

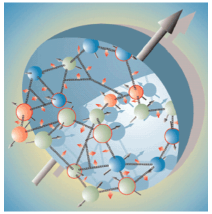

Valence quarks

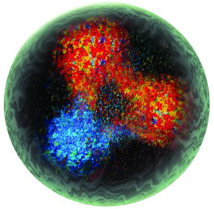

Jefferson Lab: fixed-target electron scattering

$0.1 < x_B < 0.7$

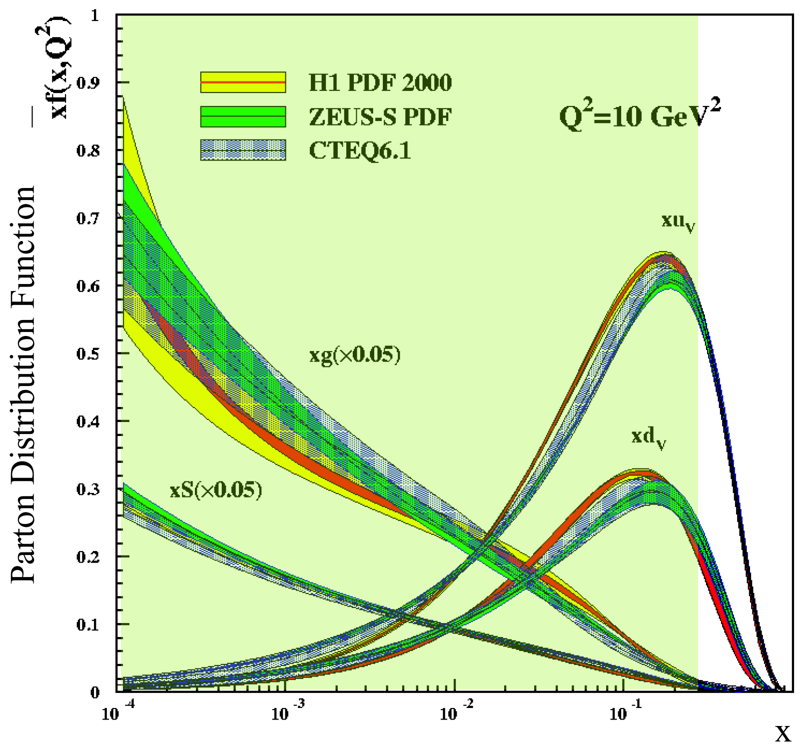

Sea quarks

HERMES: fixed gas-target electron/positron scattering

$0.02 < x_B < 0.3$

COMPASS: fixed-target muon scattering

$0.01 < x_B < 0.1$

The glue

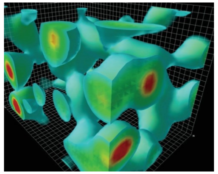

Derek Leinweber

ZEUS/H1: electron/ positron-proton collider

$10^{-4} < x_B < 0.02$

Electron-ion collider: $10^{-4} < x_B < 10^{-1}$

Luminosity 100 - 1000 times that of HERA

Kinematic landscape

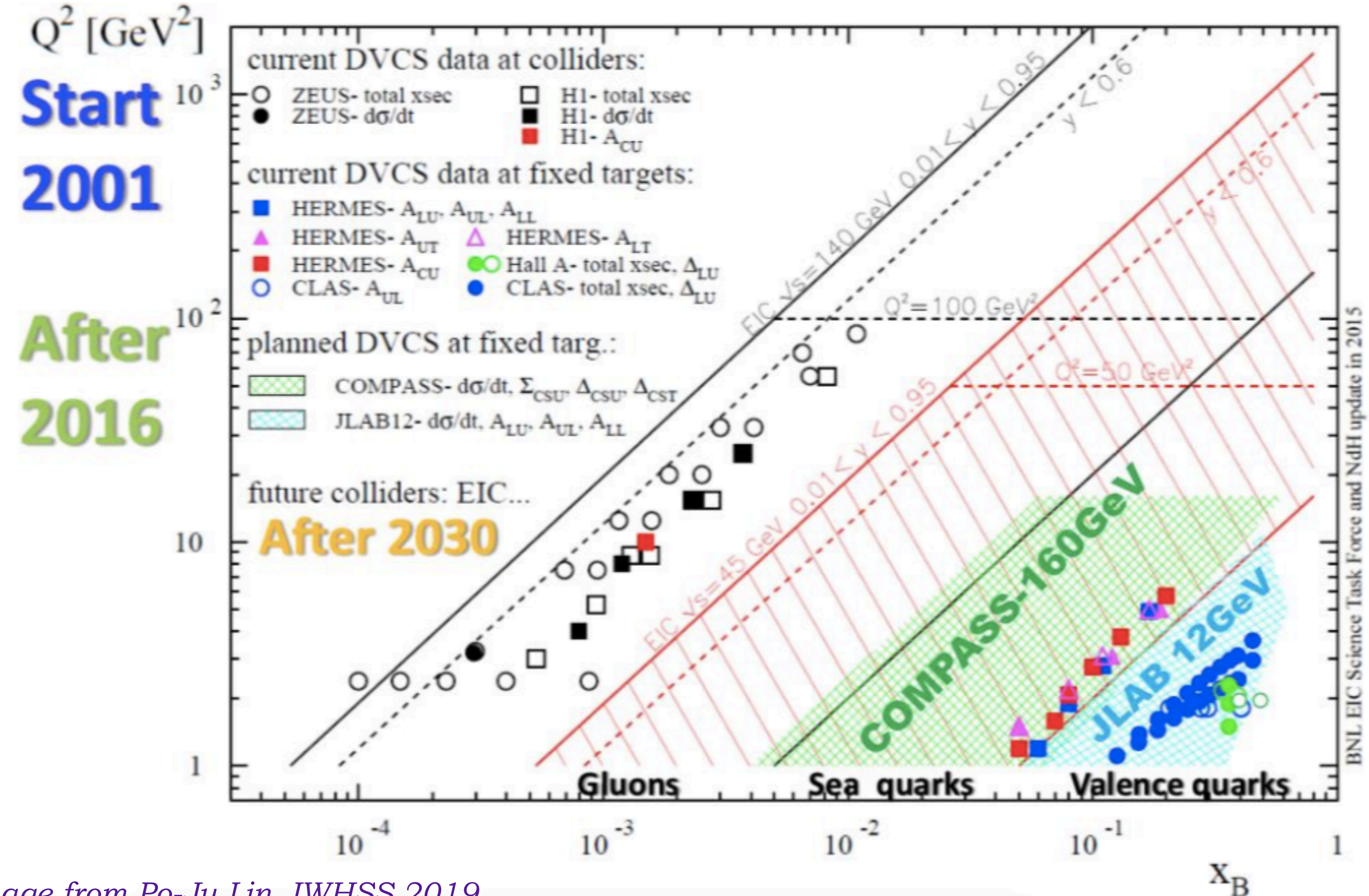

Image from Po-Ju Lin, IWHSS 2019

Jefferson Lab

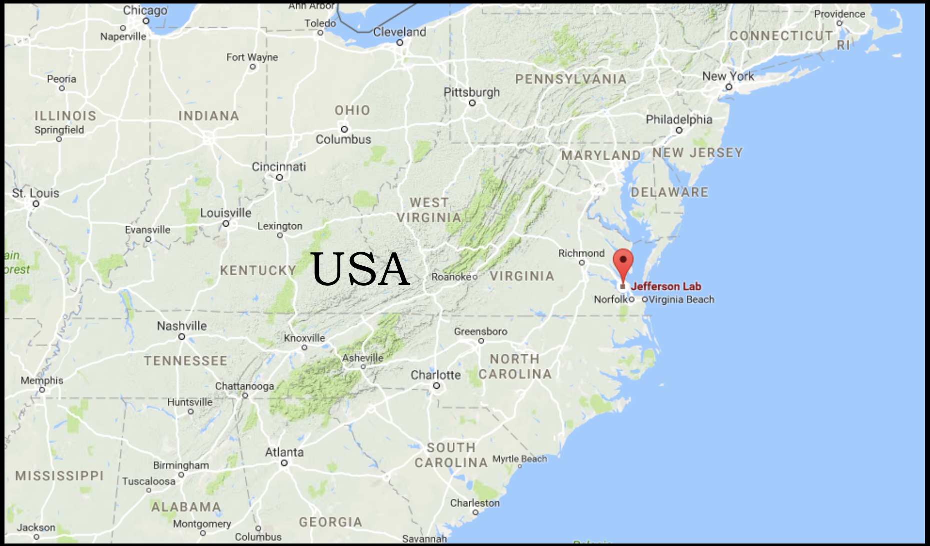

Jefferson Lab: 6 GeV era

CEBAF: Continuous Electron Beam Accelerator Facility.

- Energy up to ~6 GeV
- Energy resolution $\delta E/E_e \sim 10^{-5}$
- Electron polarisation up to ~85%

Hall A:

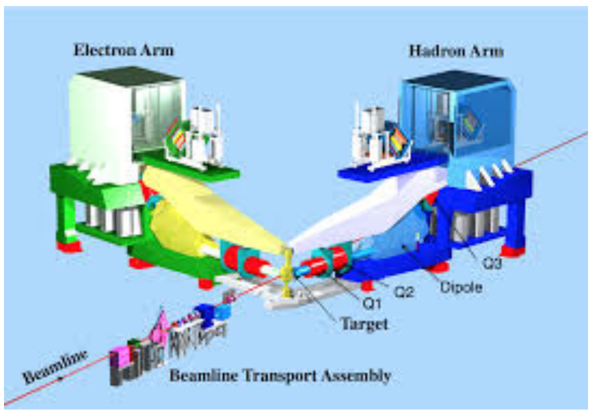

- High resolution($\delta p/p = 10^{-4}$) spectrometers, very high luminosity.

Hall B: CLAS

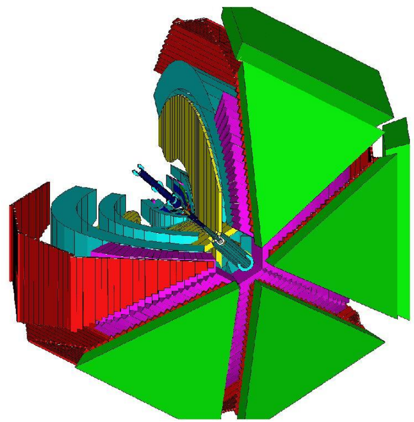

- Very large acceptance, detector array for multi-particle final states.

Hall C:

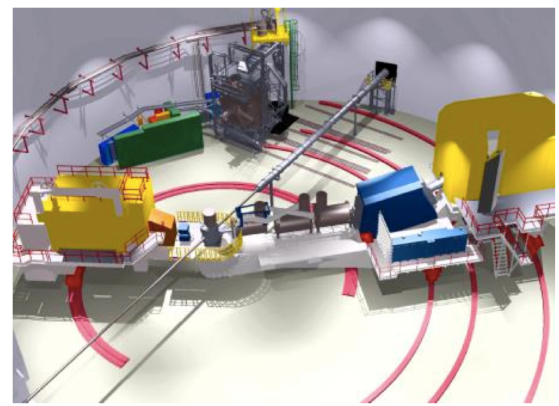

- Two movable spectrometer arms, well-defined acceptance, high luminosity

JLab @ 12 GeV

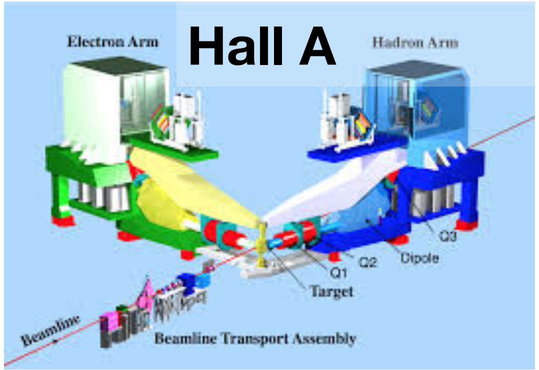

High resolution($\delta p/p = 10^{-4}$) spectrometers, very high luminosity, large installation experiments.

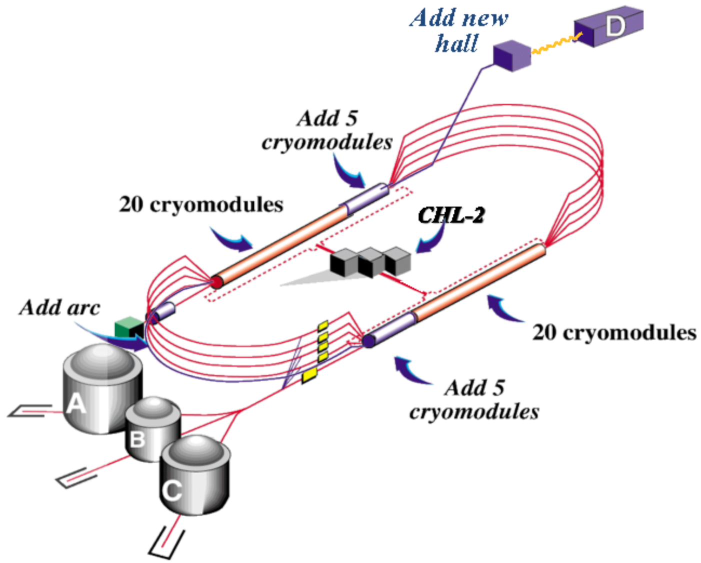

Hall C

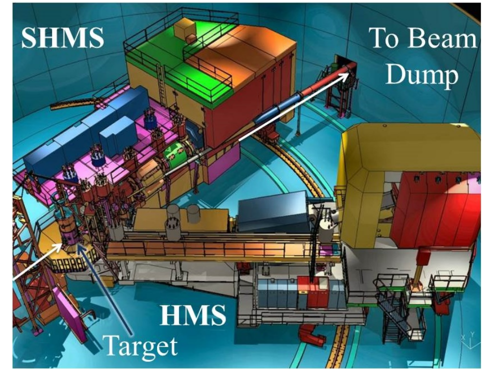

Two movable high momentum spectrometers, well-defined acceptance, very high luminosity.

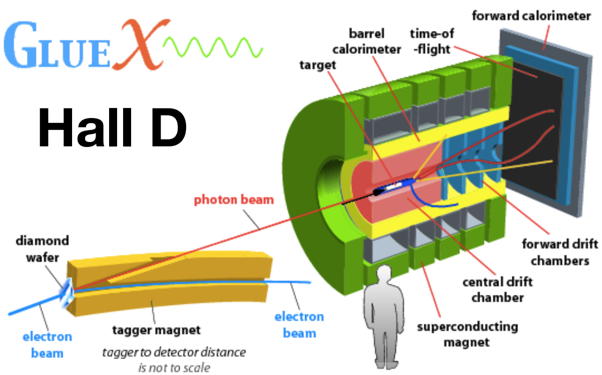

9 GeV tagged polarised photons, full acceptance

Hall B: CLAS12

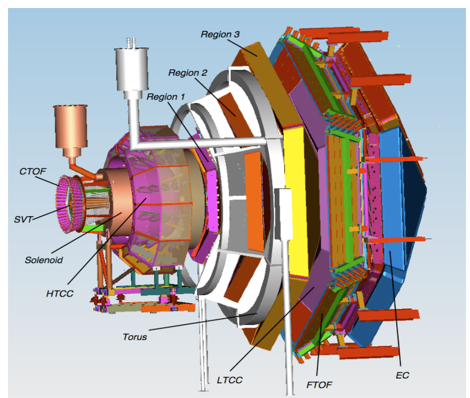

Very large acceptance, high luminosity.

JLab @ 12 GeV

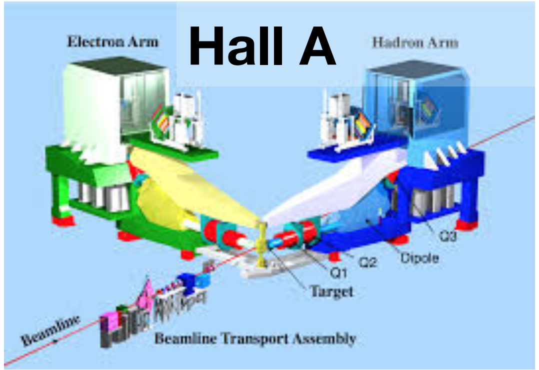

High resolution($\delta p/p = 10^{-4}$) spectrometers, very high luminosity, large installation experiments.

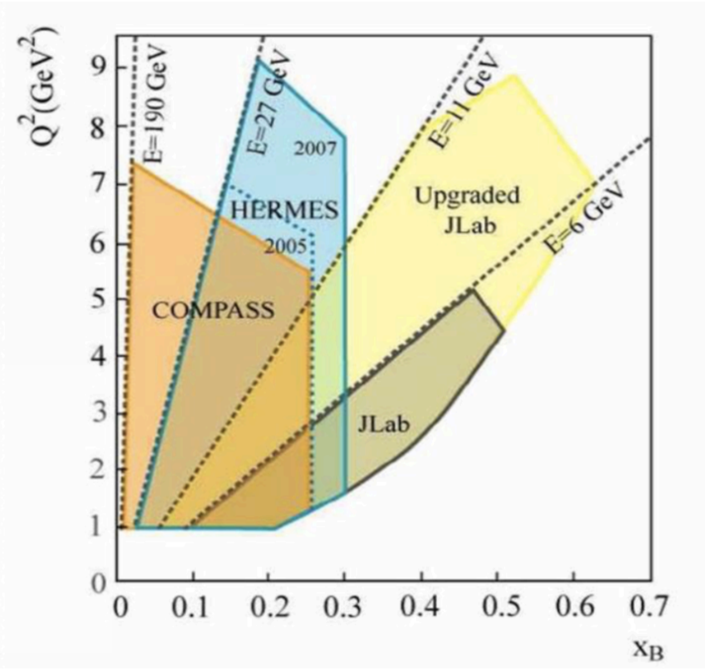

Hall C

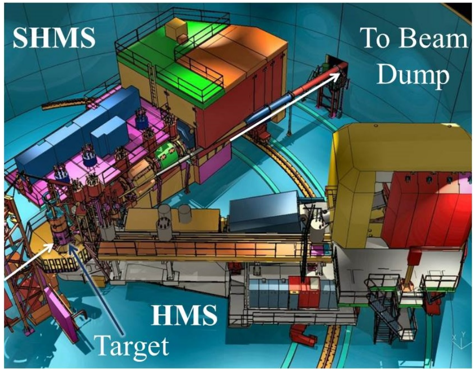

Two movable high momentum spectrometers, well-defined acceptance, very high luminosity.

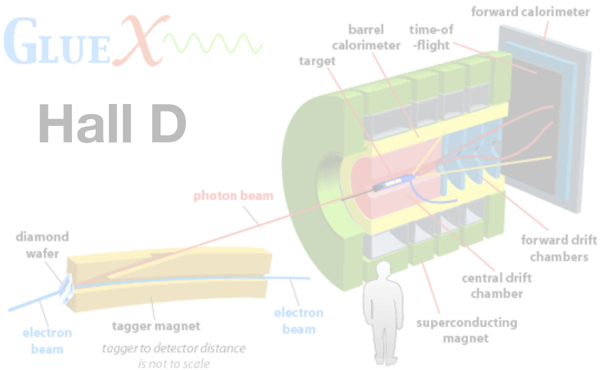

9 GeV tagged polarised photons, full acceptance

Hall B: CLAS12

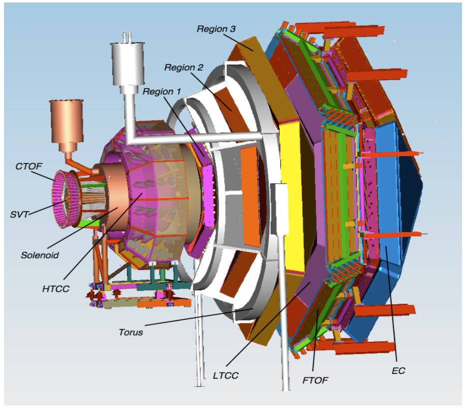

Very large acceptance, high luminosity.

CLAS12

Design luminosity

$L \sim 10^{35}\ cm^{-2}\ s^{-1}$

High luminosity & large acceptance:
Concurrent measurement of exclusive, semi-inclusive, and inclusive processes

Acceptance for photons and electrons:
- $2.5^o < \theta < 125^o$

Acceptance for all charged particles:
- $5^o < \theta < 125^o$

Acceptance for neutrons:
- $5^o < \theta < 120^o$

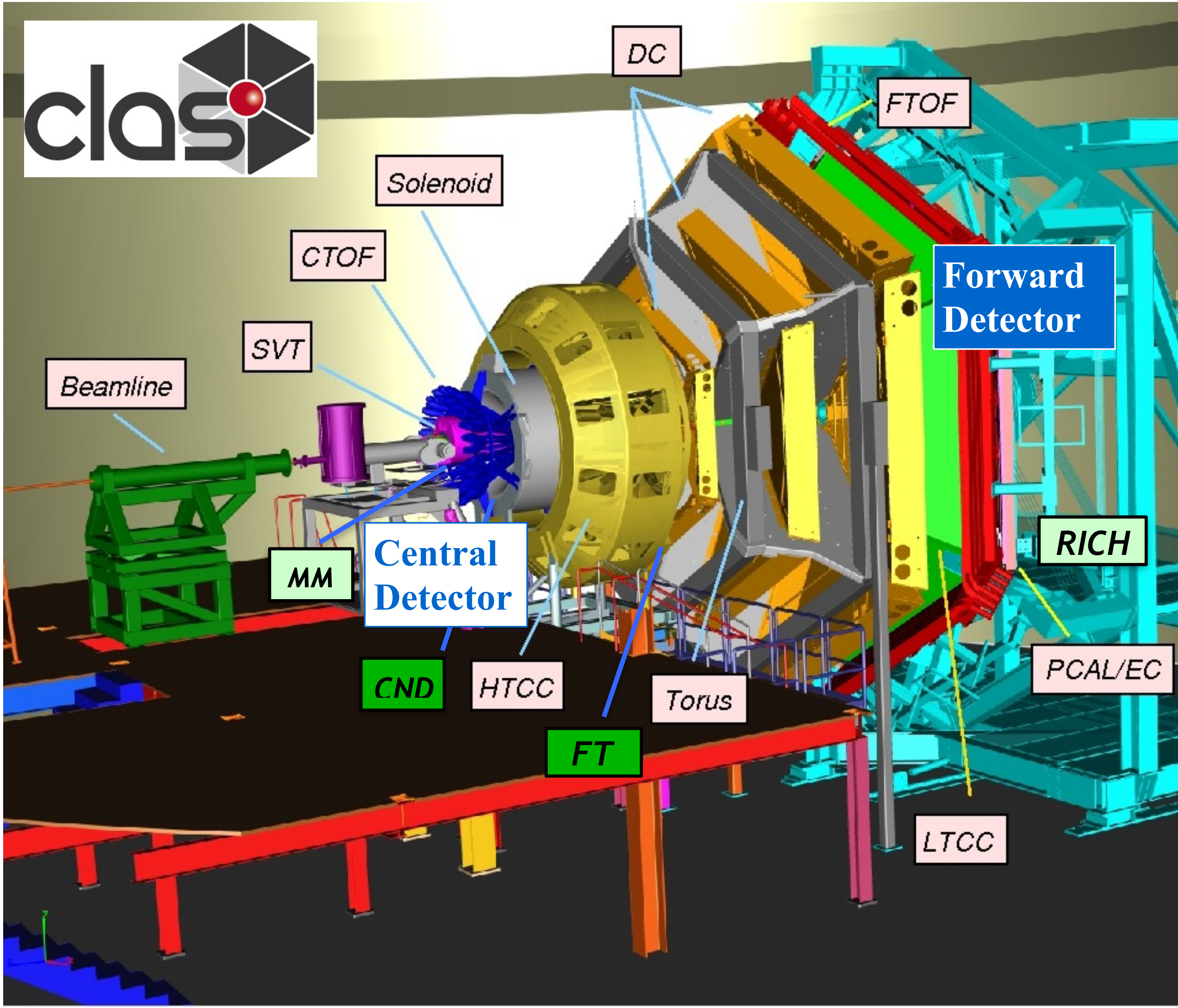

DVCS in Hall C

Detect electron with (Super) High Momentum Spectrometer, (S)HMS.

Detect photon in $PbWO_4$ calorimeter.

Sweeping magnet to reduce backgrounds in calorimeter.

Reconstruct recoiling proton through missing mass.

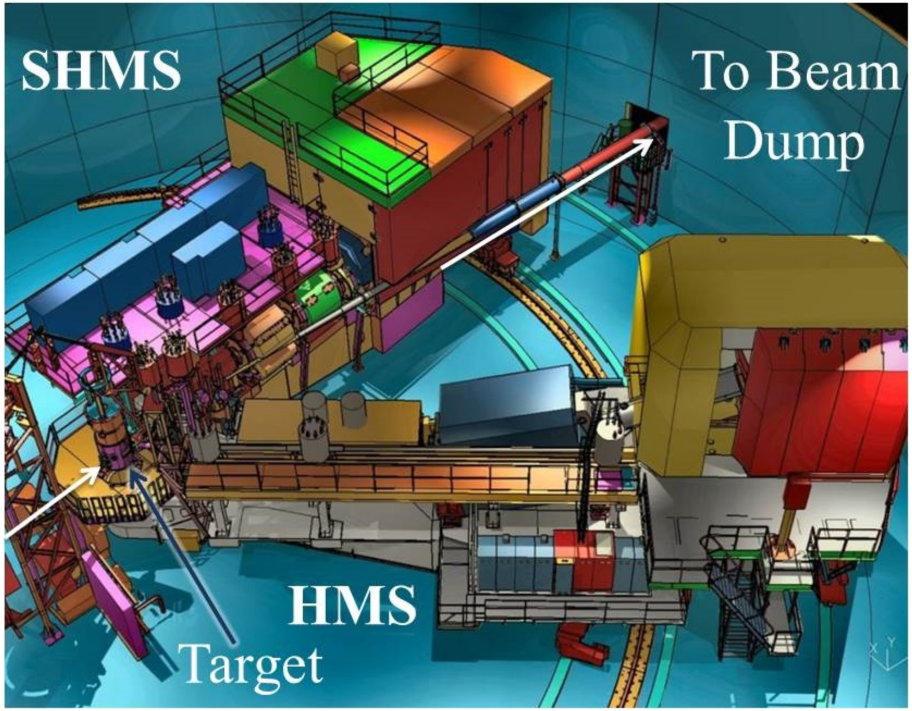

Similar principle applied in Hall A

DVCS at JLab:
6 GeV era

DVCS in Hall A

- 15 cm long liquid H_2 target
- Luminosity $=10^{37}$ cm^{-2}s^{-1}

$$ep \rightarrow e'\gamma(p')$$

Detected in High Resolution Spectrometer (SRS)

Detected in PbF_2 Calorimeter

Reconstructed through missing mass

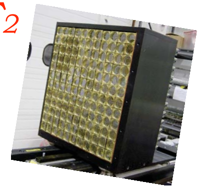

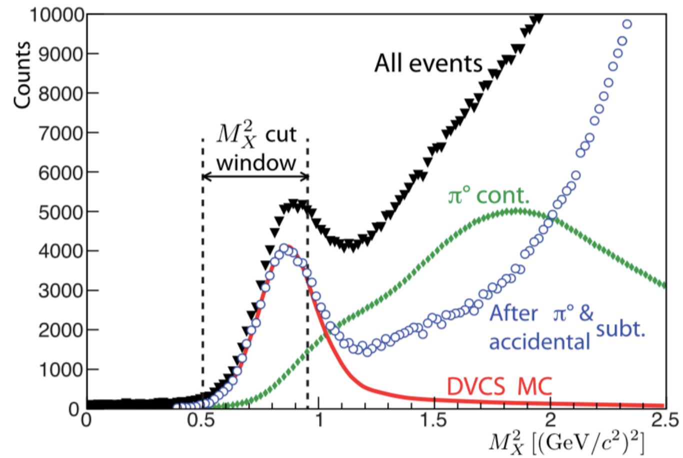

M. Defurne *et al*, ***PRC* 92** (2015) 055202.

- **E00-110 experiment** (2004): 5.75 GeV polarised electron beam
- Measure Q^2-dependence (Q^2: 1.5, 1.9, 2.3 GeV^2) of DVCS-BH cross-sections at fixed x_B (0.36) and x_B dependence at constant Q^2.

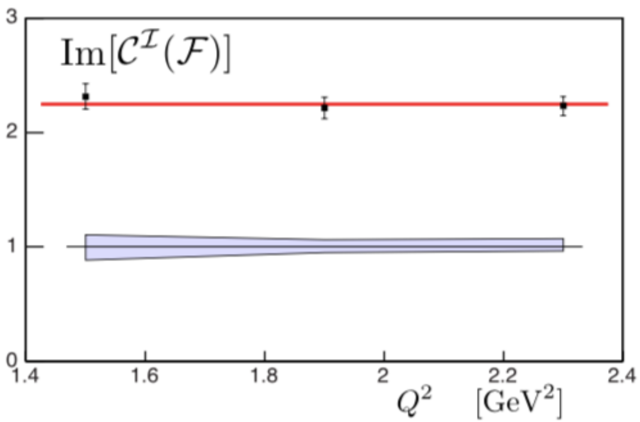

- **E07-004 experiment** (2010): Energy scan for fixed x_B, Q^2:

Q^2 (GeV^2)	x_B	E^{beam} (GeV)	$-t$ (GeV^2)
1.50	0.36	3.355 5.55	0.18, 0.24, 0.30
1.75	0.36	4.455 5.55	0.18, 0.24, 0.30, 0.36
2.00	0.36	4.455 5.55	0.18, 0.24, 0.30, 0.36

M. Defurne *et al*, ***PRC* 92** (2015) 055202.

High-precision cross-sections: Hall A

- High precision cross-section measurement in a small kinematic region: Generalised Rosenbluth separation of the DVCS² (scales as E_e^2) and the BH-DVCS interference (scales as E_e^3) terms. Addition of NLO and/or higher-twist improve model agreement.

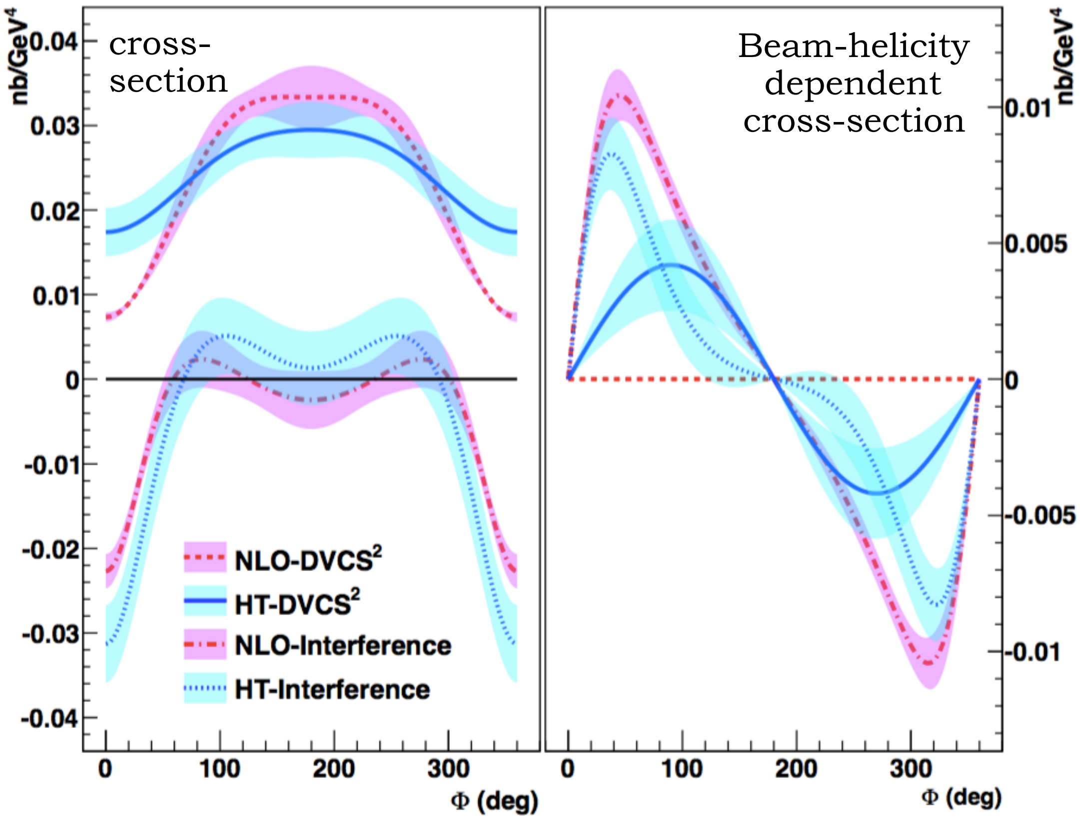

Q^2: 1.5, 1.9, 2.3 GeV² at fixed x_B 0.36
$-t$: 0.18, 0.24, 0.30

E_e: 4.5, 5.6 GeV.

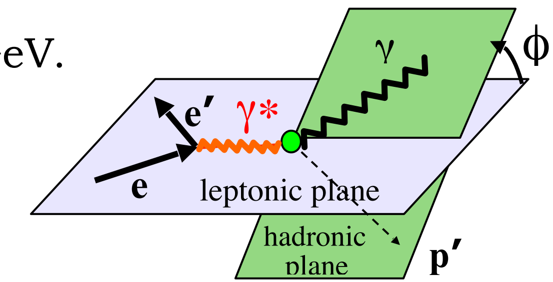

- Significant differences between pure DVCS and interference contributions.

- If NLO: sensitivity to gluons.

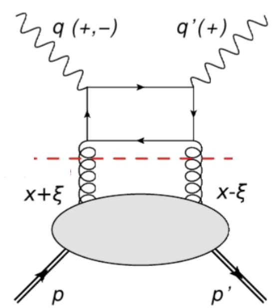

- Separation of HT and NLO effects requires scans across wider ranges of Q^2 and beam energy: JLab12.

M. Defurne *et al*, ***Nature Communications* 8** (2017) 1408.

Large kinematic coverage: CLAS

- Unpolarised DVCS cross-sections and helicity-dependent cross-section differences in a wide kinematic range:

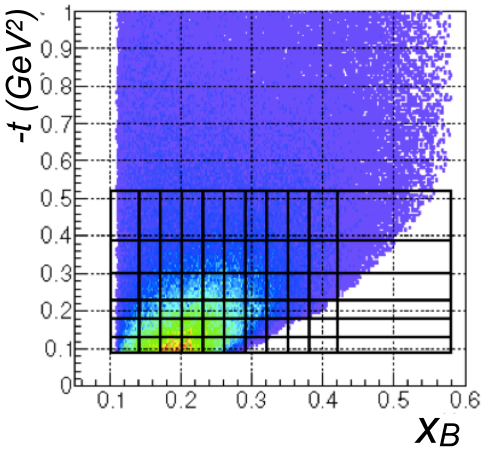

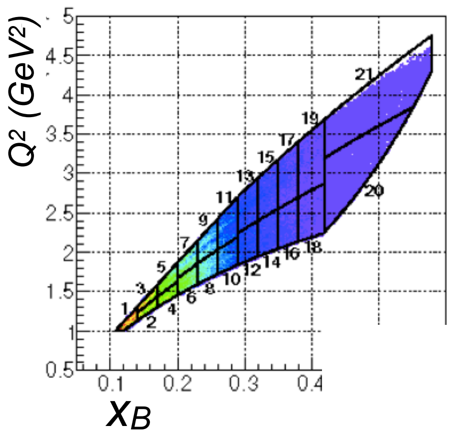

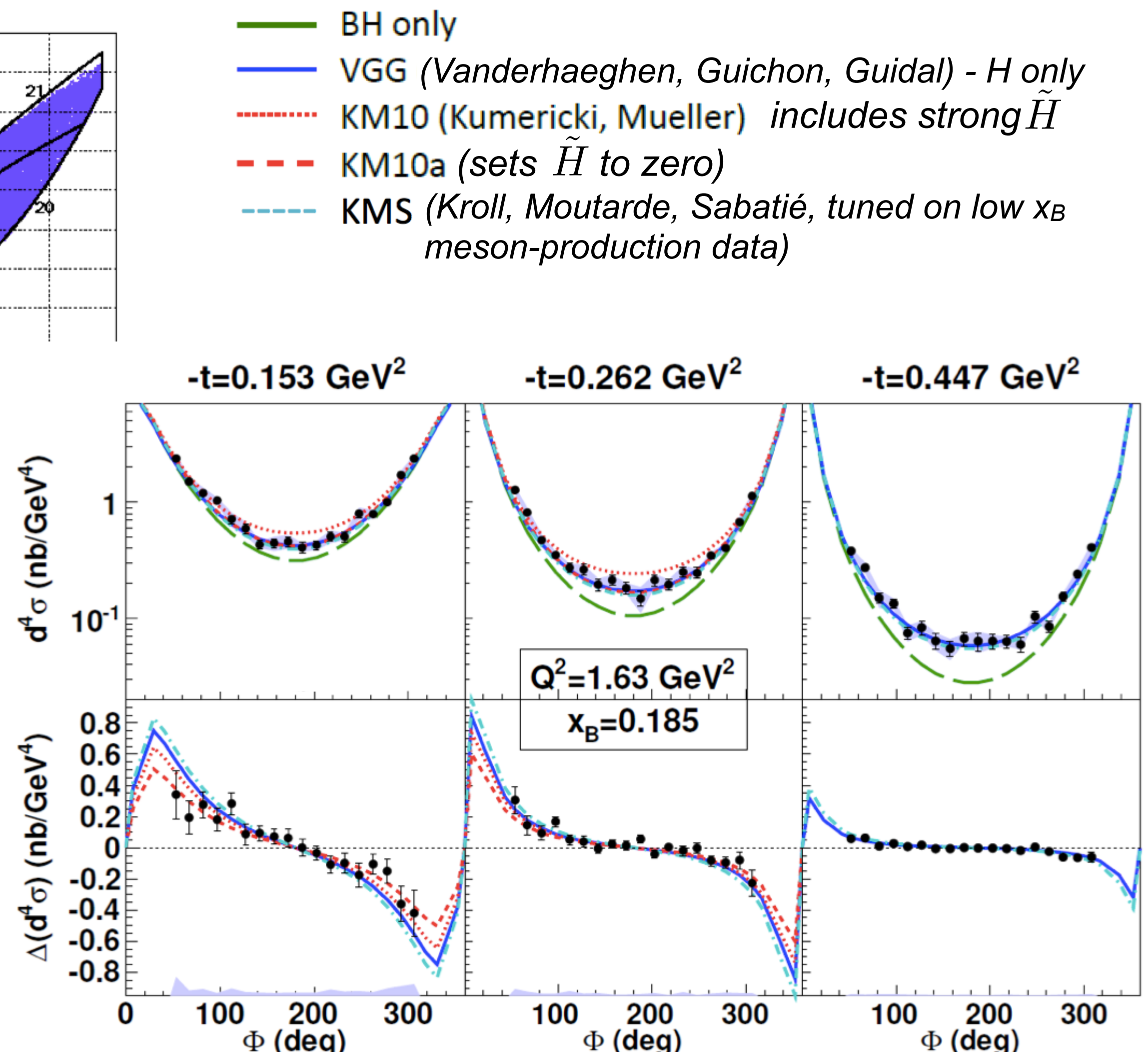

- Widest phase space coverage in valence quark region: CFF constraints.

- Dominance of GPD *H* in unpolarised cross-section.

H.-S. Jo *et al* (CLAS), ***PRL*** **115** (2015) 212003
N. Hirlinger Saylor *et al* (CLAS), ***PRC*** **98** (2018) 045203

DVCS asymmetries @ CLAS

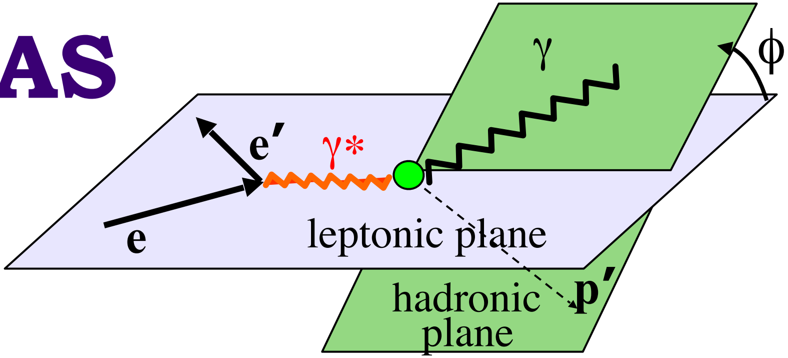

High statistics, large kinematic coverage, strong constraints on fits, simultaneous fit of BSA, TSA and DSA at common kinematics from the same dataset:

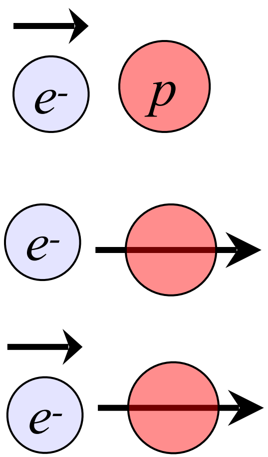

Beam-spin asymmetry (BSA): $\Delta\sigma_{LU} \sim \sin\phi\, \Im(F_1 H + \xi G_M \tilde{H} - \frac{t}{4M^2} F_2 E)\, d\phi$

Target-spin asymmetry: $\Delta\sigma_{UL} \sim \sin\phi\, \Im(F_1 \tilde{H} + \xi G_M (H + \frac{x_B}{2} E) - \xi \frac{t}{4M^2} F_2 \tilde{E} + \ldots)\, d\phi$

Double-spin asymmetry: $\Delta\sigma_{LL} \sim (A + B\cos\phi)\, \Re(F_1 \tilde{H} + \xi G_M (H + \frac{x_B}{2} E) + \ldots) d\phi$

F_1, F_2: Dirac, Pauli form factors

→ Constraints on CFFs H and $\tilde{H}$

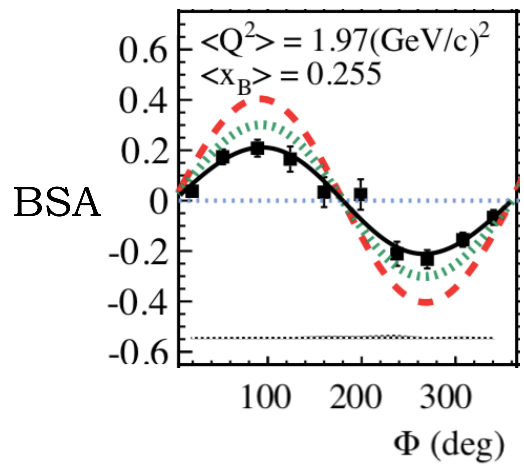

E. Seder *et al* (CLAS), ***PRL* 114** (2015) 032001
S. Pisano *et al* (CLAS), ***PRD* 91** (2015) 052014
F.-X. Girod *et al* (CLAS), ***PRL* 100** (2008) 162002

Beam- and target-spin asymmetries

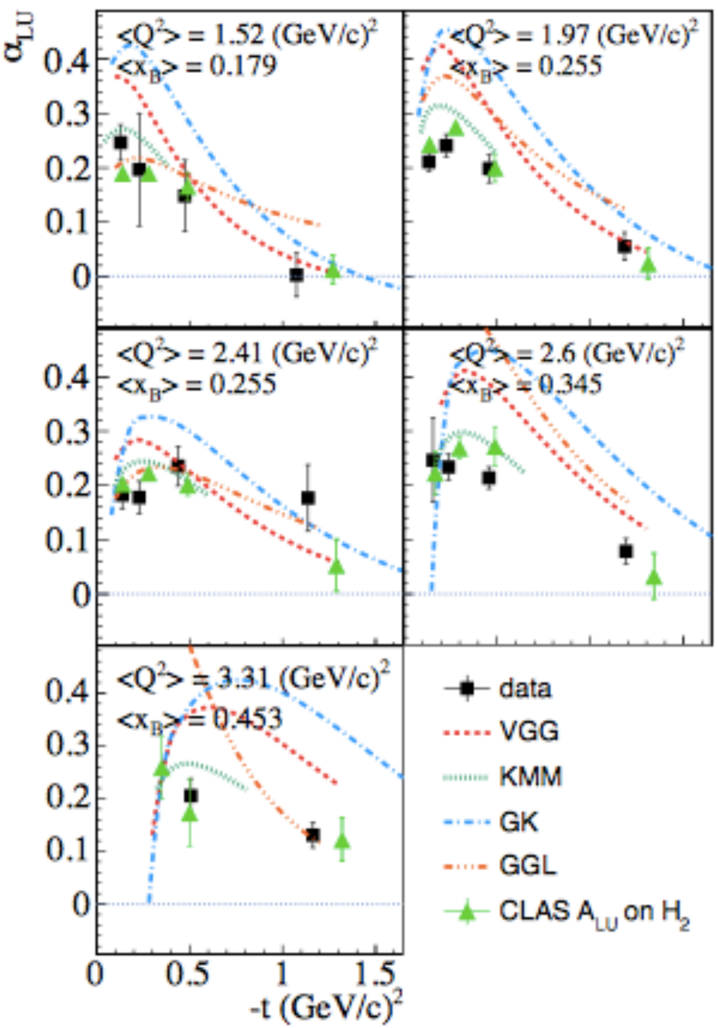

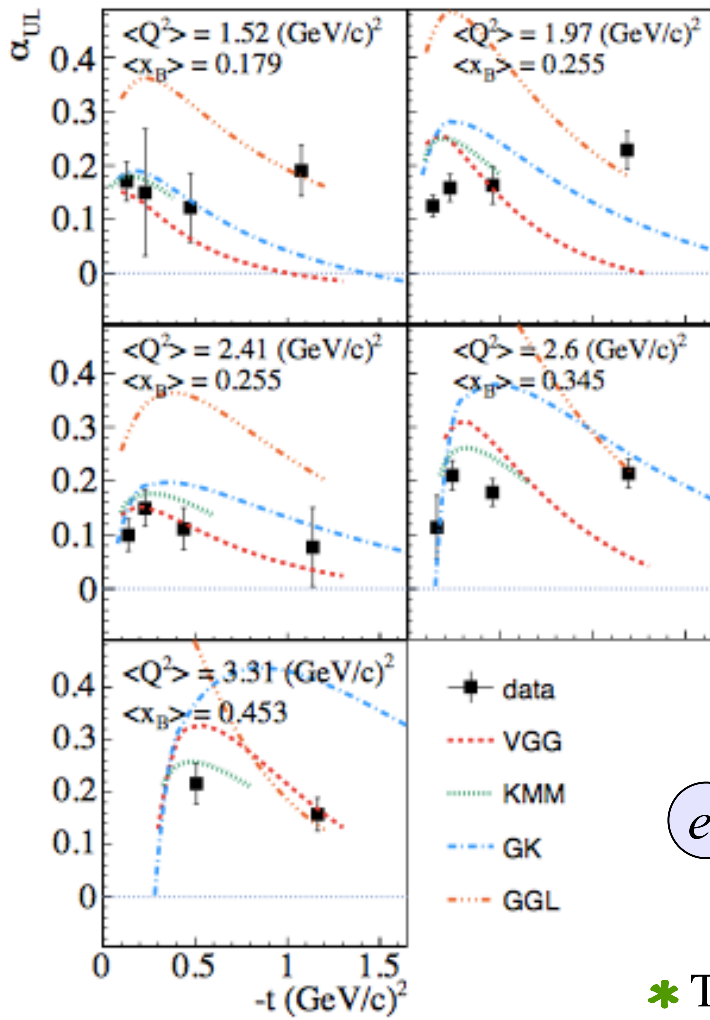

$$A = \frac{\alpha sin\phi}{1+\beta cos\phi}$$

GGL: Goldstein, Gonzalez, Liuti

GK: Kroll, Moutarde, Sabatié

KMM: Kumericki, Mueller, Murray

VGG: Vanderhaeghen, Guichon, Guidal

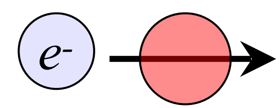

- TSA shows a flatter distribution in *t* than BSA.

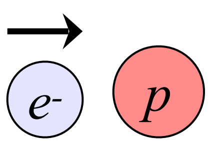

S. Pisano *et al* (CLAS), ***PRD* 91** (2015) 052014
E. Seder *et al* (CLAS), ***PRL* 114** (2015) 032001

Compton Form Factors from CLAS data

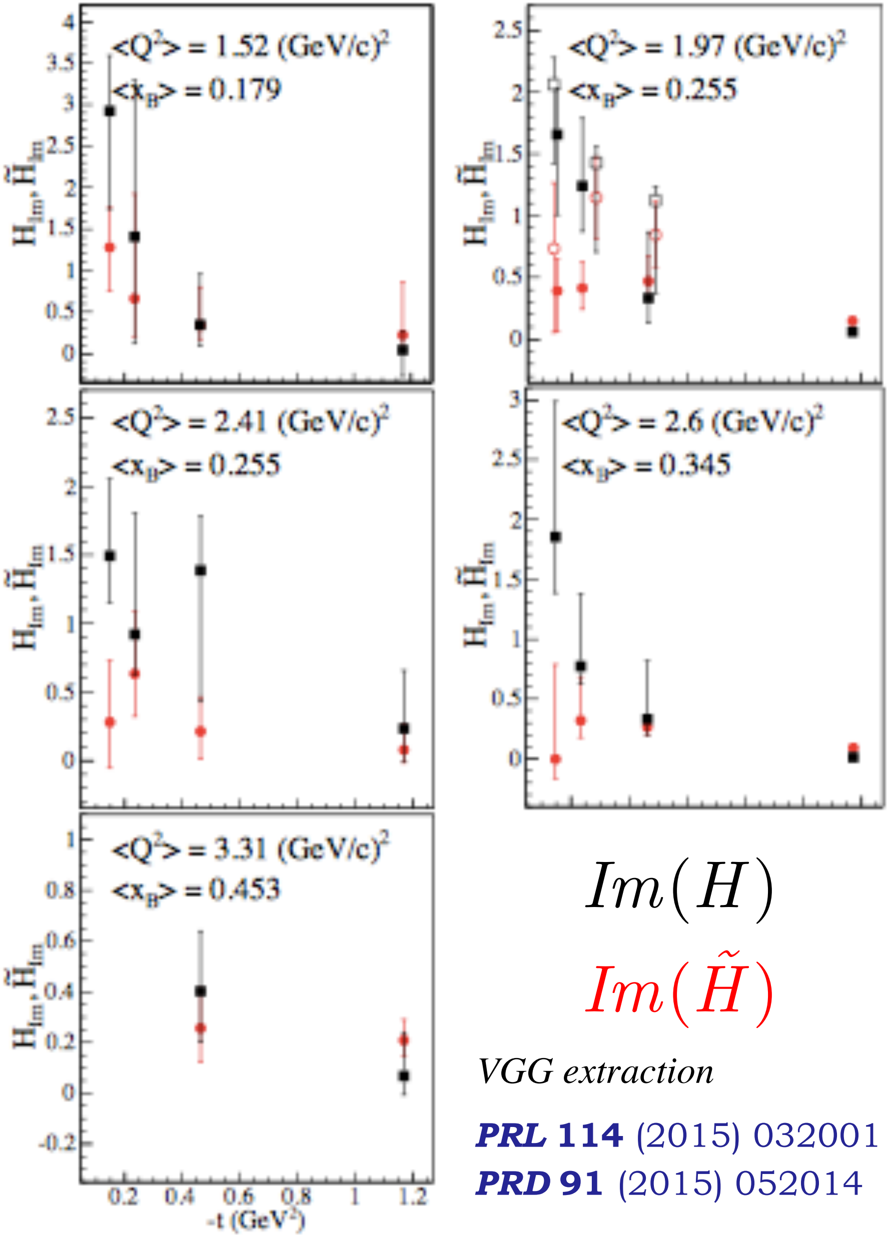

$Im(H)$

$Im(\tilde{H})$

VGG extraction

***PRL* 114** (2015) 032001

***PRD* 91** (2015) 052014

- Extracted using local fits to cross-sections and asymmetries, constrained by the VGG (Vanderhaeghen, Guichon, Guidal) model.
- Information on relative distributions of quark momenta (PDFs) and quark helicity, $\Delta q(x)$

$$H(x,0,0) = q(x) \quad \tilde{H}(x,0,0) = \Delta q(x)$$

- Indications that axial charge is more concentrated than electromagnetic charge.

$$\int_{-1}^{+1} H dx = F_1 \quad \int_{-1}^{+1} \tilde{H}\, dx = G_A$$

- Slope flatter towards higher-x: valence quarks are at centre, lower-x quarks at periphery.

Global analysis of all available data needed.

Towards nucleon tomography

- **Local fit** to extract CFFs: limits based on +/-5 * the VGG (Vanderhaeghen, Guichon, Guidal) model predictions using leading-twist amplitude based on Double Distributions.

- Assuming leading-twist and exponential dependence of GPD on t, using models to extrapolate to the zero skewness point $\xi = 0$ and assuming similar behaviour for u and d quarks there:

$$\langle b_\perp^2 \rangle^q(x) = -4 \frac{\partial}{\partial \mathbf{\Delta}_\perp^2} \ln H_-^q(x, 0, -\mathbf{\Delta}_\perp{}^2)\Big|_{\mathbf{\Delta}_\perp = 0}$$

$$H_-^q(x, 0, t) \equiv H^q(x, 0, t) + H^q(-x, 0, t) \qquad t = \Delta^2$$

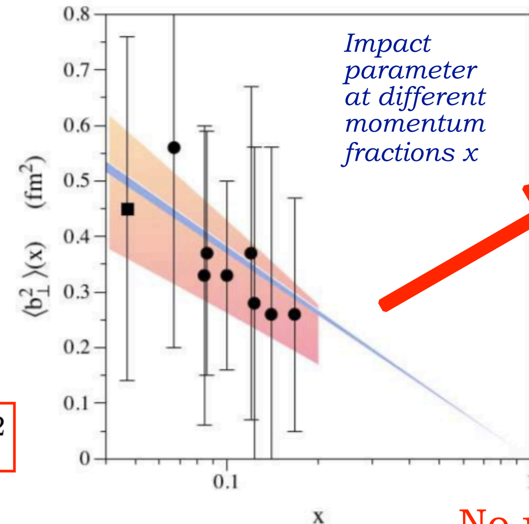

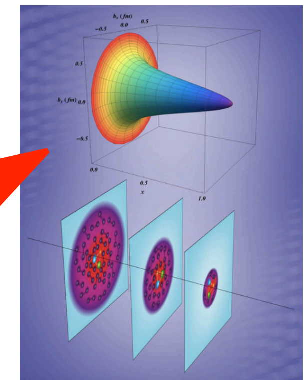

R. Dupré *et al.*, Eur. Phys. J **A 53,** (2017) 171

No uncertainties shown!

- **Global fits:** PARTONS framework using neural networks to minimise model-dependence in the extraction of CFFs.

We need more data from multiple channels and across a wide kinematic range!

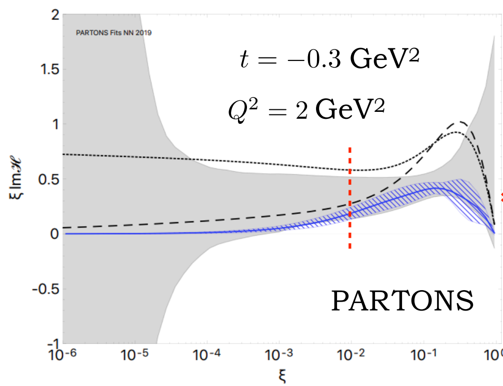

H. Moutarde *et al.*, Eur. Phys. J C79, 614 (2019)

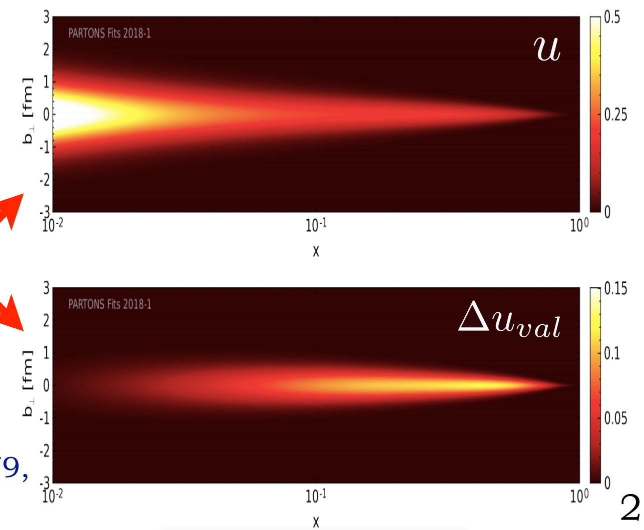

DVCS on the neutron: Hall A

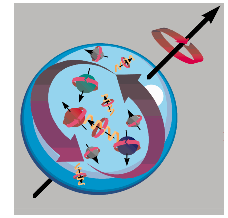

$$J_N = \frac{1}{2} = \frac{1}{2}\Sigma_q + L_q + J_g$$

- Ji's relation: $J^q = \frac{1}{2} - J^g = \frac{1}{2}\int_{-1}^{1} x dx \left\{ H^q(x,\xi,0) + E^q(x,\xi,0) \right\}$

- H^q in DVCS off the proton, first experimental constraint on E^q from neutron-DVCS beam-spin asymmetry.

$$\Delta\sigma_{LU} \sim \sin\phi \, \mathbf{Im}\{F_1 H + \xi(F_1+F_2)H - kF_2 E\} d\phi$$

M. Mazouz et al, PRL 99 (2007) 242501

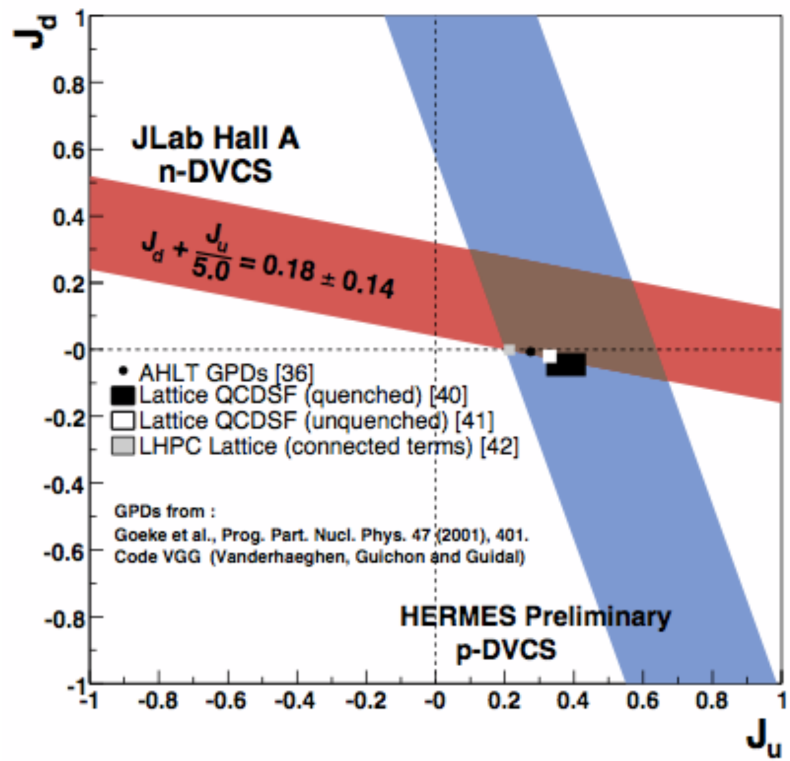

- Gives constraints on orbital angular momentum of quarks: **the spin puzzle.**

- Rosenbluth separation of interference & DVCS terms underway in neutron-DVCS cross-sections: E_e = 4.5 and 5.5 GeV (experiment E08-025).

LD_2 target $\langle Q^2 \rangle = 1.75$ GeV^2 $\langle x_B \rangle = 0.36$

DVCS on the bound proton

CLAS

- Beam spin asymmetry in DVCS from bound protons in ^{4}He (gas target).

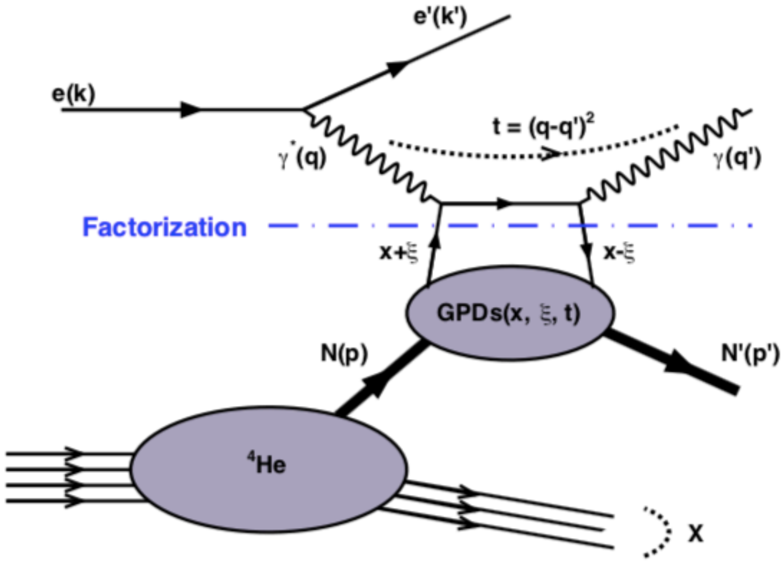

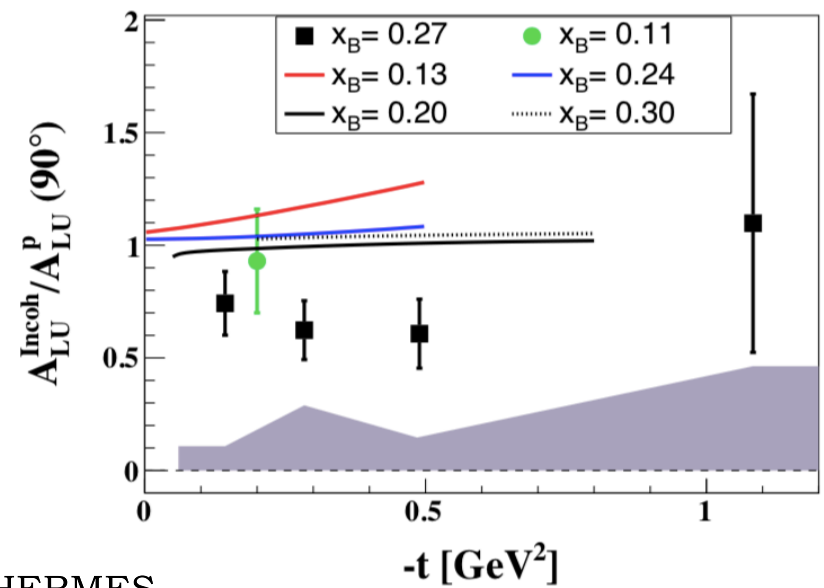

HERMES

Off-shell: S. Liuti, K. Taneja, PRC72, 032201 (2005)

On-shell: V. Guzey, A. Thomas, K. Tsushima, PLB673, 9 (2009)

- 25% - 40% lower asymmetries for bound proton compared to free, no strong dependence on t.
- Medium-modification effects, initial/final state interactions?

M. Hattawy *et al*, PRL **123**, 032502 (2019)

Imaging pressure within the nucleon

* GPDs provide indirect access to mechanical properties of the nucleon (encoded in the gravitational form factors, GFFs, of the energy-momentum tensor).

X. D. Ji, PR**D 55**, 7114-7125 (1997)
M. Polyakov, PL**B 555**, 57-62 (2016)

* Three scalar GFFs, functions of *t*: encode pressure and shear forces ($d_1(t)$), mass ($M_2(t)$) and angular momentum distributions ($J(t)$).

* Can be related to GPDs via sum rules:

$$\int x\,[H(x,\xi,t)+E(x,\xi,t)]\,\mathrm{d}x = 2J(t)$$

$$\int xH(x,\xi,t)\mathrm{d}x = M_2(t)+\frac{4}{5}\xi^2 d_1(t)$$

* Model-dependent extraction

* Neural net analysis, however: d-term almost unconstrained and consistent with zero

Possibility of extracting pressure distributions! But more data needed.

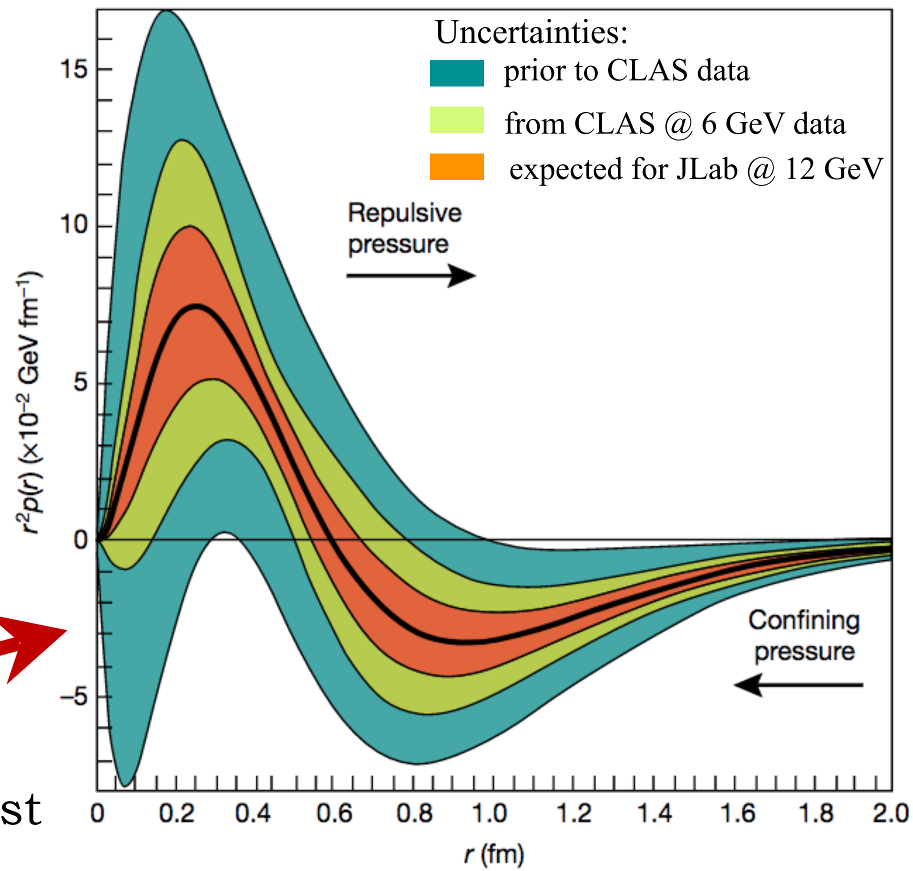

V. Burkert, L. Elouadrhiri, F.-X. Girod, Nature **557**, 396-399 (2018)

K. Kumerički, Nature **570**, E1-E2 (2019)

DVCS at JLab12:
11 GeV era

11 GeV era DVCS Cross-sections: Halls A and C

Experiments:
E12-06-114 (Hall A, 100 days),
E12-13-010 (Hall C, 53 days)

Unpolarised liquid H_2 target:

- Beam energies: 6.6, 8.8, 11 GeV
- Scans of Q^2 at fixed x_B.
- Hall A: aim for absolute cross-sections with 4% relative precision.

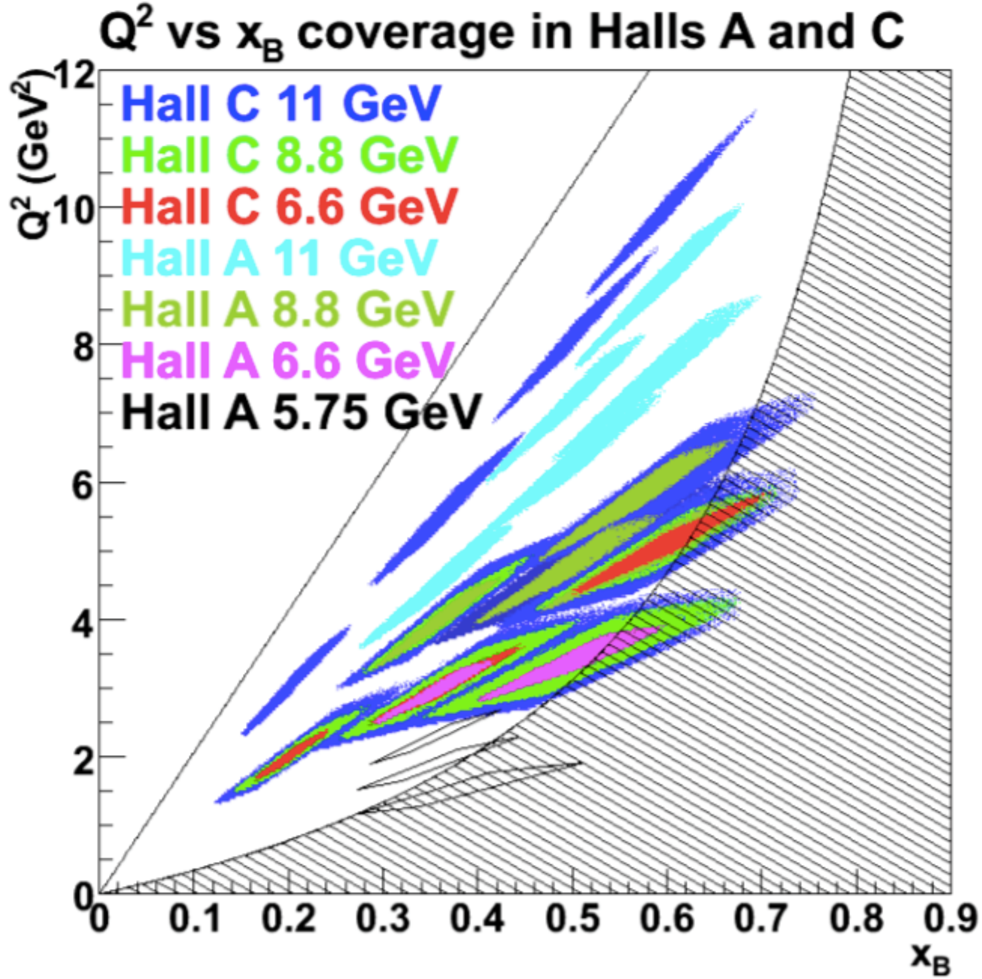

✱ Azimuthal, energy and helicity dependencies of cross-section to separate $|T_{DVCS}|^2$ and interference contributions in a wide kinematic coverage.

✱ Separate *Re* and *Im* parts of the DVCS amplitude.

DVCS in Hall A: first experiment after upgrade. 50% of data taken!

DVCS with CLAS12

E12-06-119: Unpolarised liquid H_2 target

Beam-spin asymmetry → ***Im*(H$_p$)**

First experiment with CLAS12 ~50% done

P_{beam} = 85%
L = 10^{35} $cm^{-2}s^{-1}$
1< Q^2 < 10 GeV^2
0.1 <x_B< 0.65
$-t_{min}$< $-t$ < 2.5 GeV^2

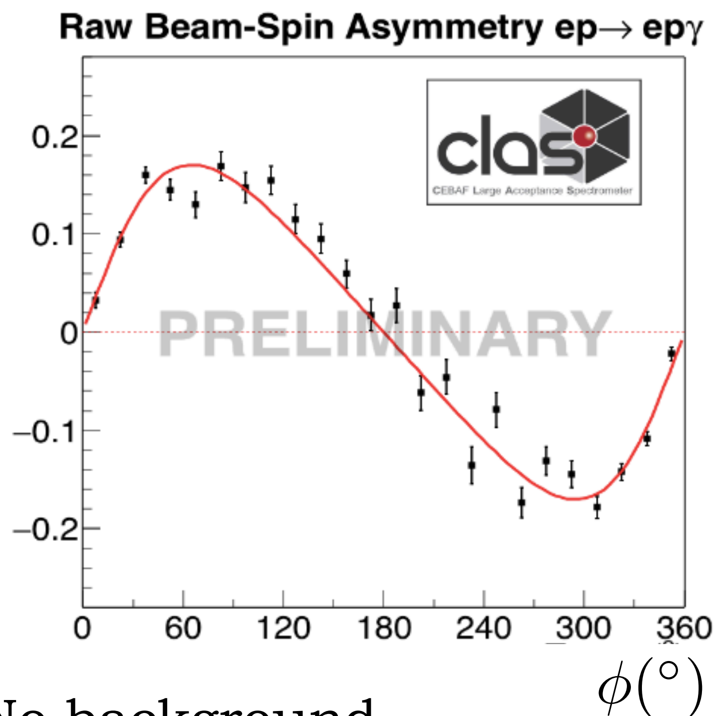

No background subtraction

$$\Delta\sigma_{LU} \sim \sin\phi\, \Im(F_1 H + \xi G_M \tilde{H} - \frac{t}{4M^2} F_2 E)\, d\phi$$

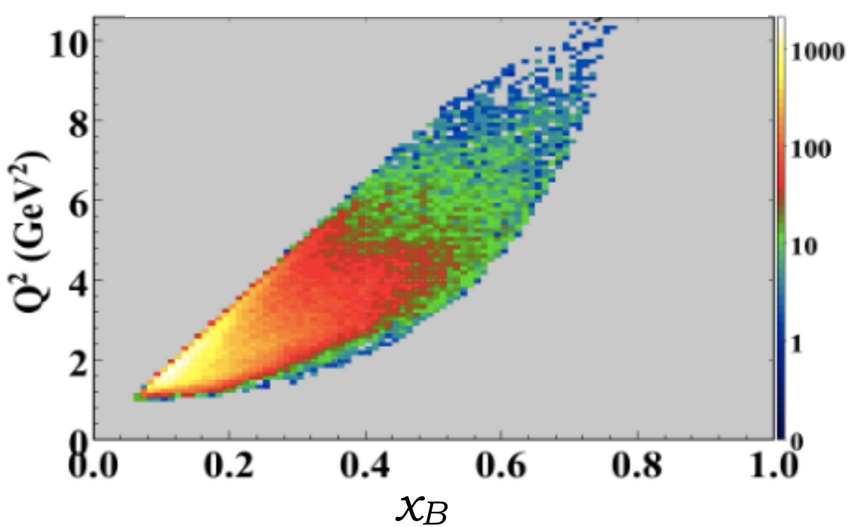

Guillaume Christiaens (Glasgow, CEA Saclay)

DVCS at lower energies with CLAS12

CLAS12

Experiment E12-16-010B

Unpolarised liquid H_2 target:

- Beam energies: 6.6, 8.8 GeV
- Simultaneous fit to beam-spin and total cross-sections.

* Rosenbluth separation of interference and $|T_{DVCS}|^2$ terms in the cross-section

* Scaling tests of the extracted CFFs

Compare with measurements from Halls A and C: cross-check model and systematic uncertainties.

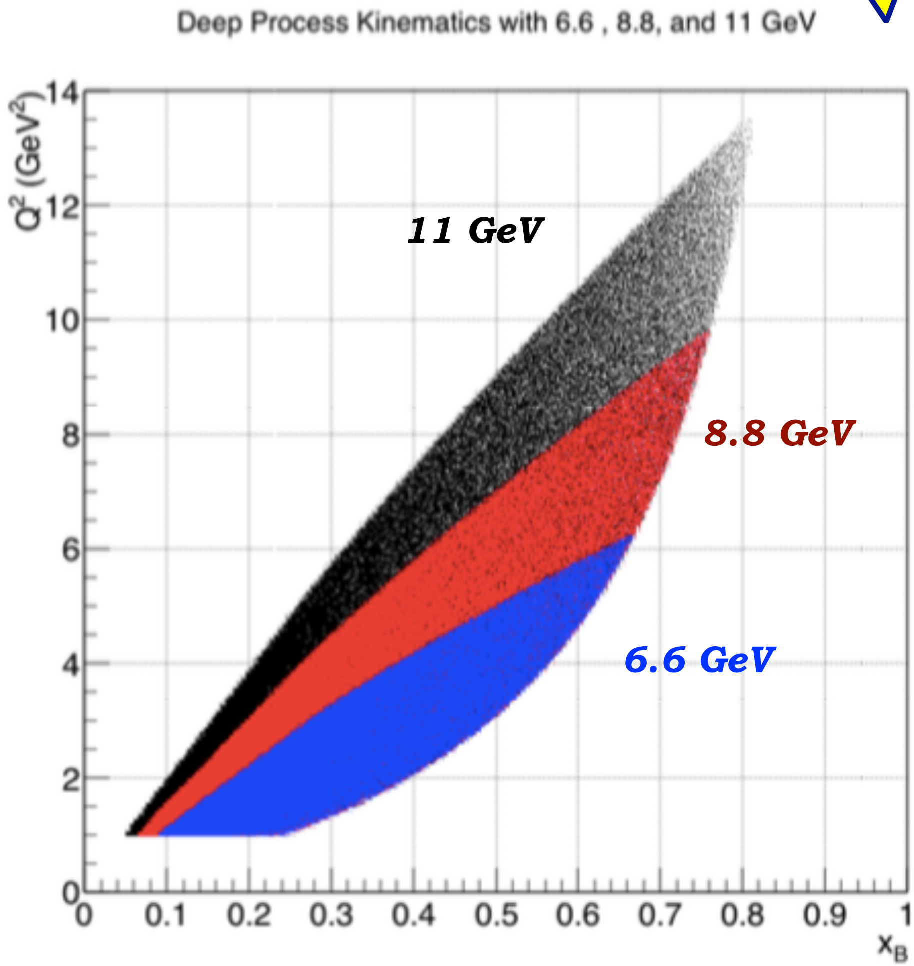

Data currently under analysis

Neutron DVCS @ 11 GeV: sensitivity to J_q

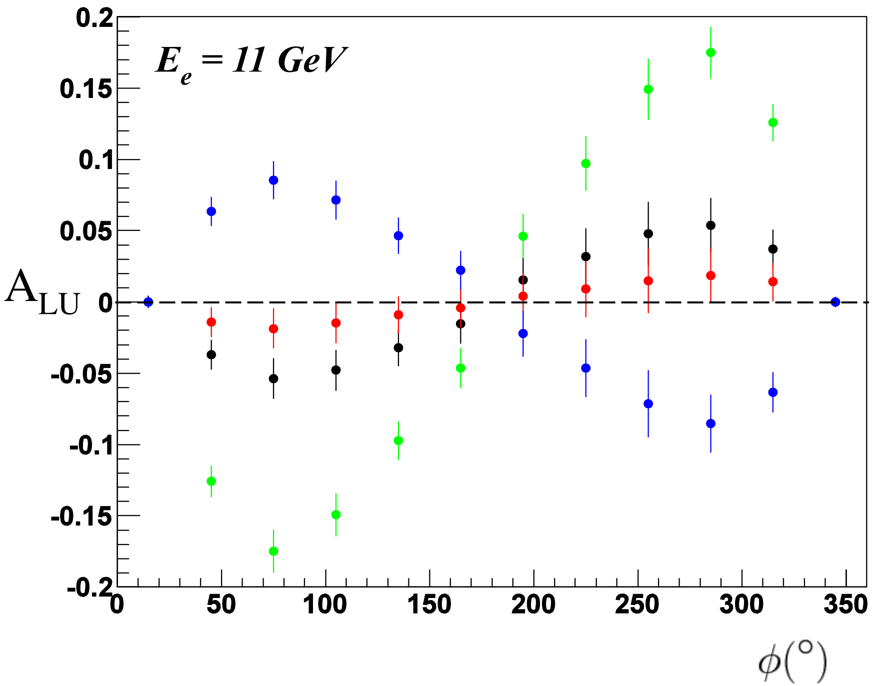

$J_u = 0.3, J_d = -0.1$ $J_u = 0.3, J_d = 0.1$

$J_u = 0.1, J_d = 0.1$ $J_u = 0.3, J_d = 0.3$

VGG (calculations by M. Guidal)

$x_B = 0.17$ $Q^2 = 2$ GeV^2 $t = -0.4$ GeV^2

- At 11 GeV, beam spin asymmetry (A_{LU}) in neutron DVCS *is* very sensitive to J_u, J_d

$$\Delta\sigma_{LU} \sim \sin\phi\, \mathbf{Im}\{F_1 H + \xi(F_1+F_2)H - kF_2 E\}d\phi$$

- Dedicated neutron detector added to CLAS12: Central Neutron Detector

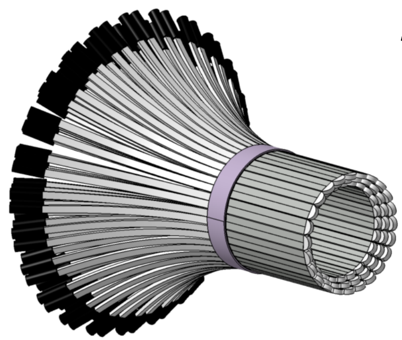

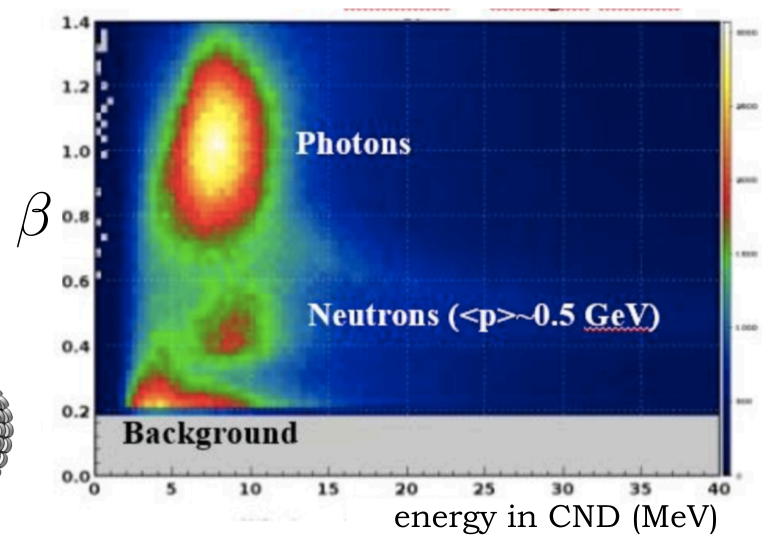

Katheryne Price (IPN Orsay)

Measurement currently in progress...

Experiment E12-11-003

CLAS12

Proton & neutron DVCS with a longitudinally polarised target

Experiments: E12-06-119
E12-06-109A

A_{UL} characterised by imaginary parts of CFFs via:

$$F_1\tilde{H} + \xi G_M\left(H + \frac{x_B}{2}E\right) - \frac{\xi t}{4M^2}F_2\tilde{E} + \ldots$$

$\rightarrow$ ***Im***$(\tilde{H}_p)$
Im(H_n)

Longitudinally polarised NH_3 and ND_3 targets:

- Dynamic Nuclear Polarisation (DNP) of target material, cooled to 1K in a *He* evaporation cryostat.
- P_{proton} > 80%
- $P_{deuteron}$ up to 50%
- Statistical error: 2% - 15% on sinφ moments
- Systematic uncertainties: ~ 12%

Tentative schedule: ~2021

Target cryostat

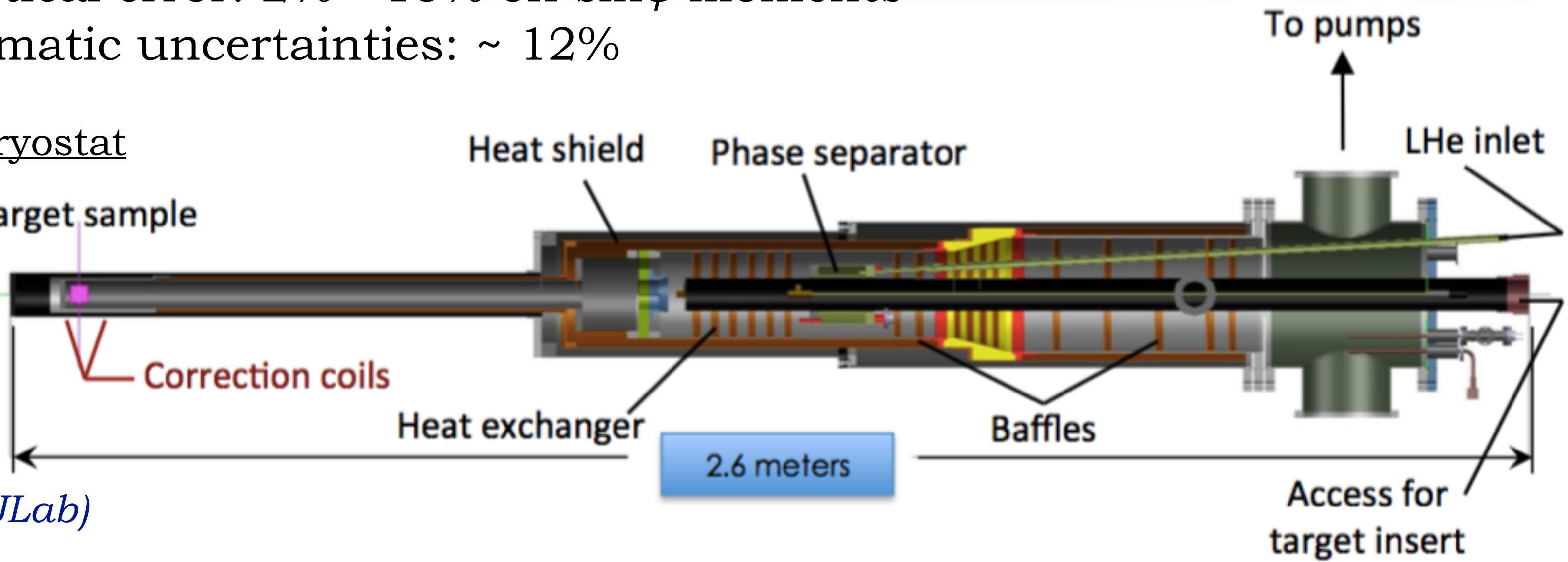

C. Keith (JLab)

CLAS12

Proton DVCS with transversely polarised target at CLAS12

C12-12-010: with transversely polarised HD target (conditionally approved).

$\Delta\sigma_{UT} \sim \cos\phi \; \mathrm{Im}\{k(F_2 H - F_1 E) + \ldots\}d\phi$

Sensitivity to ***Im(E)*** for the proton.

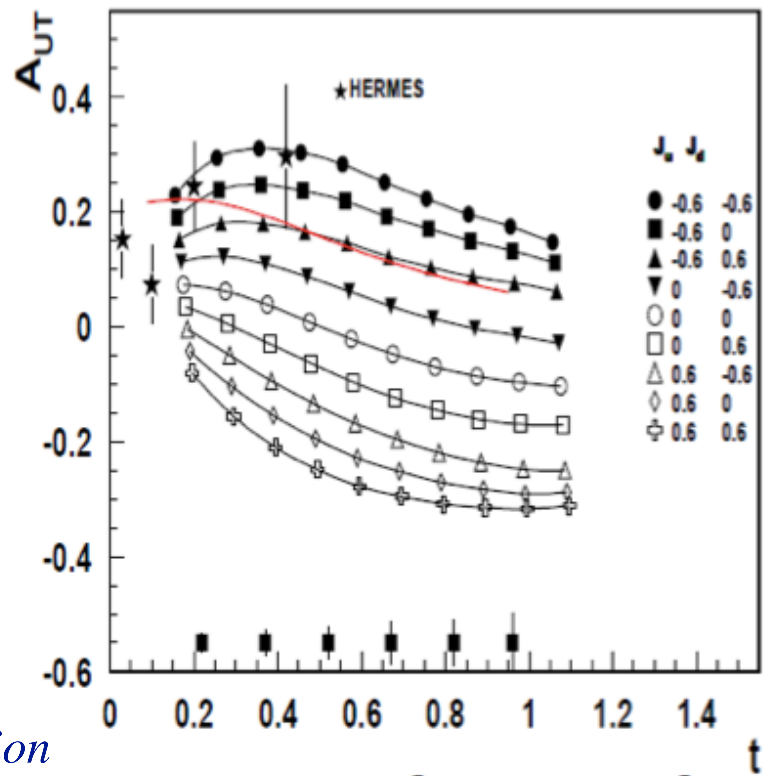

$\langle x \rangle = 0.2, \langle Q^2 \rangle = 2.5\ GeV^2$

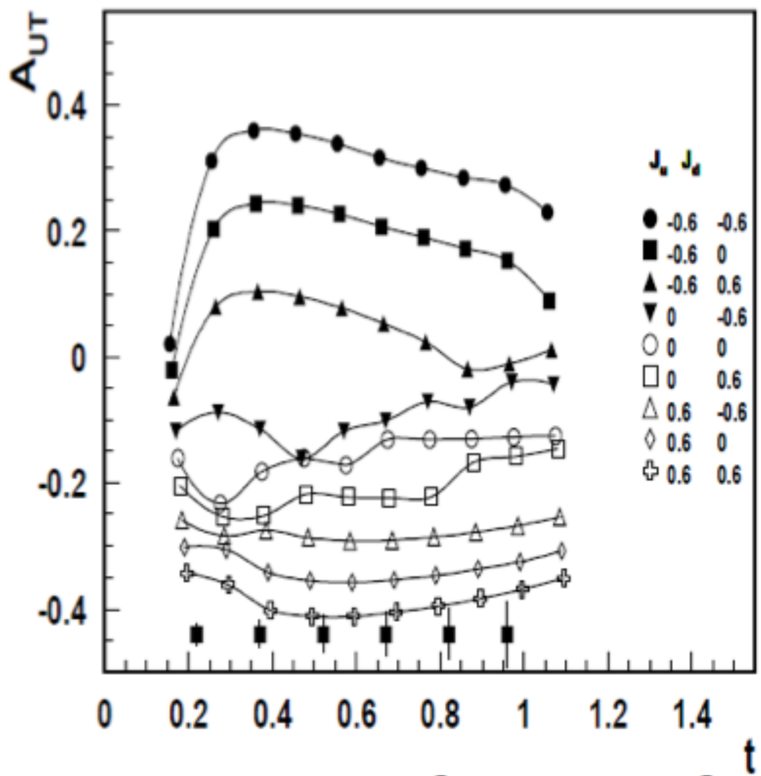

$\langle x \rangle = 0.33, \langle Q^2 \rangle = 2.5\ GeV^2$

VGG extraction (M. Guidal)

DVCS @ COMPASS: sea quarks

COMPASS @ Cern (SPS)

Compact **M**uon and **P**roton **A**pparatus for **S**tructure and **S**pectroscopy

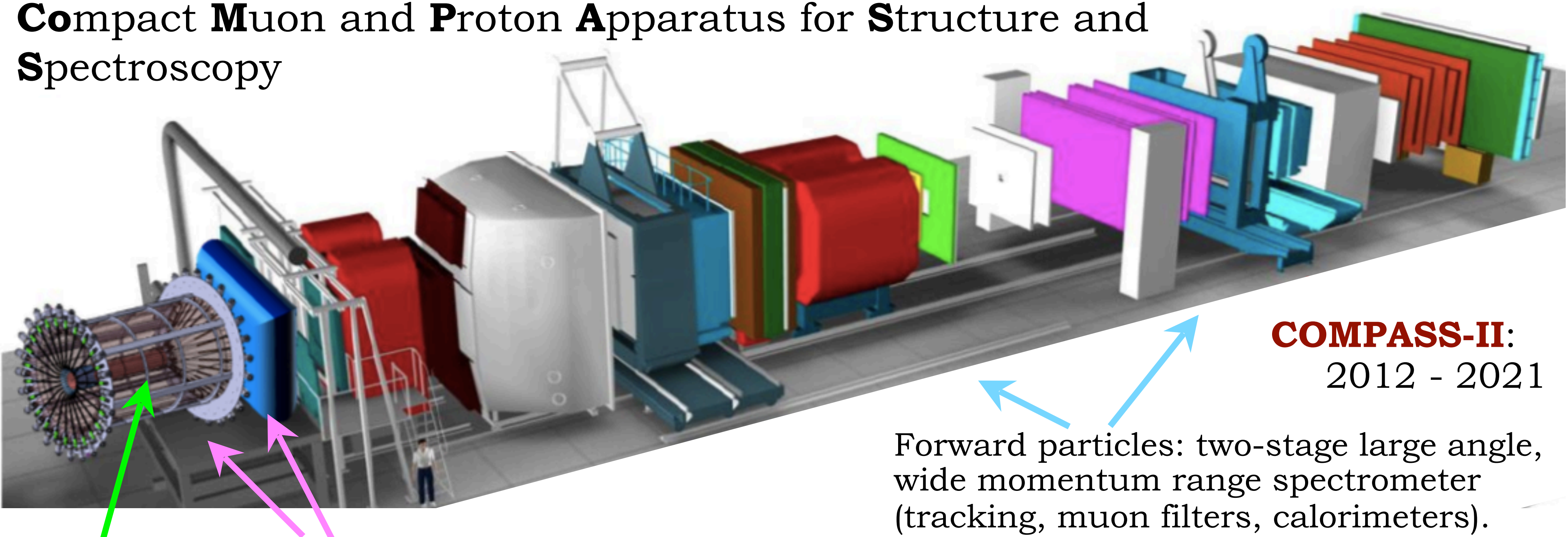

COMPASS-II: 2012 - 2021

Forward particles: two-stage large angle, wide momentum range spectrometer (tracking, muon filters, calorimeters).

2.5m liquid *H_2* target

Upgrades: new scintillator ToF CAMERA for recoil proton detection & new EM calorimeter.

DVCS : μ p → μ' p γ

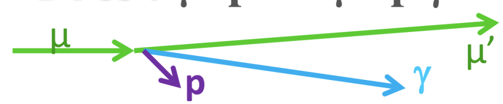

Full exclusive reconstruction

- 160 GeV 80% polarised μ^+/μ^-
- $\sim 4 \times 10^8 \mu/spill$, 9.6s/40s duty cycle

Data:
- 2008 & 2009: two v. short test runs, 40 cm LH_2 target.
- COMPASS-II: 1 month in 2012, 6 months in 2016 & 2017 each (GPD **H**).
- 2022+: transversely pol. NH_3 target (GPD **E**). LOI stage…

DVCS @ COMPASS (2012 run)

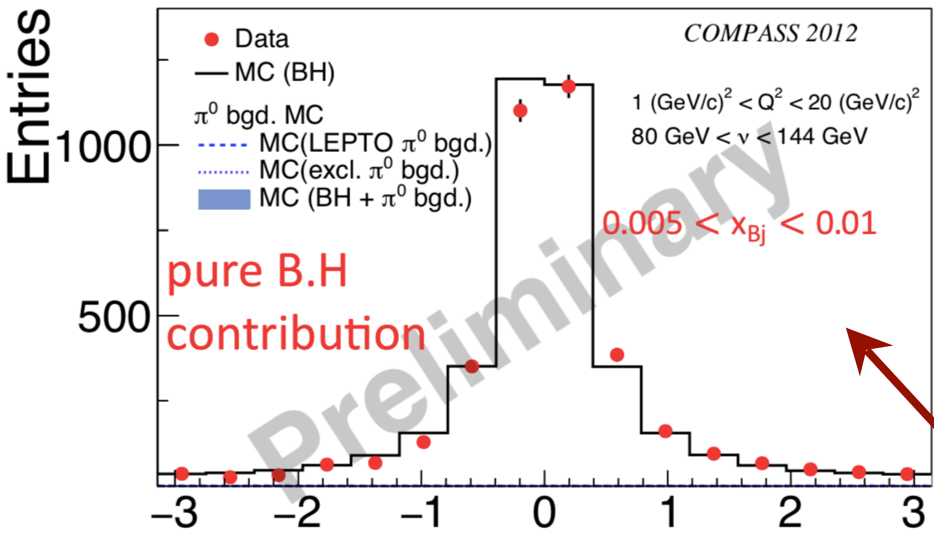

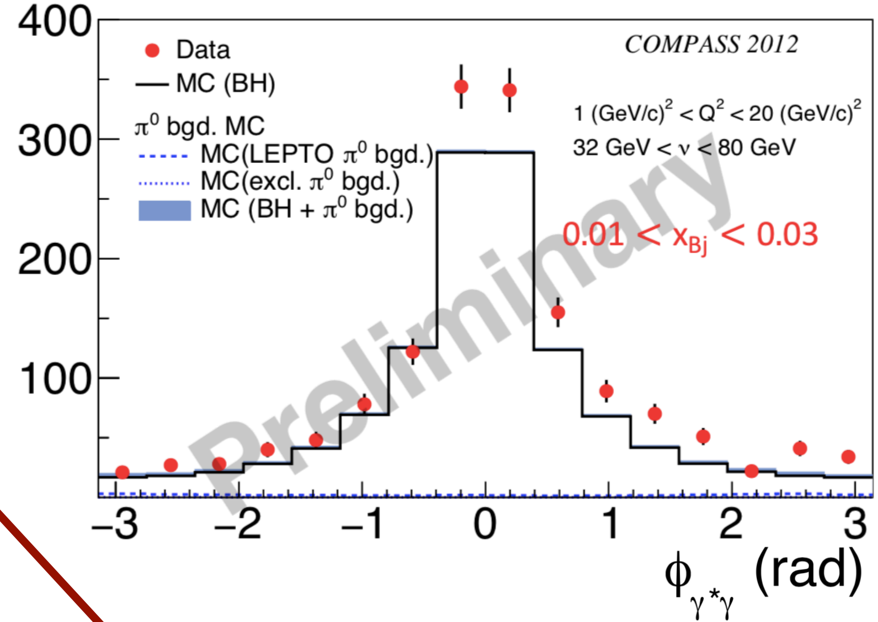

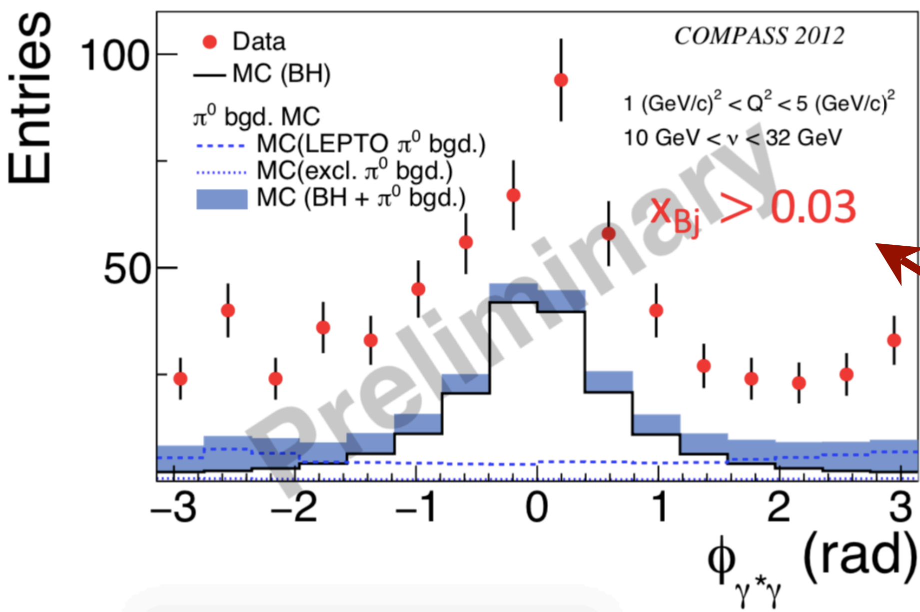

Bethe-Heitler dominates at very low x_B

DVCS dominates at these kinematics

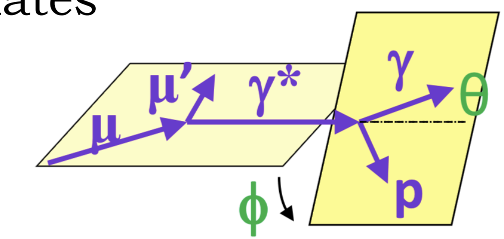

Slide mash-up from N. d'Hose and A. Ferrero

DVCS @ COMPASS (2012 run)

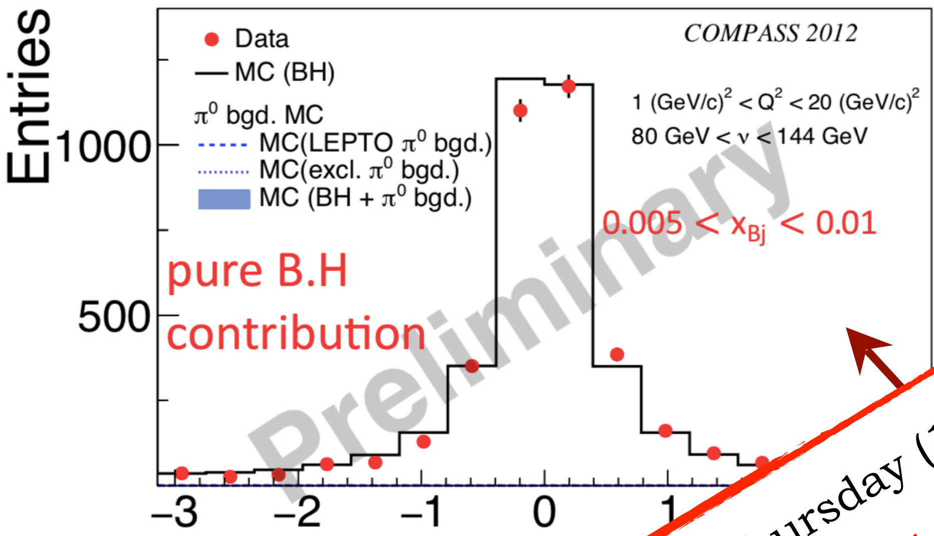

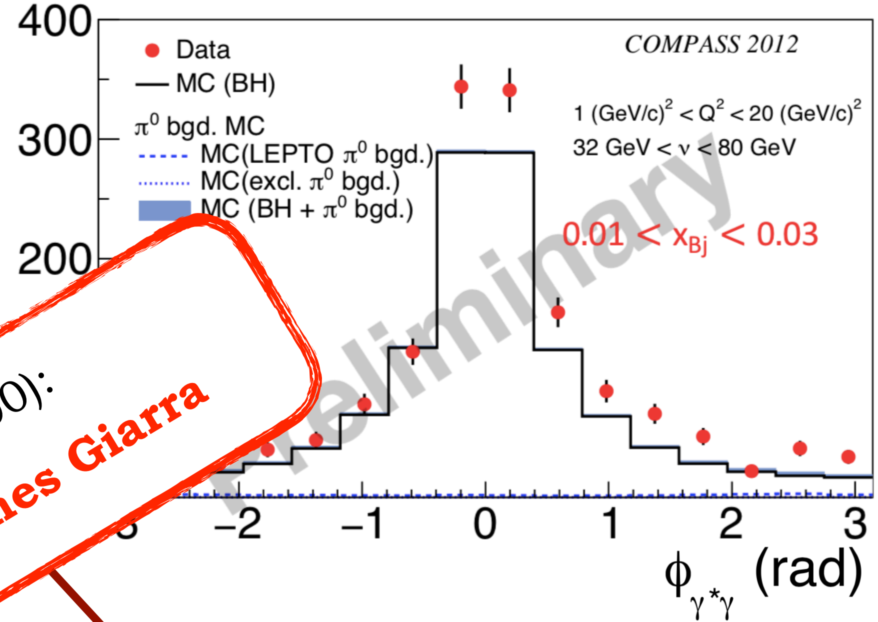

See talk on Thursday (15.00):
Johannes Giarra

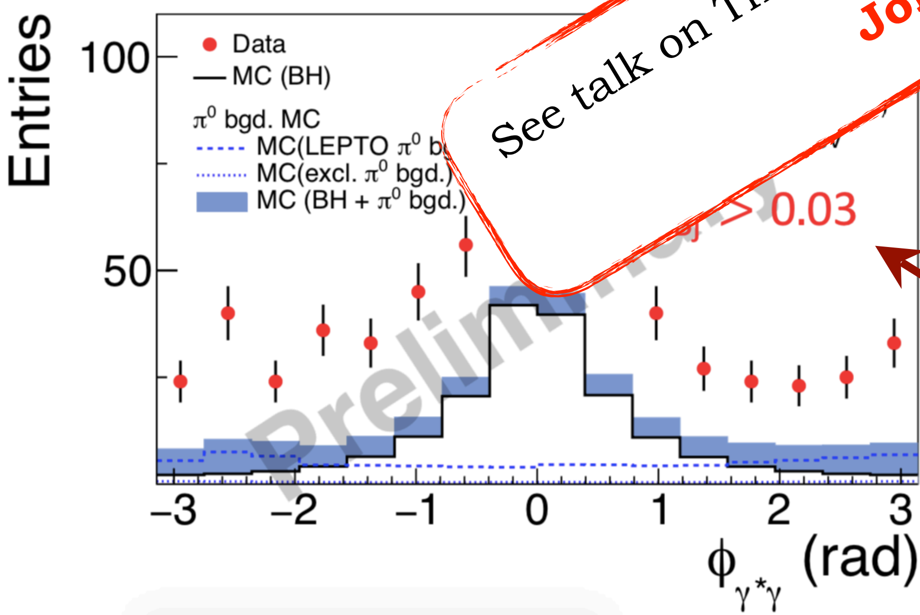

Bethe-Heitler dominates at very low x_B

DVCS dominates at these kinematics

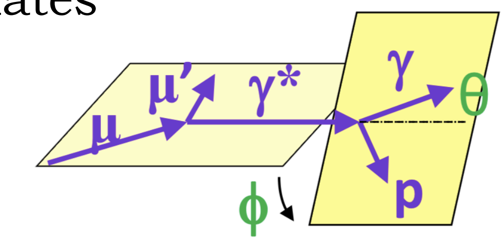

Slide mash-up from N. d'Hose and A. Ferrero

DVCS x-section and t-slope extraction

Kinematically constrained
vertex fit applied

Slide from: A. Ferrero @ SPIN 2018

$d\sigma^{DVCS}/dt = e^{-B|t|}$

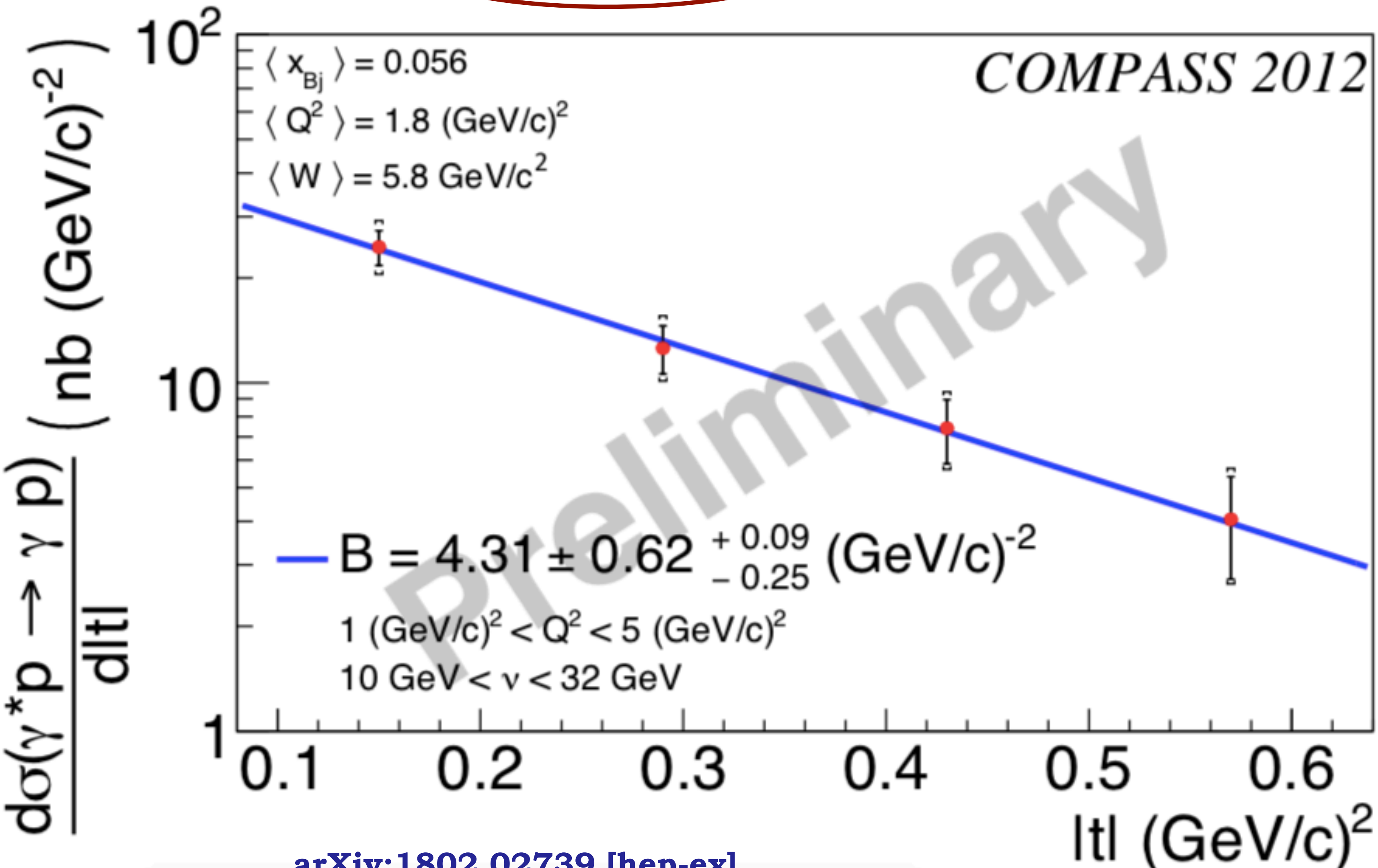

arXiv:1802.02739 [hep-ex]

DVCS x-section and t-slope extraction

Kinematically constrained vertex fit applied

$d\sigma^{DVCS}/dt = e^{-B|t|}$

Slide from: A. Ferrero @ SPIN 2018

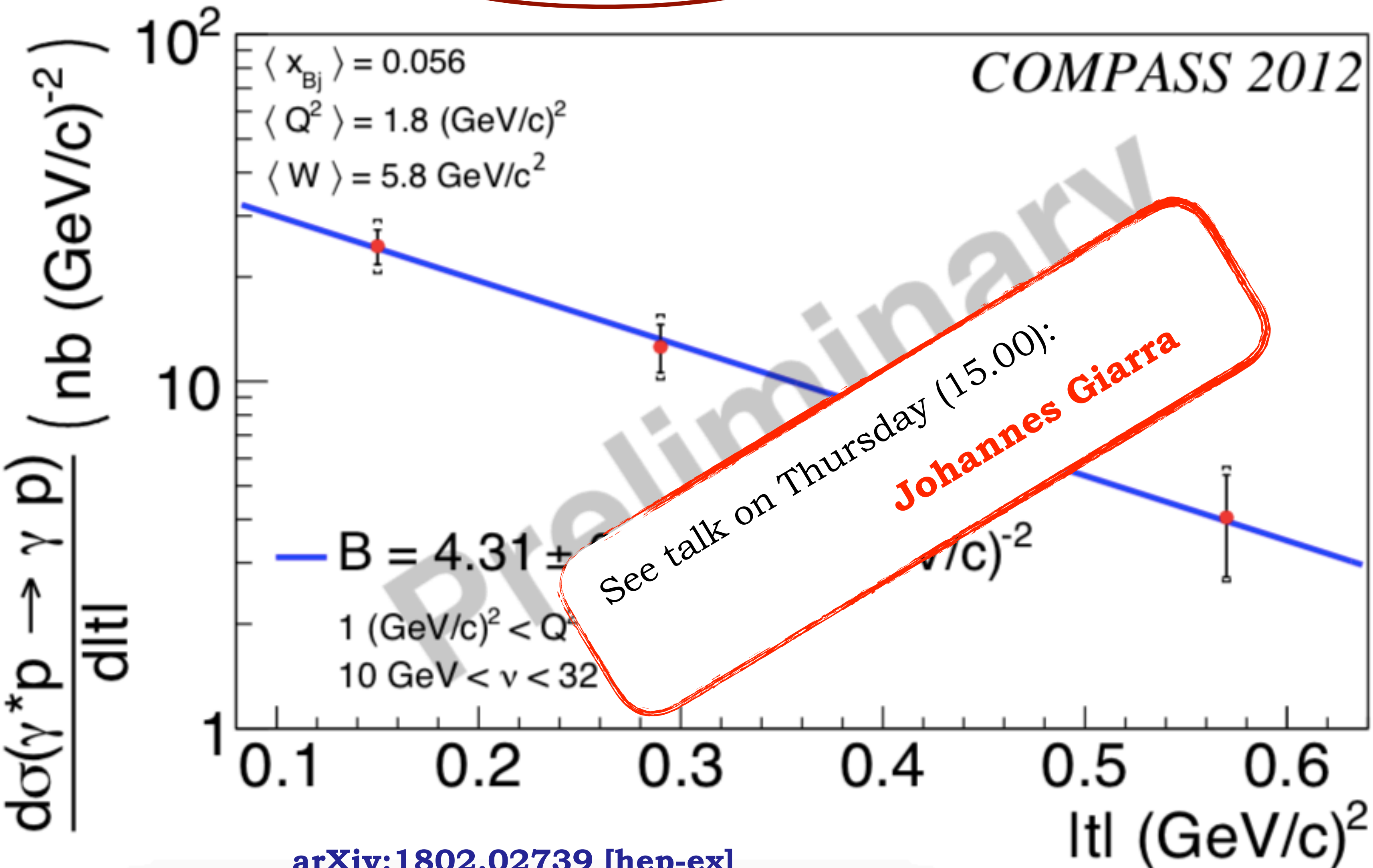

arXiv:1802.02739 [hep-ex]

Tomography of sea quarks

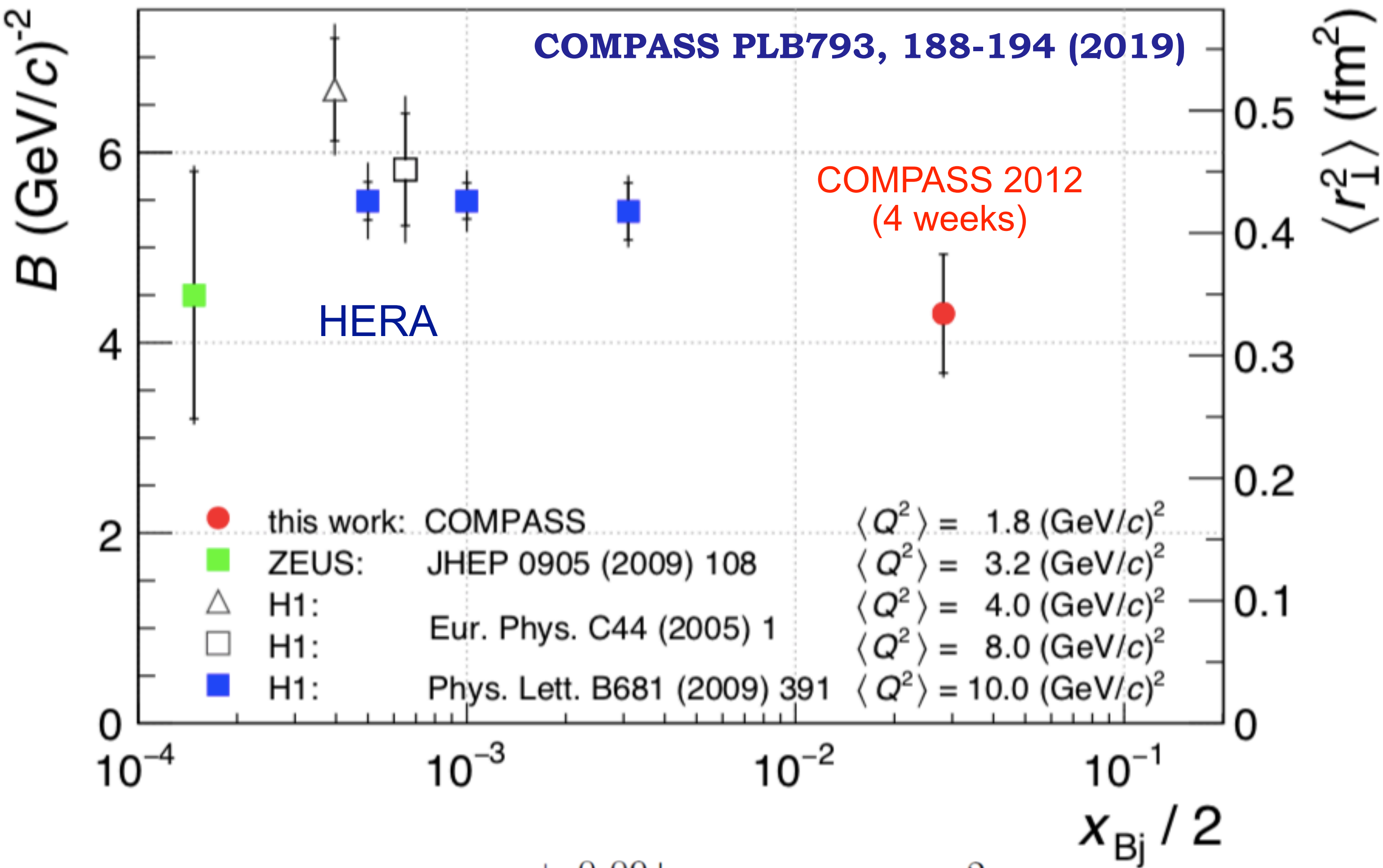

$1 < Q^2 < 5$ GeV^2

$\langle Q^2 \rangle = 1.8$ GeV^2

$\langle x_B \rangle = 0.056$

Integrated luminosity: 42.4 pb^{-1}

10 times more stats in 2016-17 runs

$$B = (4.31 \ \pm \ 0.62_{\text{stat}} \ {}^{+\,0.09}_{-\,0.25}\big|_{\text{sys}})\,(\text{GeV}/c)^{-2}$$

$$\sqrt{\langle r_\perp^2 \rangle} = (0.58 \pm 0.04_{\text{stat}} \ {}^{+\,0.01}_{-\,0.02}\big|_{\text{sys}} \ \pm 0.04_{\text{model}})\,\text{fm}$$

at average x_B = *0.056*

$\langle r_\perp^2 (x_B) \rangle \approx 2B(x_B)$

for small x_B

Tomography of sea quarks

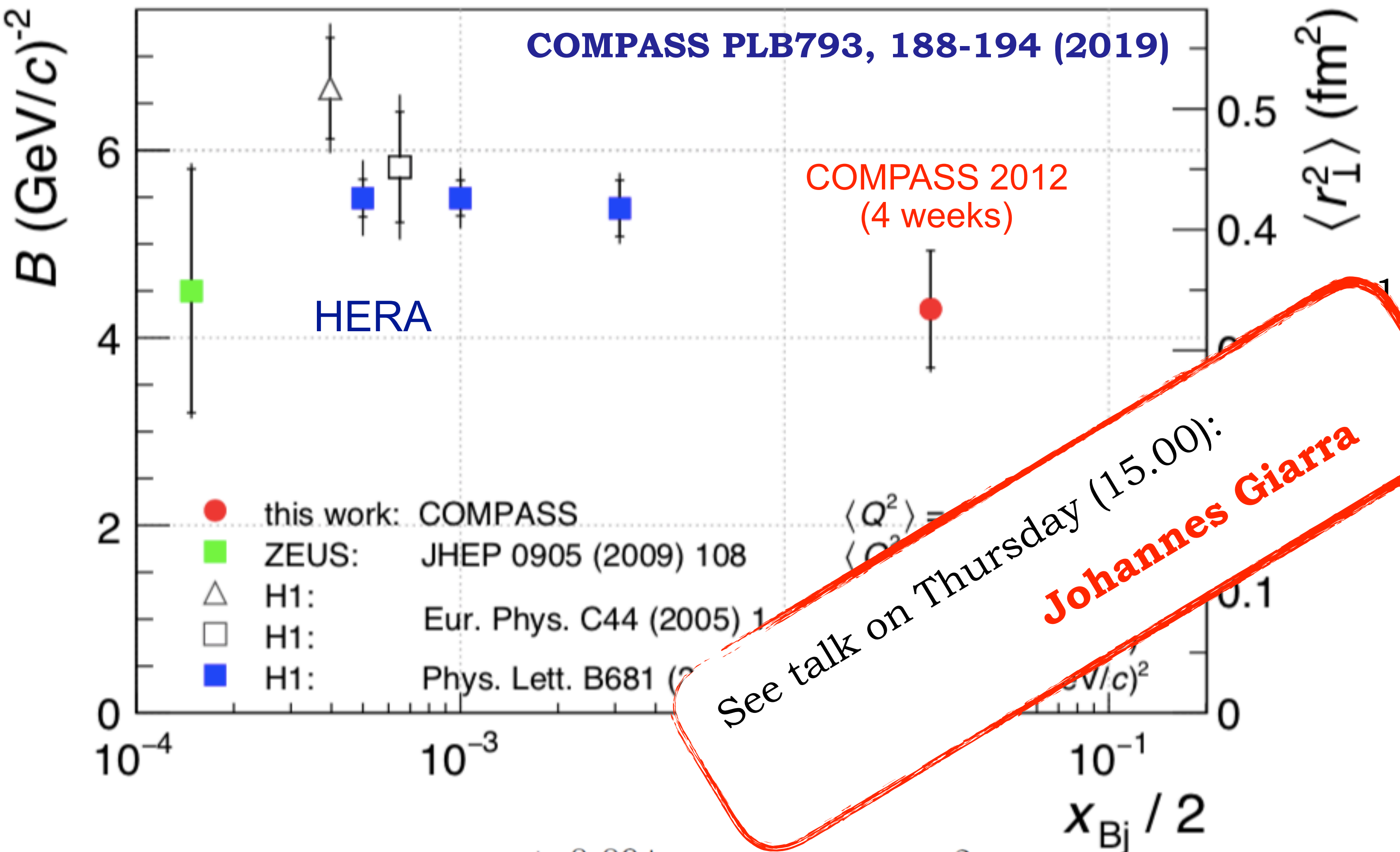

1 < Q^2 < 5 GeV^2

<Q^2> = 1.8 GeV^2

<x_B> = 0.056

Integrated luminosity: 42.4 pb^{-1}

10 times more stats in 2016-17 runs

$$B = (4.31 \pm 0.62_{\text{stat}} \,{}^{+\,0.09}_{-\,0.25}\big|_{\text{sys}})\,(\text{GeV}/c)^{-2}$$

$$\sqrt{\langle r_\perp^2 \rangle} = (0.58 \pm 0.04_{\text{stat}} \,{}^{+\,0.01}_{-\,0.02}\big|_{\text{sys}} \pm 0.04_{\text{model}})\,\text{fm}$$

at average x_B = *0.056*

$$\langle r_\perp^2(x_B)\rangle \approx 2B(x_B)$$

for small x_B

Hard Exclusive Meson Production

Hard Exclusive Meson Production

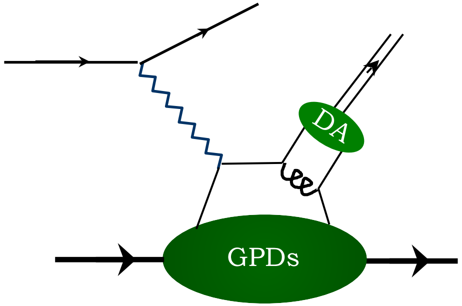

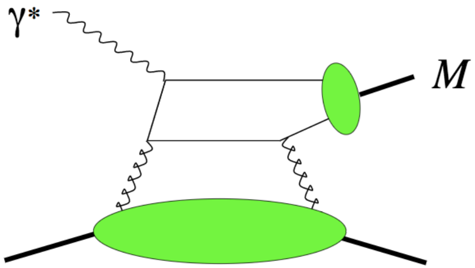

- Amplitude depends on convolution of GPDs and meson Distribution Amplitudes (DA).
- At leading order & twist, access to the four chiral-even (parton helicity-conserving) GPDs:
  - Pseudo-scalar mesons: $\tilde{H}^q, \tilde{E}^q(x, \xi, t)$
  - Vector mesons: $H^q, E^q, H^g, E^g(x, \xi, t)$

Gluon GPDs!

HEMP enables flavour decomposition of quark GPDs and gives access to gluon GPDs

Caveats:

- factorisation established only for longitudinal photons,
- factorisation sets in at a higher scale than in DVCS,
- DA not entirely understood

Extracting GPDs from HEMP is hard!

Transversity GPDs

- Predictions based solely on chiral-even GPDs ($\widetilde{H}$, $\widetilde{E}$ — longitudinal (L) photon polarisation) under-estimated pion-production cross-sections from JLab and HERMES by order of magnitude: significant transverse (T) photon polarisation at play!

- For pseudo-scalar mesons, access four chiral-odd (parton helicity-flipping) transversity GPDs (via convolutions of leading-twist GPDs with twist-3 meson DA):

$$E_T^q, \tilde{E}_T^q, H_T^q, \tilde{H}_T^q(x, \xi, t)$$

Appear in DVMP amplitude when virtual photon has transverse polarisation — not accessible at LT in DVCS.

- $\tilde{E}_T$ can be related to the transverse anomalous magnetic moment:

$$\kappa_T = \int_{-1}^{+1} \tilde{E}_T(x, \xi, t=0)\, dx$$

- and H_T to the transversity distribution: $H_T(x, 0, 0) = h_1(x)$

which describes distribution of transverse partons in a transverse nucleon

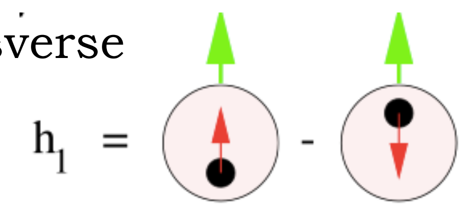

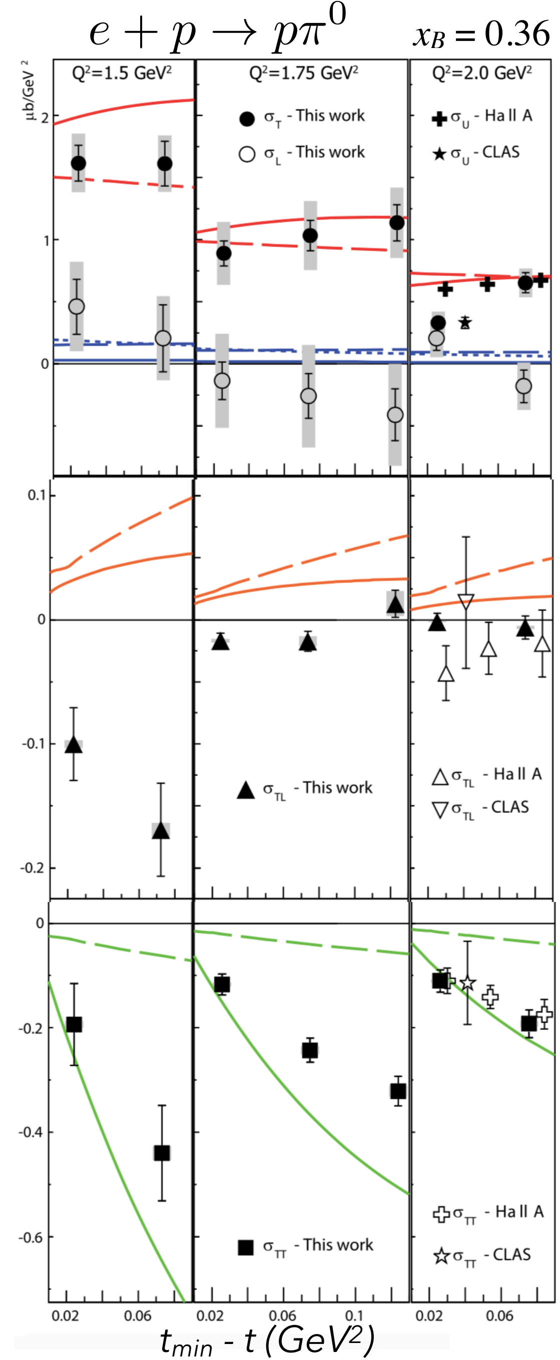

Pseudo-scalar meson production

- Separation of L/T contributions to cross-sections through Rosenbluth-like techniques / simultaneous fits at different kinematics.

- Strong transverse contribution observed in charged and neutral pion / K⁺ cross-sections: possible access to transversity GPDs.

- Attempt at GPD flavour-separation using π^0 and η BSA:

$$H_T^{\pi^0} = \left(e_u H_T^u - e_d H_T^d\right)/\sqrt{2}, \qquad H_T^{\eta} = \left(e_u H_T^u + e_d H_T^d\right)/\sqrt{6},$$

- Measurements at JLab @11 GeV: E12-07-105, E12-06-108, E12-13-010, E12-09-011

  π^0 η K in Halls A, B and C.

- π^0 at COMPASS.

—— Goloskokov Kroll (EPJ A47, 112 (2011))

- - - Goldstein, Hernandez, Liuti (PRD 84, 034007 (2011))

M. Defurne *et al*, ***PRL* 117** (2016) 262001

Vector meson production

- L/T contributions to cross-sections separated by using helicity conservation between virtual photon and meson: strong deviations from leading-twist GPD formalism (higher-twist? evolution effects? meson-size corrections?)

- Gluonic GPD H^g dominates at small x: gluonic radius.

→ GPD extraction much cleaner for heavier quarks: J/Ψ

Too close to threshold @ JLab12, but ideal for the Electron-Ion Collider (finite meson size contributions become negligible)!

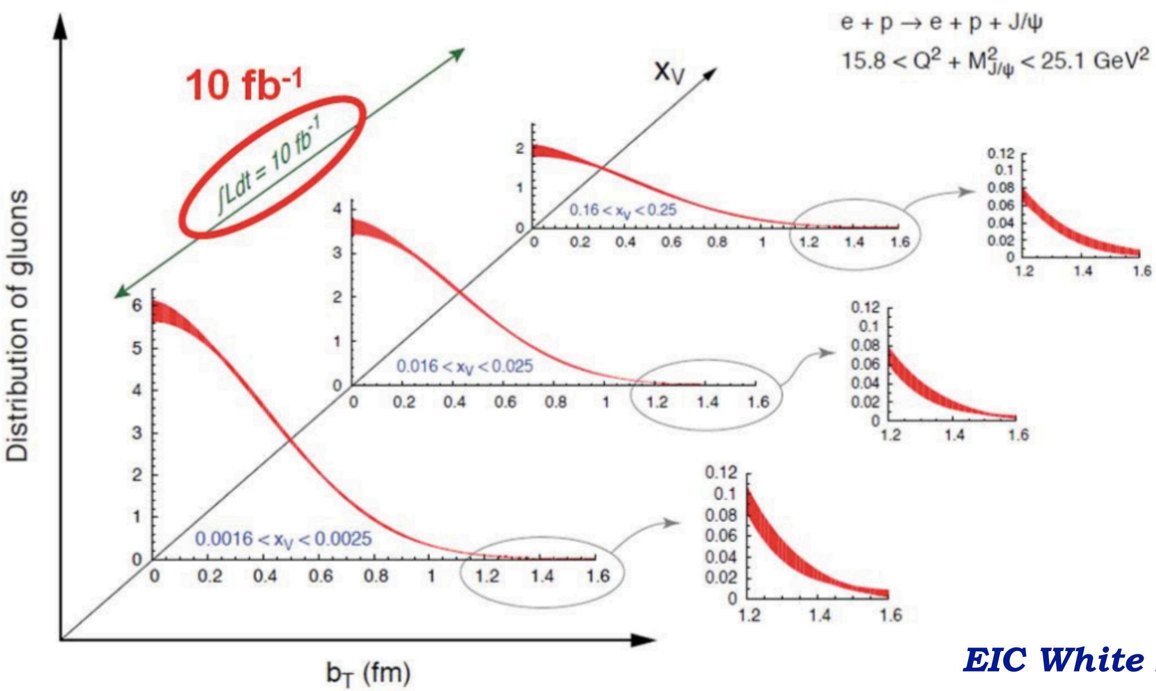

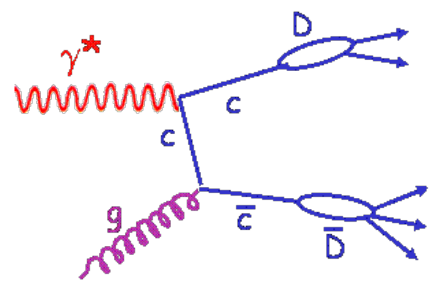

Gluon momentum fraction related to:

$$x_V = x_B(1 + M^2_{J/\Psi}/Q^2)$$

EIC White Paper, *Eur. Phy. J. A 52, 9 (2016)*

Summary

- Generalised Parton Distributions are accessible in a number of exclusive processes, of which Deeply Virtual Compton scattering is the cleanest probe.

- Experimental programme started with HERMES, JLab and COMPASS: constraints on $\mathbf{H_p}$, a little on $\mathbf{\tilde{H}_p}$, $\mathbf{E_n}$ Compton Form Factors.

- Hints of the effects of glue in the valence region.

- Sensitivity to transversity GPDs in pseudo-scalar meson production.

- Vector mesons: GPD interpretation tricky, strong deviations from leading-twist formalism.

- Full imaging of the nucleon from the valence to the quark-gluon sea has to await the Electron Ion Collider.

Stay tuned!

Thank you!

Back-up

Meson production at JLab 12 GeV

Cross-sections and spin asymmetries in the 11 GeV kinematics:

- Hard exclusive electroproduction of η and π^0 (E12-06-108, CLAS12)
- Exclusive ϕ meson electroproduction (E12-12-007, CLAS12)
- DVCS and neutral pion cross-sections (E12-13-010, Hall C)
- Scaling study of the L-T separated pion electroproduction cross-section (E12-07-105, Hall C)
- Studies of the L-T separated kaon electroproduction cross-section from 5-11 GeV (E12-09-011, Hall C)
- Near-threshold electroproduction of J/Ψ (E12-12-006, Hall A)
- Time-like Compton scattering and J/Ψ electroproduction (E12-12-001, CLAS12). *Analysis under-way!*

Meson production at COMPASS

Unpolarised target:

$e\,p \rightarrow e\,\pi^0\,p$

$$\frac{d^2\sigma}{dt\,d\phi_\pi} = \frac{1}{2\pi}\left[\left(\frac{d\sigma_T}{dt} + \epsilon\frac{d\sigma_L}{dt}\right) + \epsilon\cos 2\phi_\pi \frac{d\sigma_{TT}}{dt} + \sqrt{2\epsilon(1+\epsilon)}\cos\phi_\pi \frac{d\sigma_{LT}}{dt}\right]$$

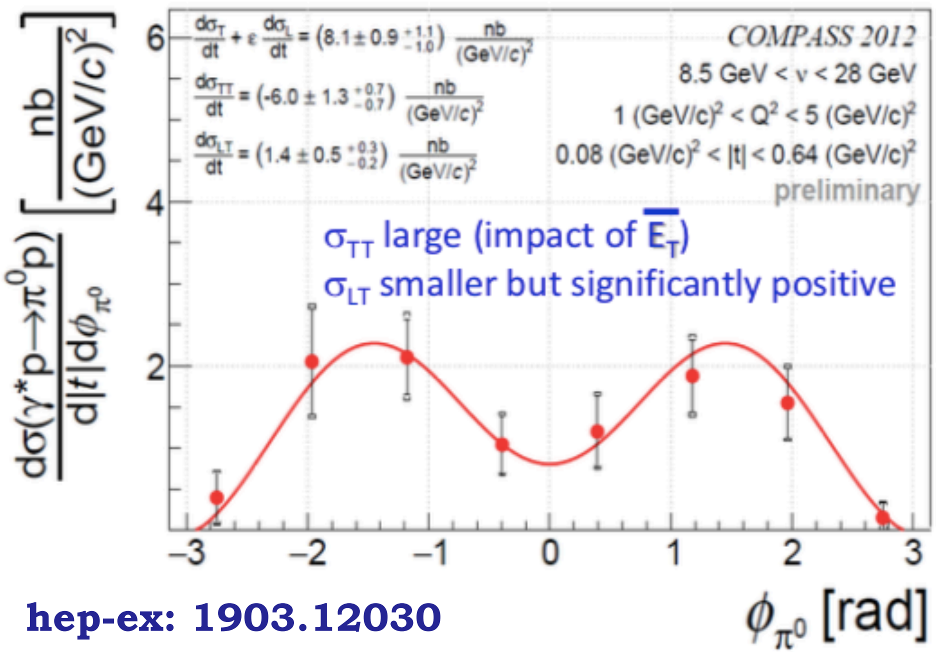

A dip at small t would indicate a large impact of $\overline{E}_T$

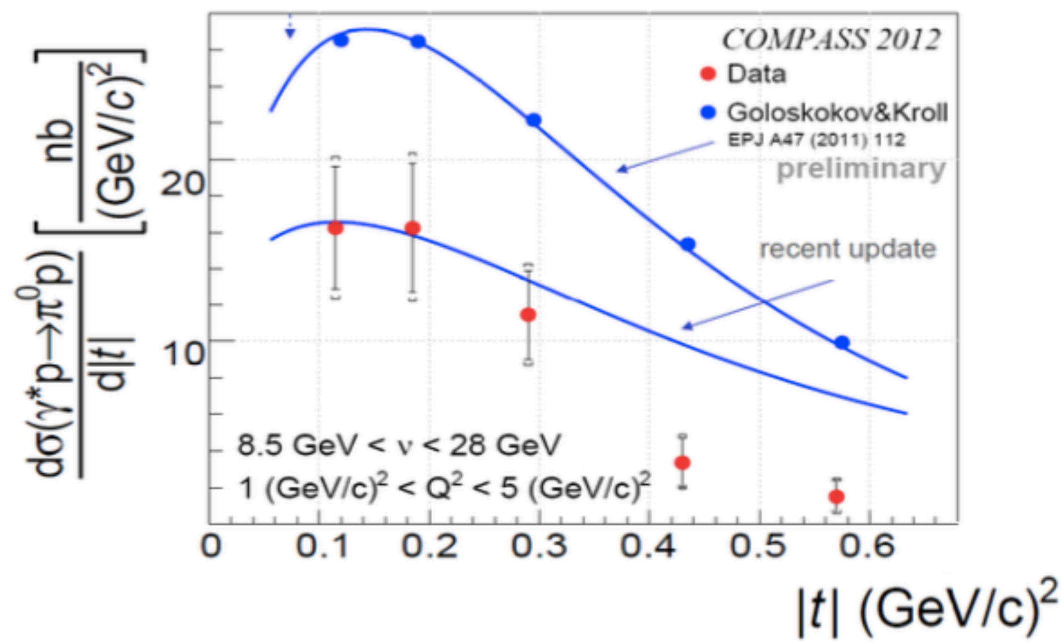

hep-ex: 1903.12030

Transversely-polarised target: ρ^0 and ω

Sensitivity to $\mathbf{H_T}$

NPB865, 1-20 (2012)
PLB731, 19 (2014)
NPB915, 454-475 (2017)

Slide from Po-Ju Lin, IWHSS 2019

Summary

JLab 6 GeV programme:

* Indications of higher-twist or higher-orders at play in DVCS: hint of gluons?
* Constraints for GPD models: most info on *Re* and *Im* parts of $\mathbf{H_p}$ CFF, a little on $\mathbf{\tilde{H}_p}$, $\mathbf{E_n}$.
* First attempt at tomography with the limited data.
* DVCS on a bound protons and a nuclear target (helium).
* Significant contributions from transverse photon polarisation: possible access to transversity GPDs in pseudo-scalar meson production.
* Vector mesons: GPD interpretation tricky, strong deviations from leading-twist formalism.

JLab 12 GeV programme:

* High precision — separation of DVCS and interference terms: sensitivity to higher twist / higher orders, gluons.
* Extensive mapping of a wider kinematic region — strides towards tomography.
* Extraction of *Re* and *Im* parts of **H** CFF, $\mathbf{\tilde{H}}$, **E**, flavour-separation: *u*/*d*.
* Access to transversity GPDs.
* Many more channels to be measured: meson-production, time-like Compton scattering, double DVCS, photon-meson-pair production: significant constraints on GPDs in the valence region.

Stay tuned!

HEMP Cross-section

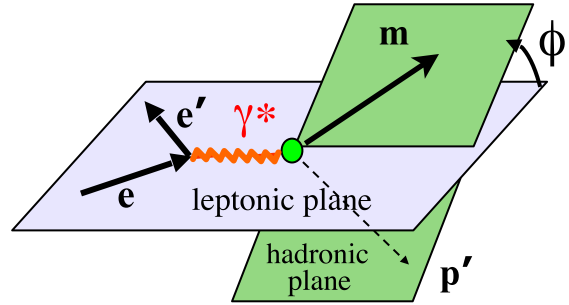

Virtual photon flux

unpolarised

$$\frac{2\pi}{\Gamma}\frac{d^4\sigma}{dQ^2\,dx_B\,dt\,d\phi_{meson}} = \sigma_T + \epsilon\sigma_L + \epsilon\sigma_{TT}\cos 2\phi + \sqrt{\epsilon(1+\epsilon)}\sigma_{LT}\cos\phi$$

polarised beam → $+P_b\sqrt{\epsilon(1-\epsilon)}\sigma_{LT'}\sin\phi$

longitudinally polarised target → $+P_{tg}\left(\sqrt{\epsilon(1+\epsilon)}\sigma_{UL}^{\sin\phi}\sin\phi + \epsilon\sigma_{UL}^{\sin 2\phi}\sin 2\phi\right)$

Target and beam longitudinally polarised → $+P_bP_{tg}\left(\sqrt{1-\epsilon^2}\sigma_{LL} + \sqrt{\epsilon(1-\epsilon)}\sigma_{LL}^{\cos\phi}\cos\phi\right)$

ϵ: ratio of the fluxes of longitudinally (L) and transversely (T) polarised virtual photons.

σ_i: structure functions, related to scattering amplitudes (i = L, T, LT, ...), *eg:*

$$\frac{d\sigma_L}{dt} = \frac{4\pi\alpha}{k'}\frac{1}{Q^6}\left\{(1-\xi^2)|\langle\tilde{H}\rangle|^2 - 2\xi^2\mathrm{Re}[\langle\tilde{H}\rangle^*\langle\tilde{E}\rangle] - \frac{t'}{4m^2}\xi^2|\langle\tilde{E}\rangle|^2\right\}$$

where $\langle F\rangle \equiv \sum_\lambda \int_{-1}^{1} dx\,\mathcal{H}_{\mu'\lambda'\mu\lambda}F$

hard-scattering kernel

GPD

Transversity GPDs

- For pseudo-scalar mesons, access four chiral-odd (parton helicity-flipping) transversity GPDs (via convolutions of leading-twist GPDs with twist-3 meson DA): $E_T^q, \tilde{E}_T^q, H_T^q, \tilde{H}_T^q(x,\xi,t)$

  Appear in DVMP amplitude when virtual photon has transverse polarisation — not accessible at LT in DVCS.

- $\tilde{E}_T$ can be related to the transverse anomalous magnetic moment:

$$\kappa_T = \int_{-1}^{+1} \tilde{E}_T(x,\xi,t=0)\,dx$$

- and H_T to the transversity distribution: $H_T(x,0,0) = h_1(x)$

  which describes distribution of transverse partons in a transverse nucleon

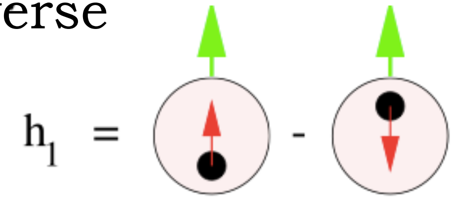

- The combination $\bar{E}_T = 2\tilde{H}_T + E_T$ is related to spatial density of transversely polarised quarks in an unpolarised nucleon.

DVCS at lower energies with CLAS12

Projected extraction of CFFs (red) compared to generated values (green). Three curves on the *Re(H)* show three different scenarios for the D-term.

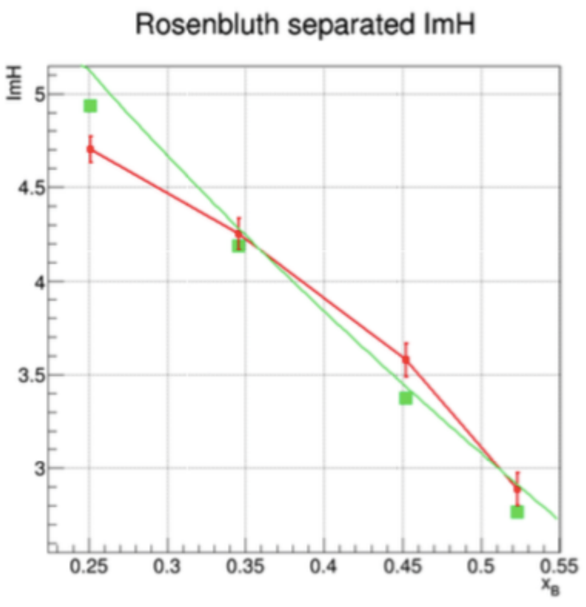

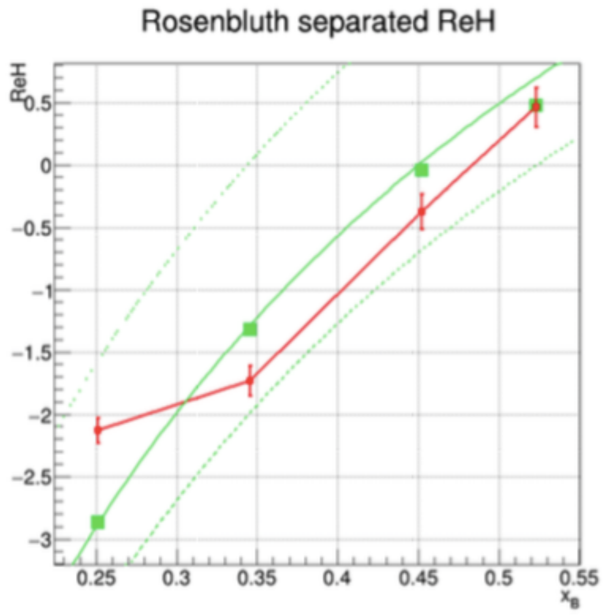

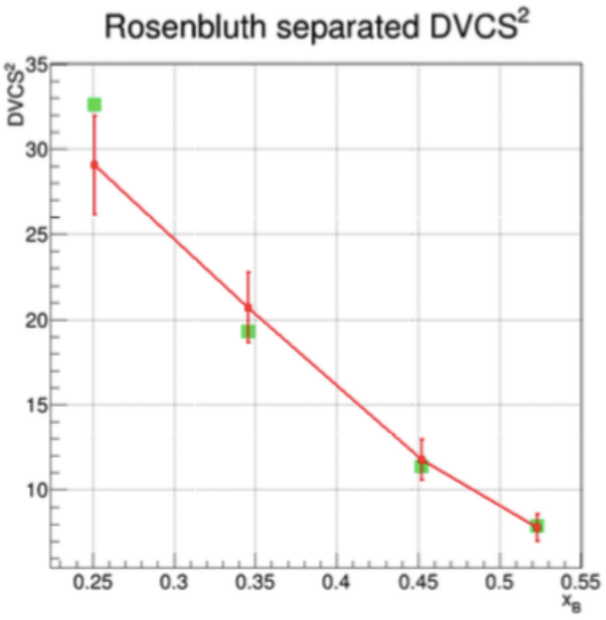

F.-X. Girod et al.

An abridged history of nucleon structure

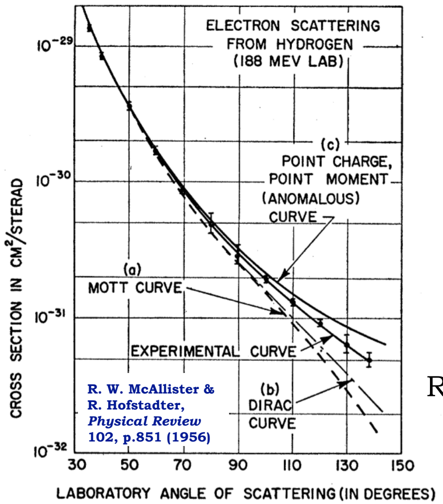

Robert Hofstadter
1915 - 1990
(Wikipedia)

1956: Elastic scattering at Stanford: the proton has internal structure! *Hofstadter: Nobel Prize 1961.*

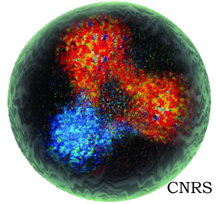

1960s: the Quark Model. Nucleons are composed of three valence quarks! *Gell-Mann (Nobel Prize 1969), Zweig.*

1968: Deep Inelastic scattering at SLAC: scaling observed. The proton consists of point-like charges: partons! *Friedman, Kendall, Taylor: Nobel Prize 1990*

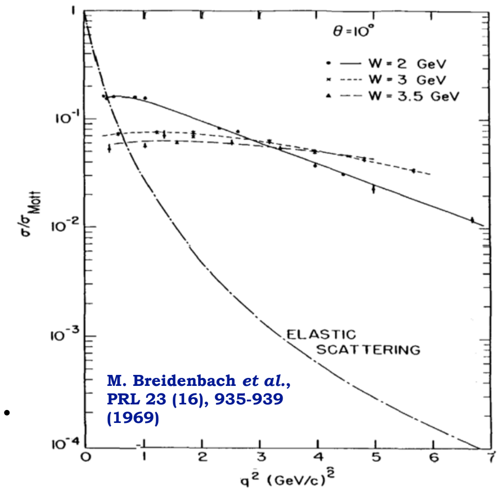

1972: Theory of QCD developed.

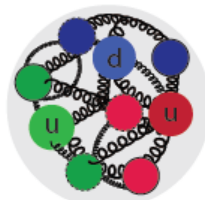

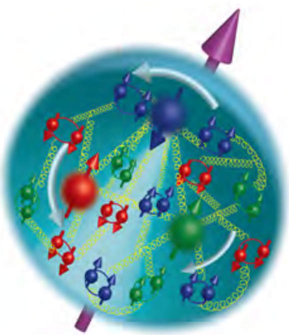

1970s-1990s: Deep Inelastic Scattering reveals a rich structure: quark-gluon sea, flavour distributions, puzzles of spin and mass… what you see depends on how closely you look!

21st Century: High-precision imaging of quarks and gluons. 3D tomography of the nucleon: spatial and momentum distributions inside it, mechanical properties of the nucleon, …

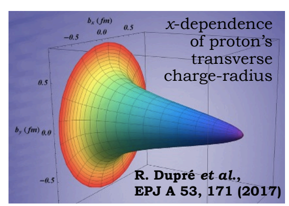

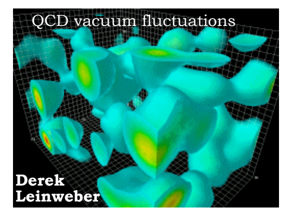

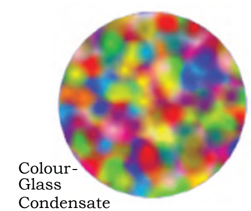

Nucleon at different scales

Valence quarks

Jefferson Lab: fixed-target electron scattering

$0.1 < x_B < 0.7$

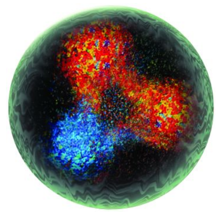

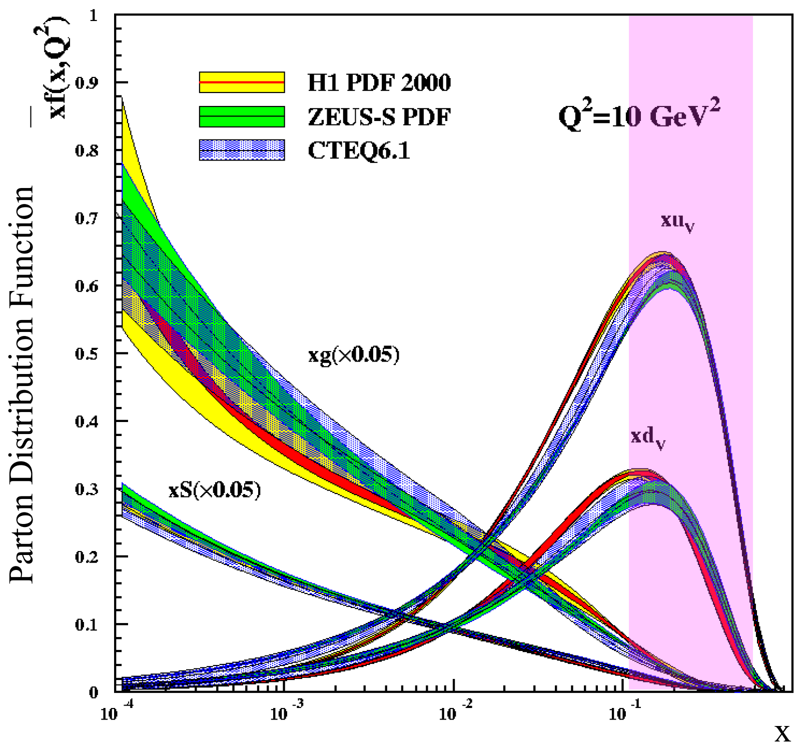

Nucleon at different scales

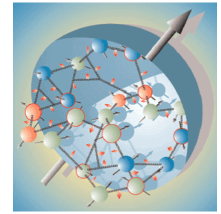

Valence quarks

Jefferson Lab: fixed-target electron scattering

$0.1 < x_B < 0.7$

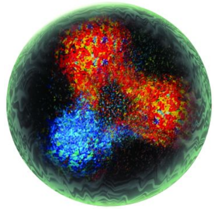

Sea quarks

HERMES: fixed gas-target electron/positron scattering

$0.02 < x_B < 0.3$

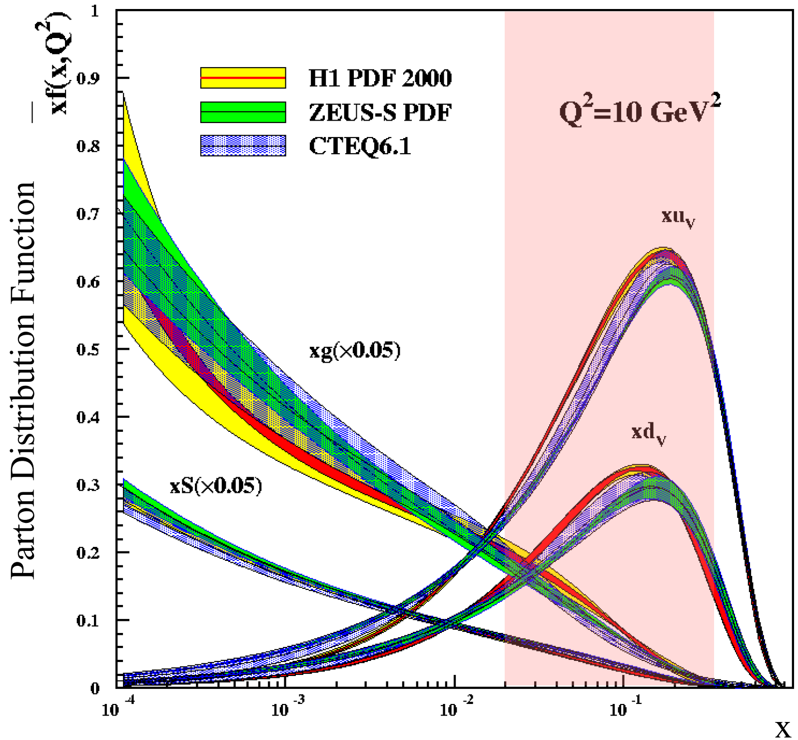

Nucleon at different scales

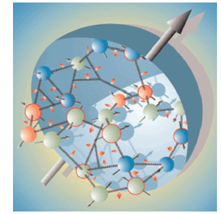

Valence quarks

Jefferson Lab: fixed-target electron scattering

$0.1 < x_B < 0.7$

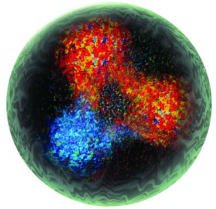

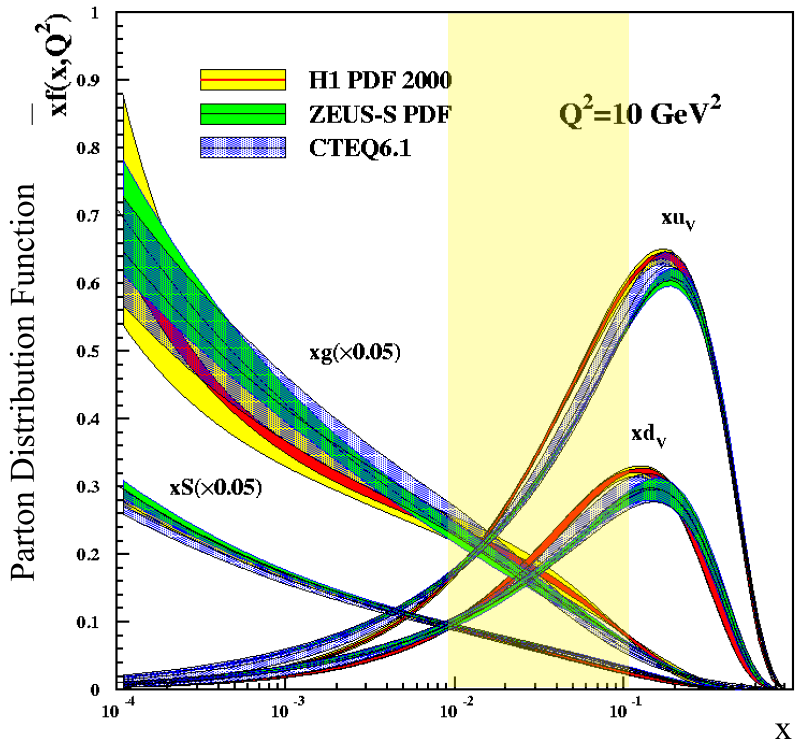

Sea quarks

HERMES: fixed gas-target electron/positron scattering

$0.02 < x_B < 0.3$

COMPASS: fixed-target muon scattering

$0.01 < x_B < 0.1$

Nucleon at different scales

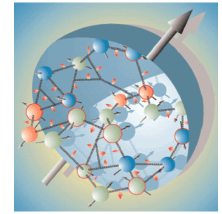

Valence quarks

Jefferson Lab: fixed-target electron scattering

$0.1 < x_B < 0.7$

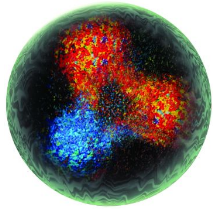

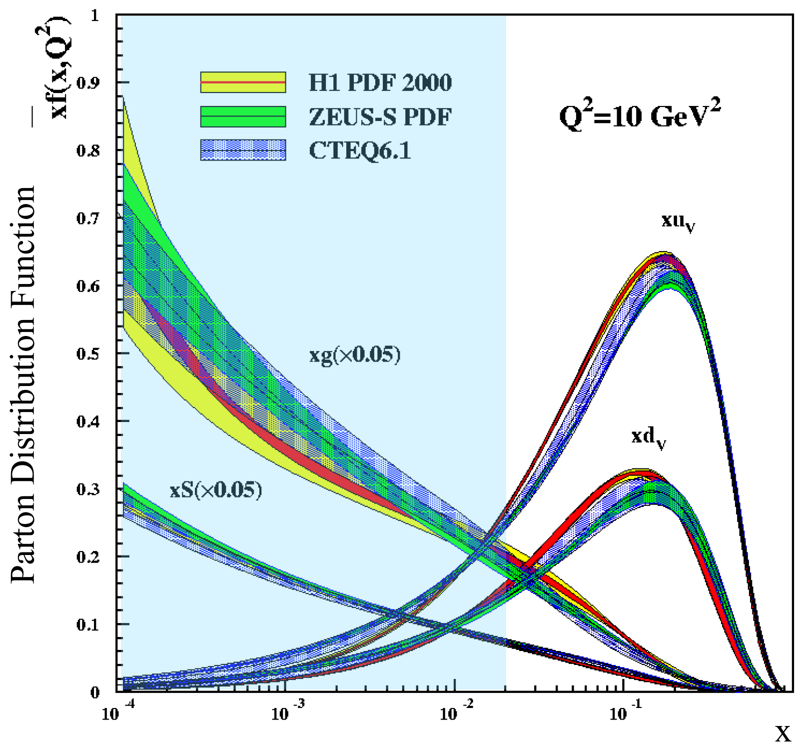

Sea quarks

HERMES: fixed gas-target electron/positron scattering

$0.02 < x_B < 0.3$

COMPASS: fixed-target muon scattering

$0.01 < x_B < 0.1$

The glue

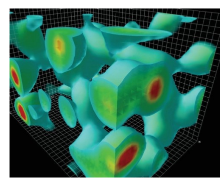

Derek Leinweber

ZEUS/H1: electron/ positron-proton collider

$10^{-4} < x_B < 0.02$

Nucleon at different scales

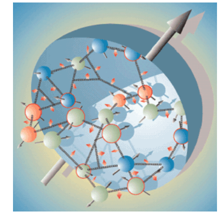

Valence quarks

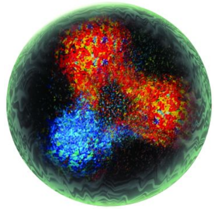

Jefferson Lab: fixed-target electron scattering

$0.1 < x_B < 0.7$

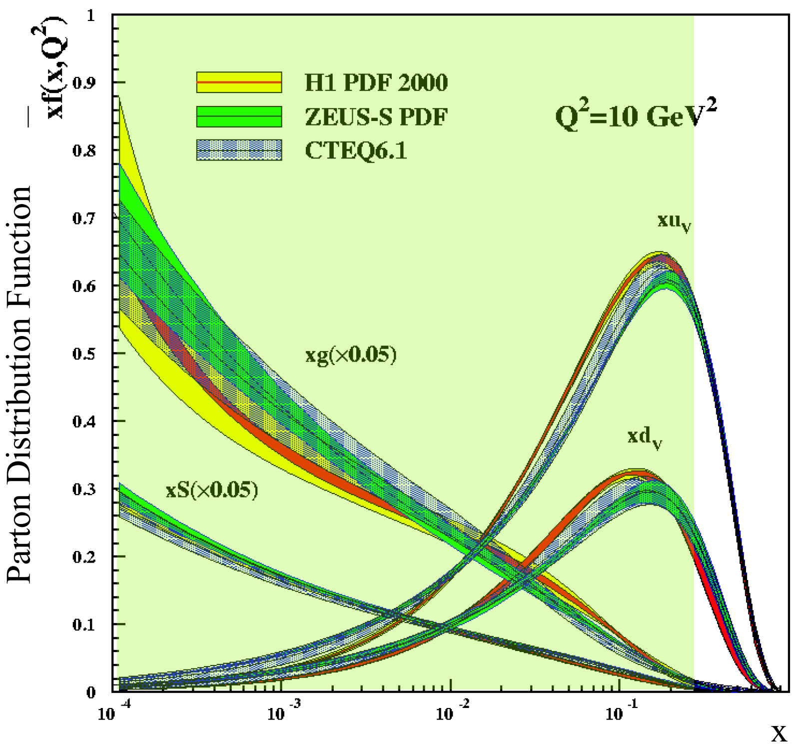

Sea quarks

HERMES: fixed gas-target electron/positron scattering

$0.02 < x_B < 0.3$

COMPASS: fixed-target muon scattering

$0.01 < x_B < 0.1$

The glue

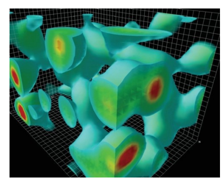

Derek Leinweber

ZEUS/H1: electron/ positron-proton collider

$10^{-4} < x_B < 0.02$

Electron-ion collider: $10^{-4} < x_B < 10^{-1}$

Luminosity 100 - 1000 times that of HERA

Kinematic landscape

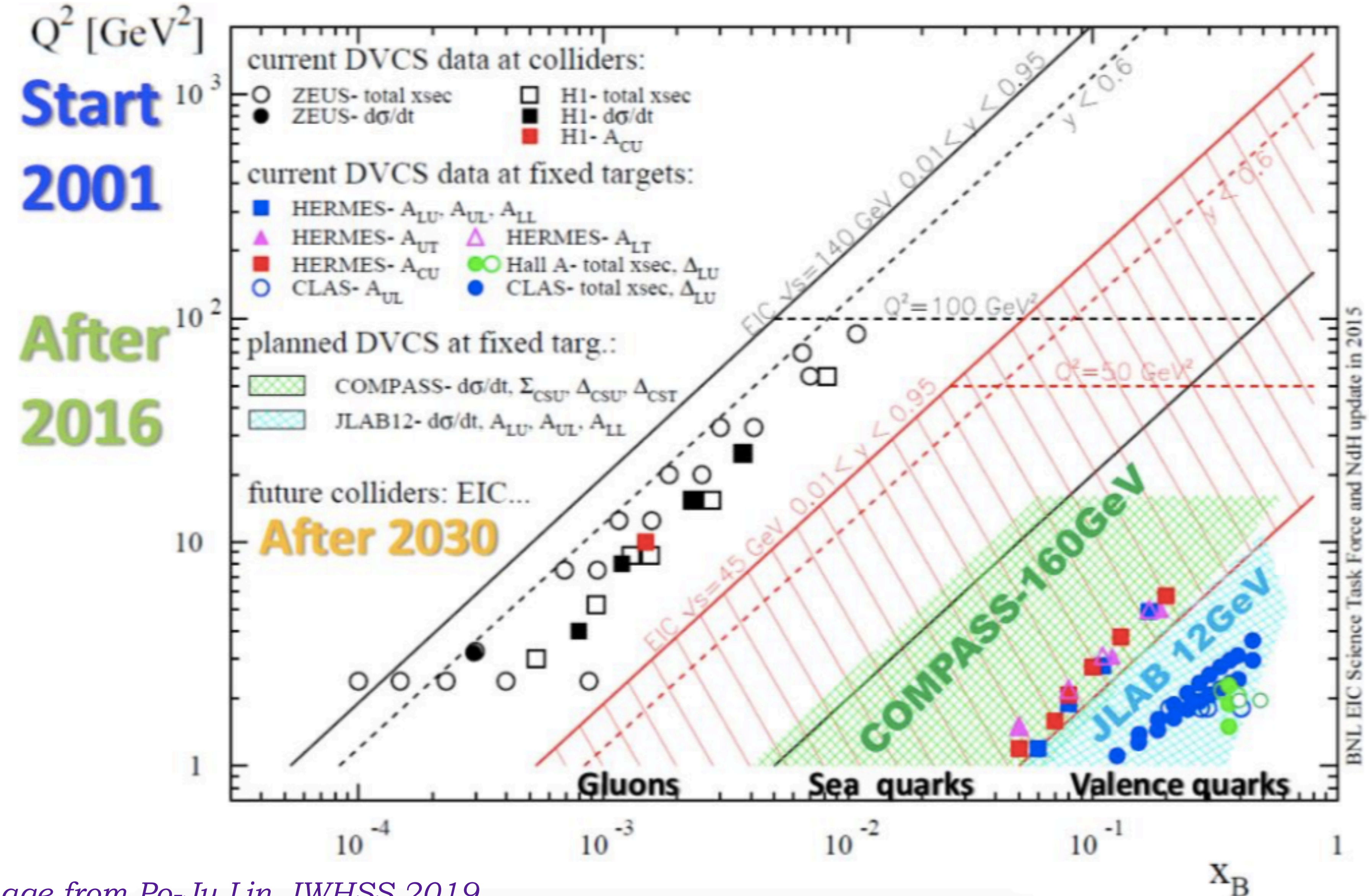

Image from Po-Ju Lin, IWHSS 2019

DVCS in Hall A

Detect electron in the Left High Resolution Spectrometer (HRS-L): 0.01% momentum resolution

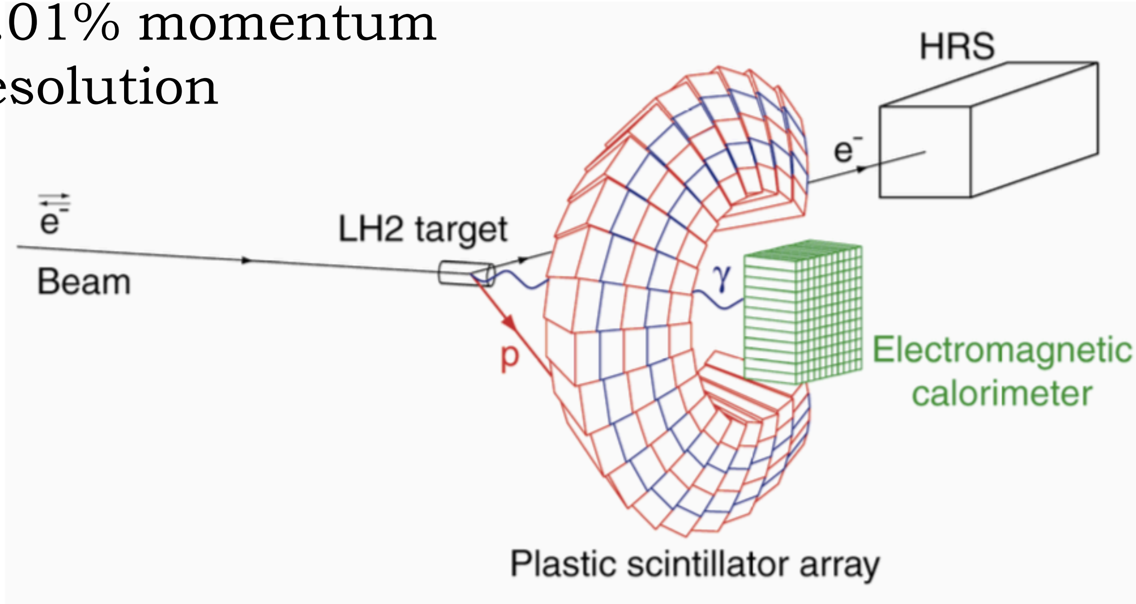

Detect photon in PbF_2 calorimeter: < 3% energy resolution

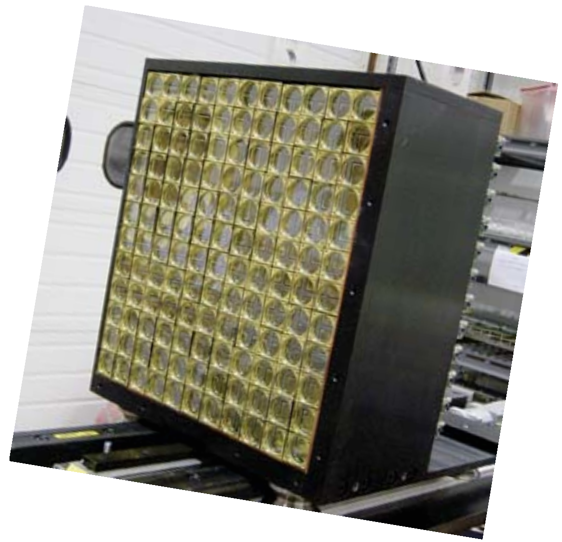

Plastic scintillator array built for proton detection, but not used in most recent measurements / re-analyses.

First DVCS cross-sections in valence region

Hall A

- E00-110: Hall A, ran in 2004, high precision, narrow kinematic range.

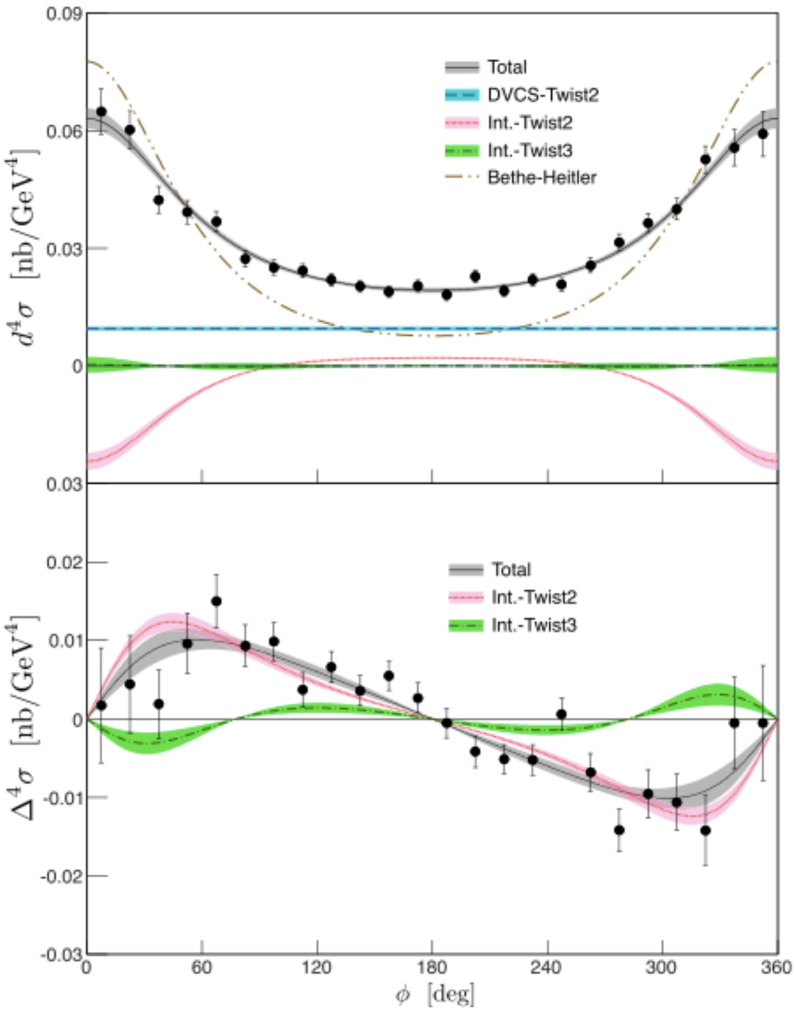

$x_B = 0.36, Q^2 = 2.3\ GeV^2, -t = 0.32\ GeV^2$

- Luminosity $=10^{37}$ cm^{-2}s^{-1}.
- Measure Q^2-dependence (Q^2: 1.5, 1.9, 2.3 GeV^2) of DVCS-BH cross-sections at fixed x_B (0.36).
- Also x_B dependence at constant Q^2.
- CFFs show scaling in DVCS: leading twist (twist-2) dominance at this moderate Q^2.

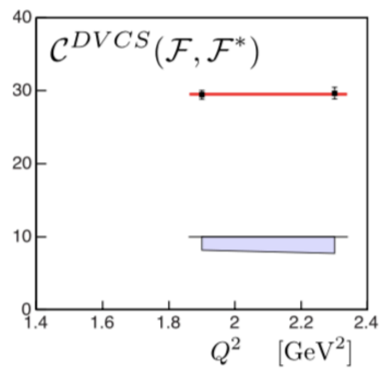

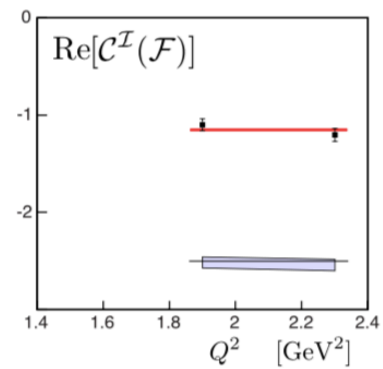

M. Defurne *et al*, ***PRC* 92** (2015) 055202.

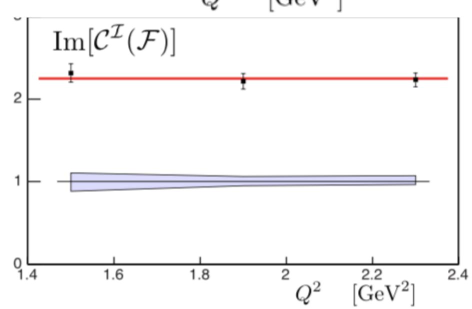

- Strong deviation of unpolarised DVCS cross-section from BH: extraction of $|T_{DVCS}|^2$ amplitude as well as interference terms.

First DVCS cross-sections in valence region

Hall A

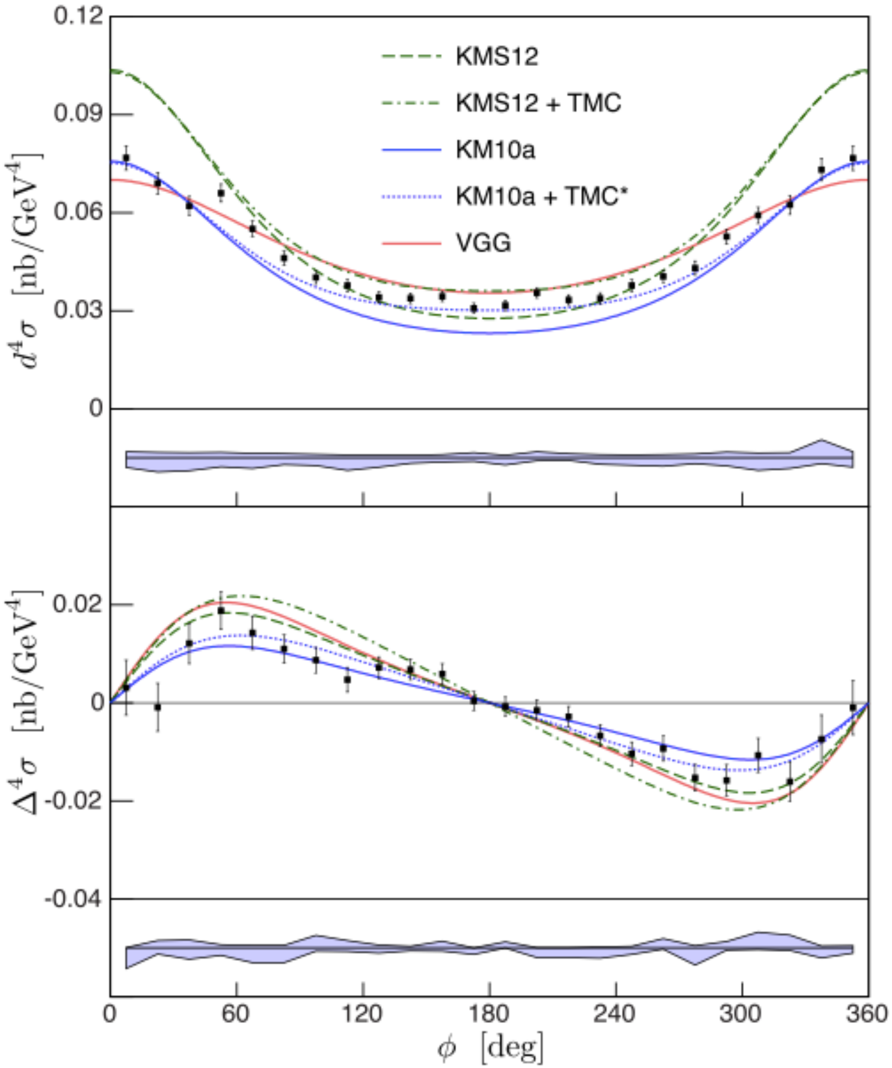

$x_B = 0.36, Q^2 = 1.9\ GeV^2, -t = 0.32\ GeV^2$

- High precision of the data: sensitivity to subtle differences in model predictions.

VGG model: Vanderhaeghen, Guichon, Guidal

KMS model: Kroll, Moutarde, Sabatié

KM model: Kumericki, Mueller

TMC: kinematic twist-4 target-mass and finite-t corrections, calculated for proton DVCS and estimated for KMS12.

- KMS parameters tuned on very low x_B meson-production data: not adapted to valence quarks.

→ TMC*: TMC extracted from the KMS12 model and applied to KM10a.

- TMC improve agreement for KM10a model, especially at $\phi = 180°$. Higher-twist effects?

The devil is in the detail…

M. Defurne *et al*, ***PRC* 92** (2015) 055202.

Here comes the twist...

- Twist: powers of $\frac{1}{\sqrt{Q^2}}$ in the DVCS amplitude. Leading-twist (LT) is twist-2.
- Order: introduces powers of α_s
- LO requires $Q^2 >> M^2$ (M: target mass)

  Bold assumption for JLab 6 GeV kinematics!

- CFFs can be classified according to real and virtual photon helicity:

$\mathcal{F}_{++}$

helicity of real produced photon

helicity of virtual incoming photon

  - Helicity-conserved CFFs — $\mathcal{F}_{++}$
  - Helicity-flip (transverse) — $\mathcal{F}_{-+}$
  - Longitudinal to transverse flip — $\mathcal{F}_{0+}$

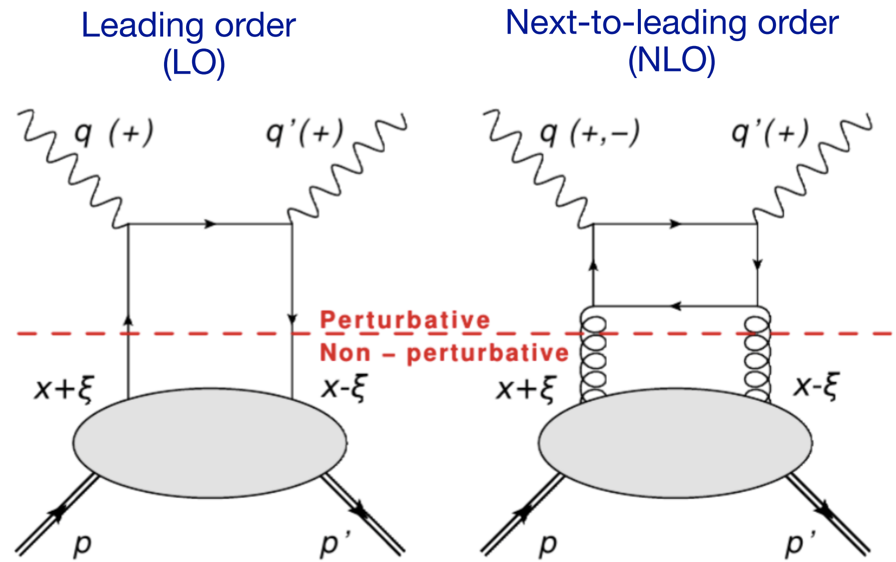

- CFFs contributing to the scattering amplitude:
  - LT in LO: only $\mathcal{F}_{++}$
  - LT in NLO: both $\mathcal{F}_{++}$ and $\mathcal{F}_{-+}$
  - Twist-3: $\mathcal{F}_{0+}$

Here comes the twist…

- At finite Q^2 and non-zero t there's ambiguity in defining the light-cone axis:
  - Traditional GPD phenomenology uses the Belitsky convention, in plane of q and P:
    A. Belitsky *et al*, ***Nucl. Phys. B878*** (2014), 214
  - New, Braun definition using q and q': more natural.
    V. Braun *et al*, ***Phys. Rev. D89*** (2014), 074022

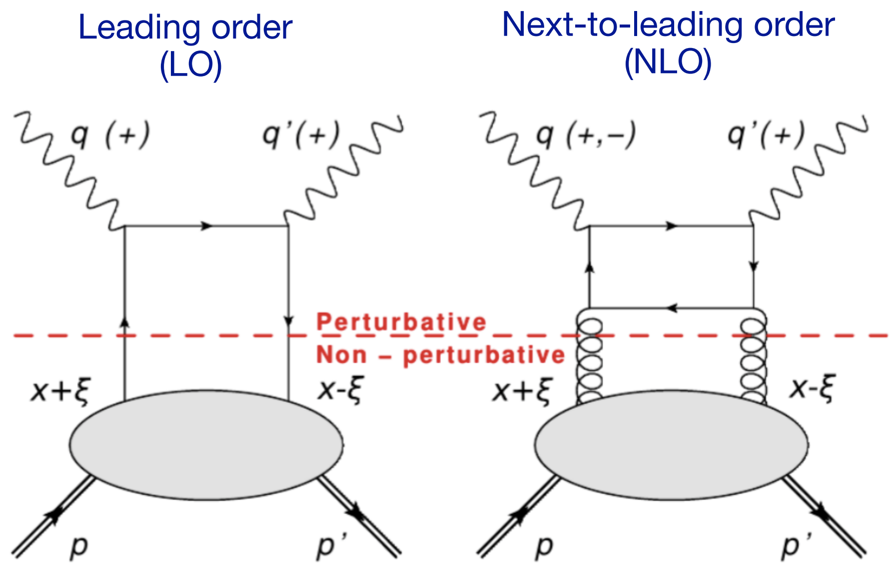

Reformulating CFFs in this frame absorbs most kinematic power corrections (TMC):

$$\mathcal{F}_{++} = \mathbb{F}_{++} + \frac{\chi}{2}\left[\mathbb{F}_{++} + \mathbb{F}_{-+}\right] - \chi_0 \mathbb{F}_{0+}$$
$$\mathcal{F}_{-+} = \mathbb{F}_{-+} + \frac{\chi}{2}\left[\mathbb{F}_{++} + \mathbb{F}_{-+}\right] - \chi_0 \mathbb{F}_{0+}$$
$$\mathcal{F}_{0+} = -(1+\chi)\mathbb{F}_{0+} + \chi_0\left[\mathbb{F}_{++} + \mathbb{F}_{-+}\right]$$

Belitsky CFFs

Braun CFFs

Assuming LO and LT in the Braun frame:

$$\mathcal{F}_{++} = (1 + \tfrac{\chi}{2})\mathbb{F}_{++}$$
$$\mathcal{F}_{-+} = \tfrac{\chi}{2}\mathbb{F}_{++}$$
$$\mathcal{F}_{0+} = \chi_0 \mathbb{F}_{++}$$

HT/HO contributions in the Belitsky frame, scaled by kinematic factors χ and χ_0.

Non-negligible at the Q^2 and x_B of the Hall A cross-section measurement:

$\chi_0 = 0.25,\ \chi = 0.06$ for $Q^2 = 2$ GeV^2, $x_B = 0.36,\ t = -0.24$ GeV^2

M. Defurne *et al*, ***Nature Communications 8*** (2017) 1408

Hints of higher twist or higher orders

- Including either higher order or higher twist effects (HT) improves the match with data:

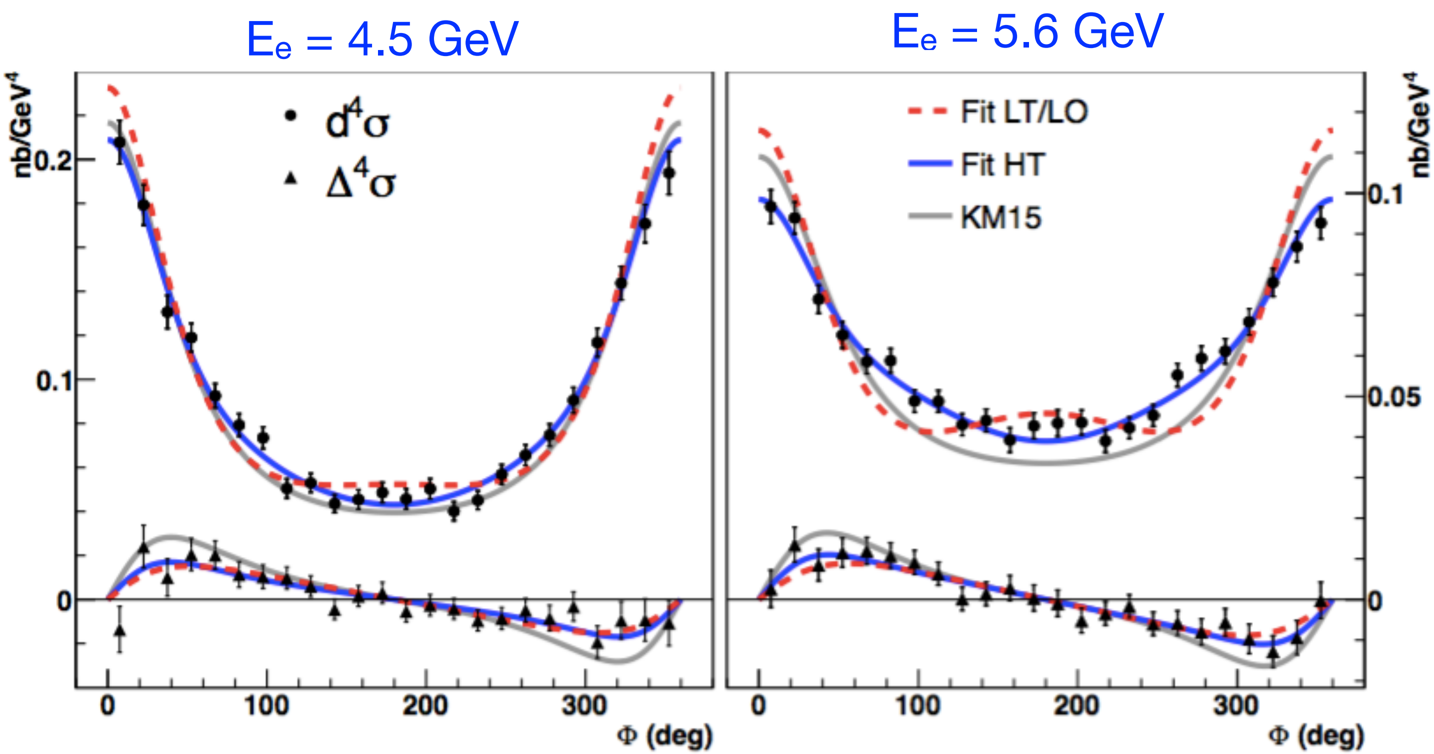

Higher-order and / or higher-twist terms are important! A glimpse of gluons.

Wider range of beam energy needed to identify the dominant effect → **JLab at 11 GeV.**

M. Defurne *et al*, ***Nature Communications* 8** (2017) 1408.

Rosenbluth separation of DVCS² and BH-DVCS terms

Hall A

- Generalised Rosenbluth separation of the DVCS² (scales as E_e^2) and the BH-DVCS interference (scales as E_e^3) terms in the cross-section is possible but NLO and/or higher-twist required: experiment E07-007 @ two beam energies: 4.5 and 5.6 GeV.

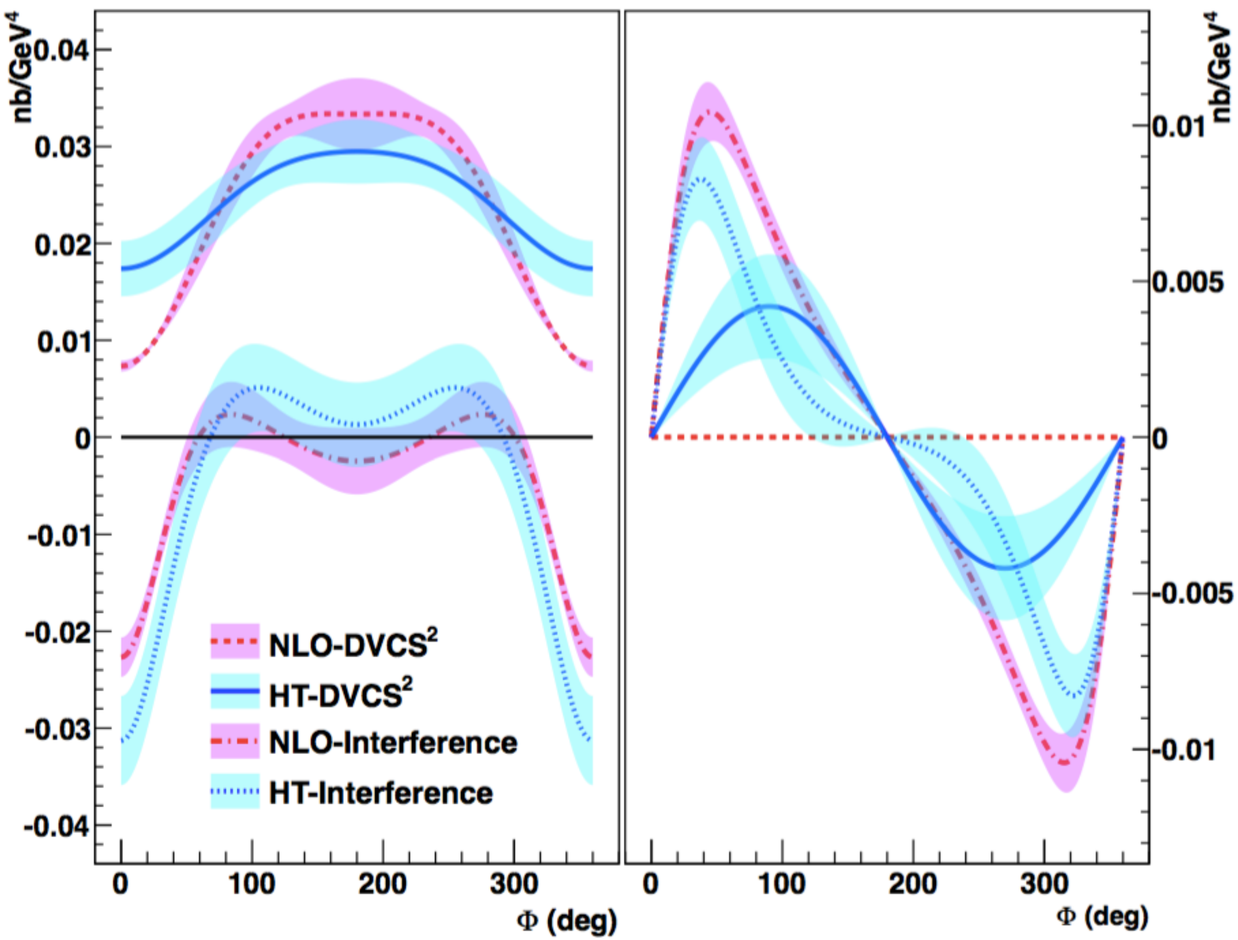

- Significant differences between pure DVCS and interference contributions.
- Helicity-dependent cross-section has a sizeable DVCS² contribution in the higher-twist scenario.
- Separation of HT and NLO effects requires scans across wider ranges of Q^2 and beam energy: JLab12!

M. Defurne *et al*, ***Nature Communications* 8** (2017) 1408.

Large kinematic coverage: CLAS

* Unpolarised DVCS cross-sections and helicity-dependent cross-section differences in a wide kinematic range:

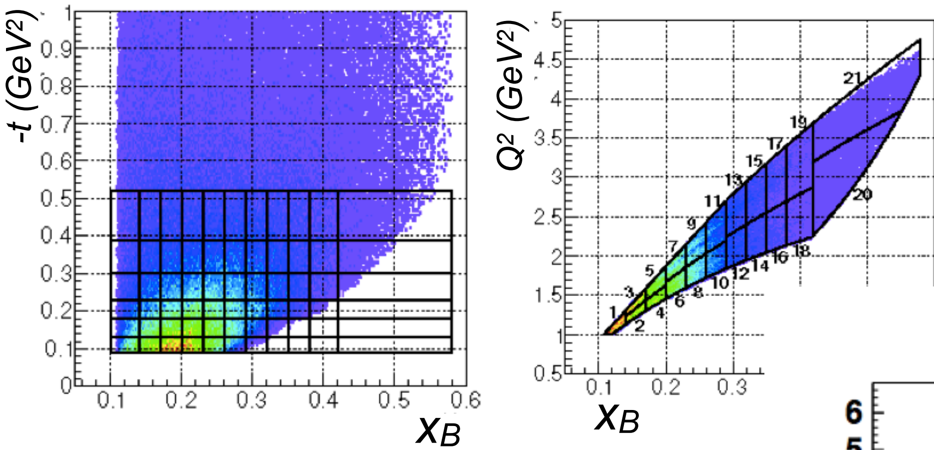

* CFFs extracted in a VGG fit.

$$F_{Im}(\xi, t) = F(\xi, \xi, t) \mp F(-\xi, \xi, t)$$

VGG (Vanderhaeghen, Guichon, Guidal) prediction

Ae^{bt}

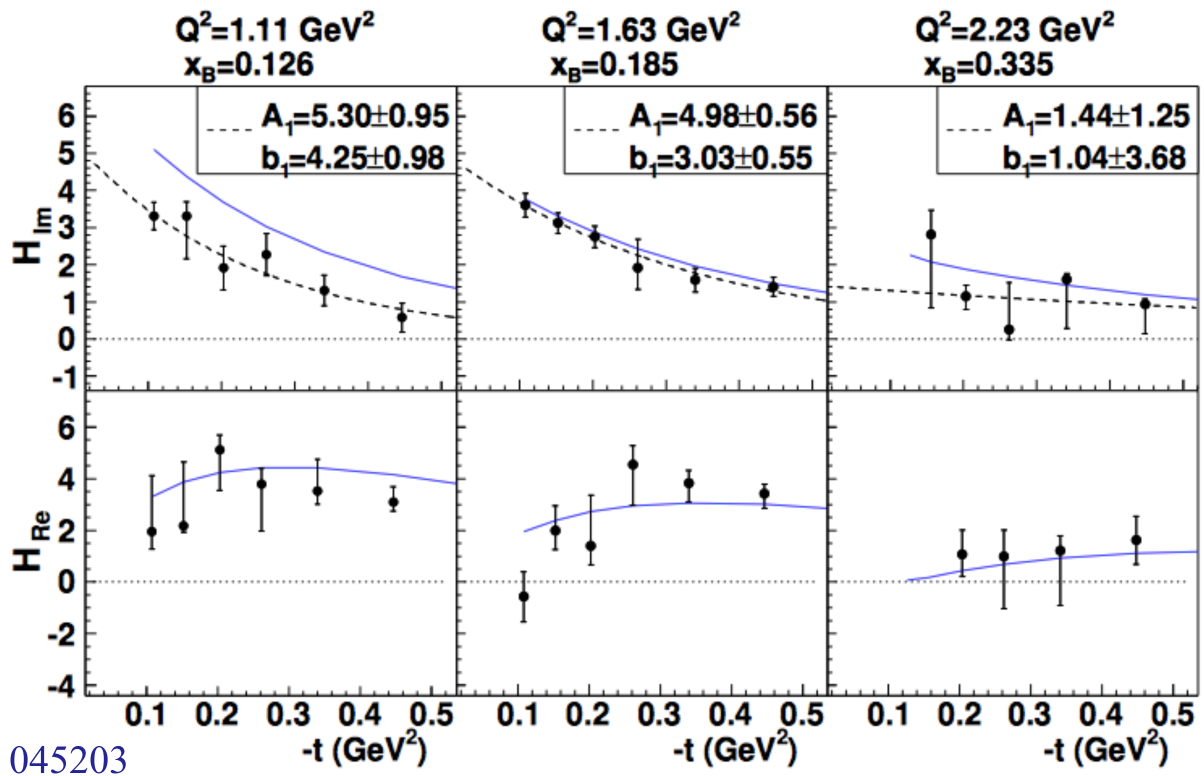

* Dominance of GPD *H* in unpolarised cross-section.

* H_{Im} slope in t becomes flatter at higher x_B

Valence quarks at centre, sea quarks spread out towards the periphery.

H.-S. Jo *et al* (CLAS), ***PRL* 115** (2015) 212003

N. Hirlinger Saylor *et al* (CLAS), ***PRC* 98** (2018) 045203

Which DVCS experiment?

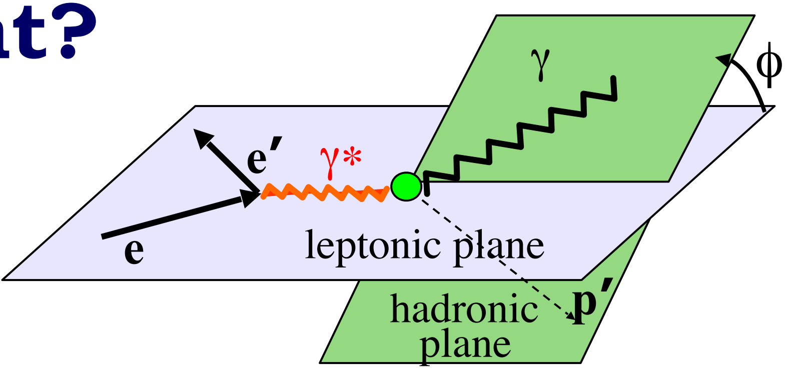

Real parts of CFFs accessible in cross-sections, beam-charge and double polarisation asymmetries,

imaginary parts of CFFs in single-spin asymmetries.

Beam, target polarisation

For example:

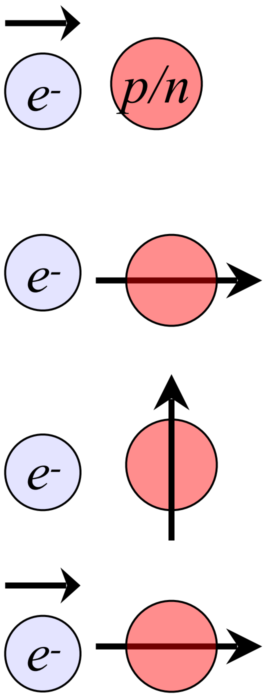

Proton	Neutron

$$\Delta\sigma_{LU} \sim \sin\phi\, \Im(F_1 H + \xi G_M \tilde{H} - \frac{t}{4M^2} F_2 E)\, d\phi$$

$Im\{\boldsymbol{H}_{\mathbf{p}}, \tilde{H}_{\mathrm{p}}, E_{\mathrm{p}}\}$

$Im\{H_{\mathrm{n}}, \tilde{H}_{\mathrm{n}}, \boldsymbol{E}_{\mathbf{n}}\}$

$$\Delta\sigma_{UL} \sim \sin\phi\, \Im(F_1 \tilde{H} + \xi G_M (H + \frac{x_B}{2} E) - \xi \frac{t}{4M^2} F_2 \tilde{E} + \ldots)\, d\phi$$

$Im\{\boldsymbol{H}_{\mathbf{p}}, \tilde{\boldsymbol{H}}_{\mathbf{p}}\}$

$Im\{\boldsymbol{H}_{\mathbf{n}}, E_{\mathrm{n}}, \tilde{E}_{\mathrm{n}}\}$

$$\Delta\sigma_{UT} \sim \cos\phi\, \Im(\frac{t}{4M^2}(F_2 H - F_1 E) + \ldots) d\phi$$

$Im\{\boldsymbol{H}_{\mathbf{p}}, \boldsymbol{E}_{\mathbf{p}}\}$

$Im\{\boldsymbol{H}_{\mathbf{n}}\}$

$$\Delta\sigma_{LL} \sim (A + B\cos\phi)\, \Re(F_1 \tilde{H} + \xi G_M (H + \frac{x_B}{2} E) + \ldots) d\phi$$

$Re\{\boldsymbol{H}_{\mathbf{p}}, \tilde{\boldsymbol{H}}_{\mathbf{p}}\}$

$Re\{\boldsymbol{H}_{\mathbf{n}}, E_{\mathrm{n}}, \tilde{E}_{\mathrm{n}}\}$

Beam-spin Asymmetry (A_{LU})

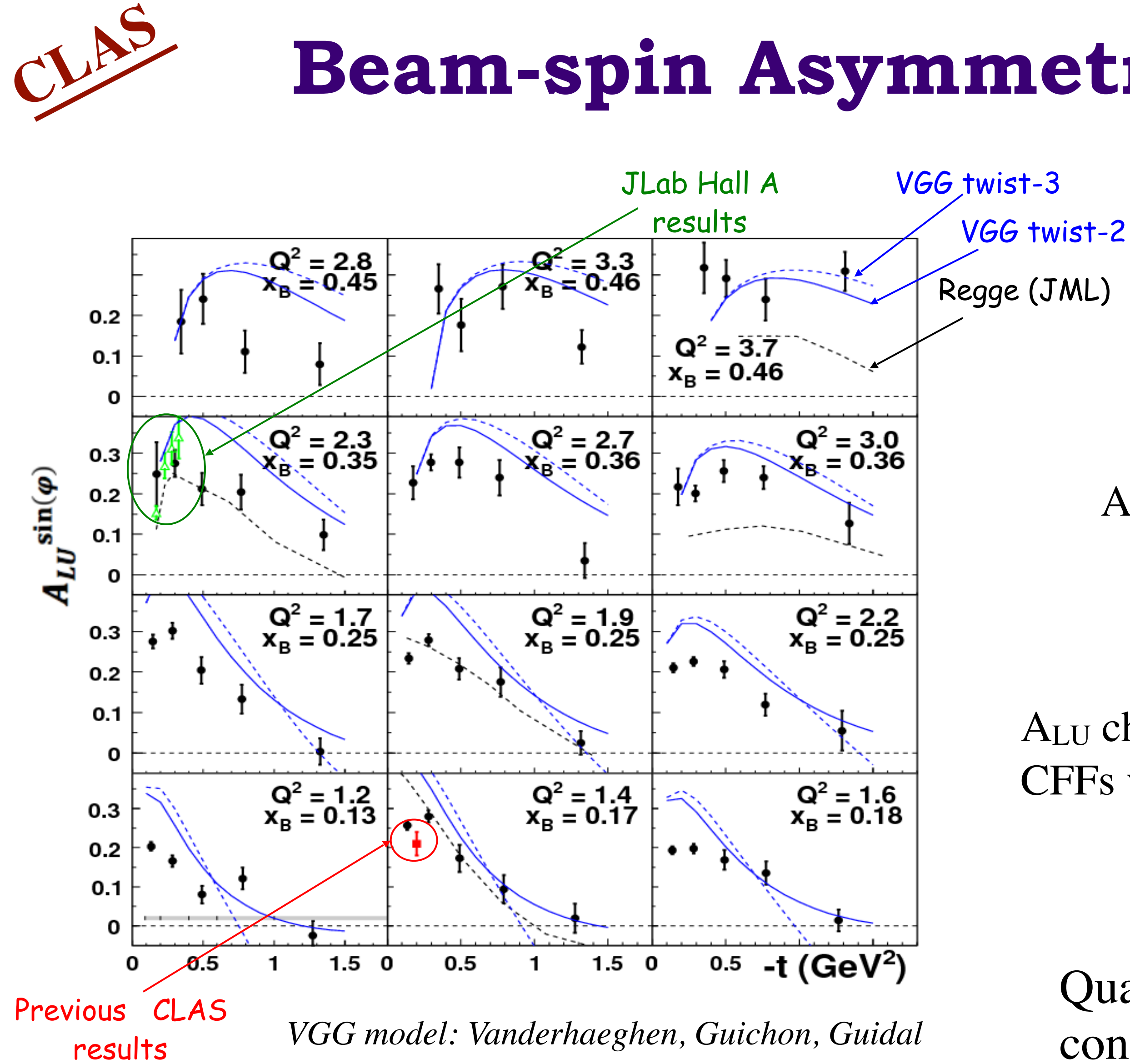

VGG model: Vanderhaeghen, Guichon, Guidal

Follows first CLAS measurement:
S. Stepanyan *et al* (CLAS), ***PRL* 87** (2001) 182002

A_{LU} from fit to asymmetry:

$$A_i = \frac{\alpha_i \sin\phi}{1 + \beta_i \cos\phi}$$

A_{LU} characterised by imaginary parts of CFFs via:

$$F_1 H + \xi G_M \tilde{H} - \frac{t}{4M^2} E$$

Qualitative agreement with models, constraints on fit parameters.

F.-X. Girod *et al* (CLAS), ***PRL* 100** (2008) 162002.

Target-spin Asymmetry (A_{UL})

Follows first CLAS measurement:
S. Chen *et al* (CLAS), ***PRL* 97** (2006) 072002

A_{UL} from fit to asymmetry:

$$A_i = \frac{\alpha_i \sin\phi}{1 + \beta_i \cos\phi}$$

A_{UL} characterised by imaginary parts of CFFs via:

$$F_1 \tilde{H} + \xi G_M (H + \frac{x_B}{2} E) - \frac{\xi t}{4M^2} F_2 \tilde{E} + \ldots$$

High statistics, large kinematic coverage, strong constraints on fits, simultaneous fit with BSA and DSA from the same dataset.

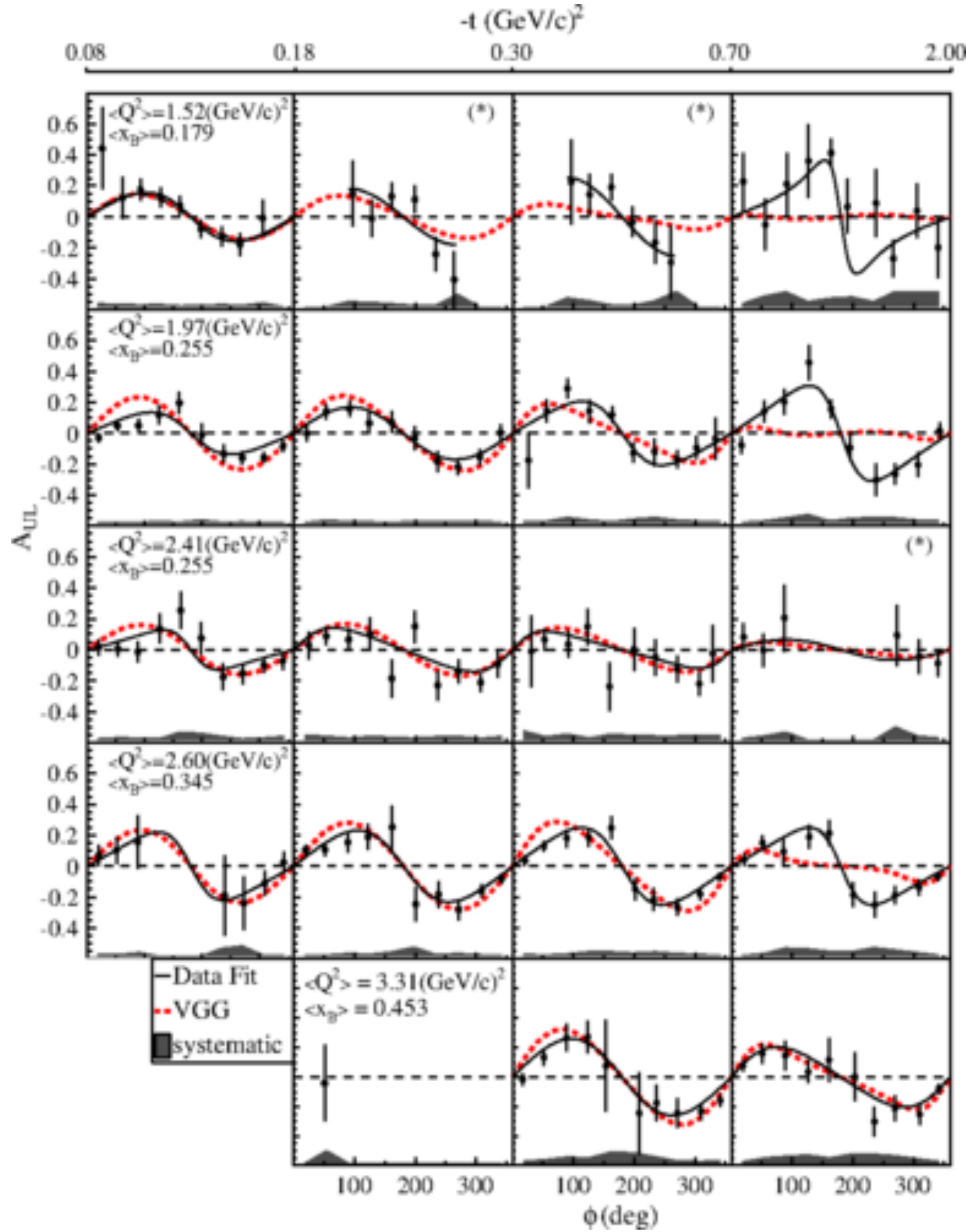

E. Seder *et al* (CLAS), ***PRL* 114** (2015) 032001

S. Pisano *et al* (CLAS), ***PRD* 91** (2015) 052014

Beam- and target-spin asymmetries

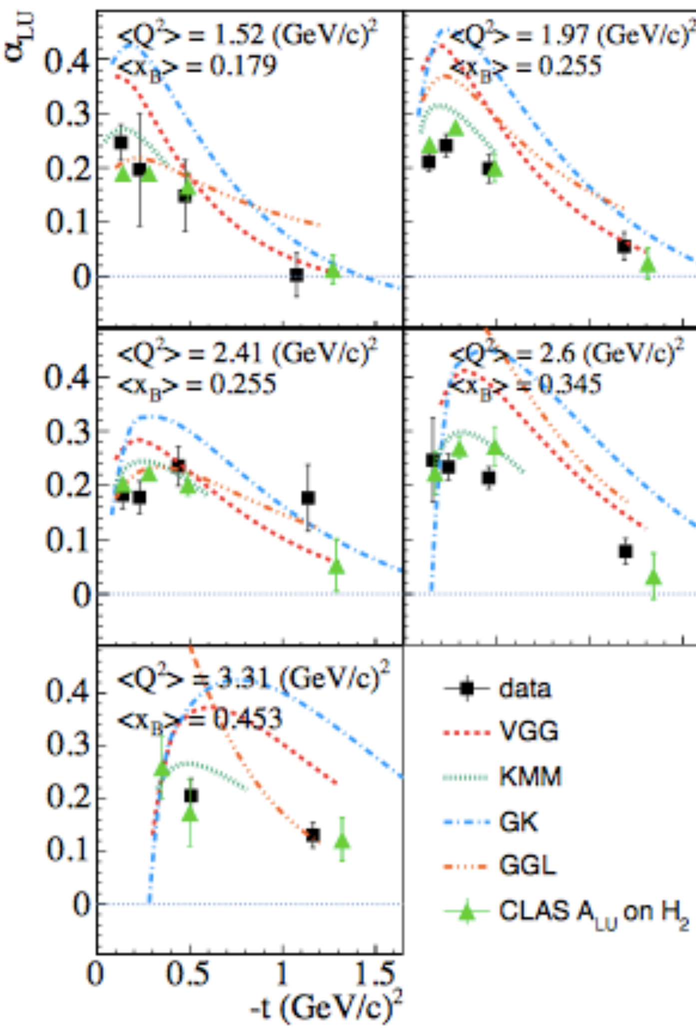

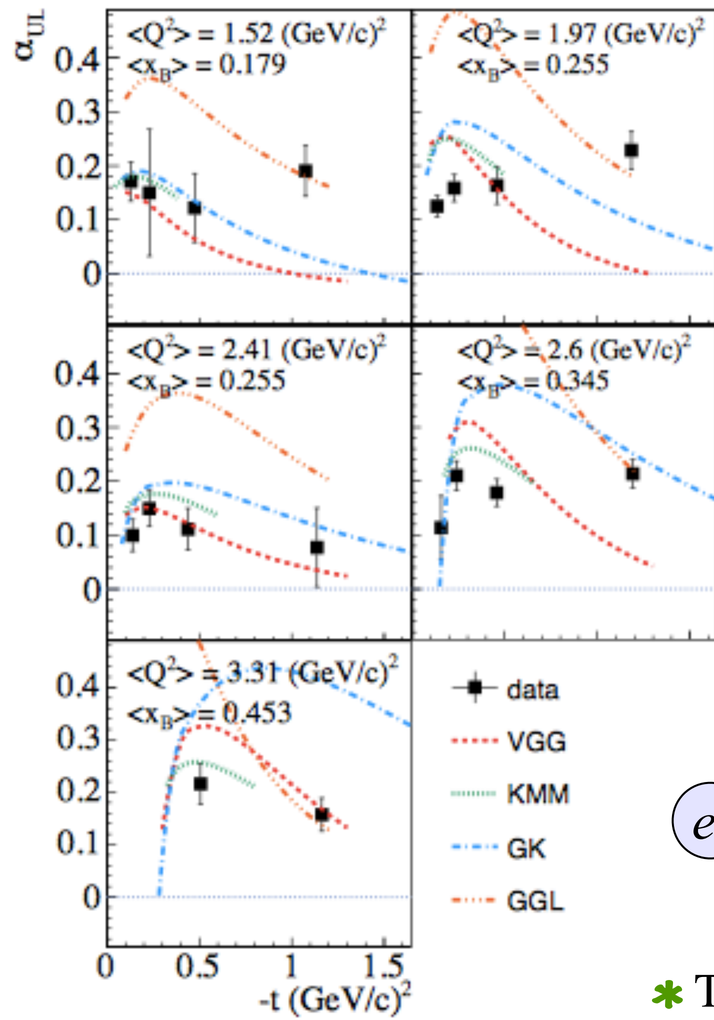

$$A = \frac{\alpha sin\phi}{1+\beta cos\phi}$$

GGL: Goldstein, Gonzalez, Liuti

GK: Kroll, Moutarde, Sabatié

KMM: Kumericki, Mueller, Murray

VGG: Vanderhaeghen, Guichon, Guidal

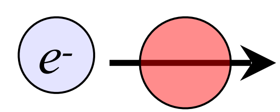

* TSA shows a flatter distribution in *t* than BSA.

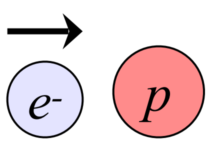

S. Pisano *et al* (CLAS), ***PRD* 91** (2015) 052014
E. Seder *et al* (CLAS), ***PRL* 114** (2015) 032001

Double-spin asymmetry

At leading twist, double-spin asymmetry (DSA) can be expressed as:

$$A_{\rm LL}(\phi) \sim \frac{c^{\rm BH}_{0,\rm LP} + c^{\mathcal{I}}_{0,\rm LP} + (c^{\rm BH}_{1,\rm LP} + c^{\mathcal{I}}_{1,\rm LP})\cos\phi}{c^{\rm BH}_{0,\rm unp} + (c^{\rm BH}_{1,\rm unp} + c^{\mathcal{I}}_{1,\rm unp} + \ldots)\cos\phi\ldots}$$

$$c^{\mathcal{I}}_{0,\rm LP}, c^{\mathcal{I}}_{1,\rm LP} \propto \Re\mathrm{e}[F_1\widetilde{\mathcal{H}} + \xi(F_1+F_2)(\mathcal{H} + \frac{x_B}{2}\mathcal{E}) - \xi(\frac{x_B}{2}F_1 + \frac{t}{4M^2}F_2)\widetilde{\mathcal{E}}]$$

At CLAS kinematics, leading-twist dominance of these CFFs

- Fit function for the phi-dependence of the asymmetry: $\dfrac{\kappa_{\rm LL} + \lambda_{\rm LL}\cos\phi}{1+\beta\cos\phi}$

Shares denominator with BSA and TSA!
If measurements at same kinematics, can do a simultaneous fit.

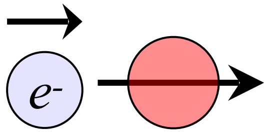

Double-spin Asymmetry (A_{LL})

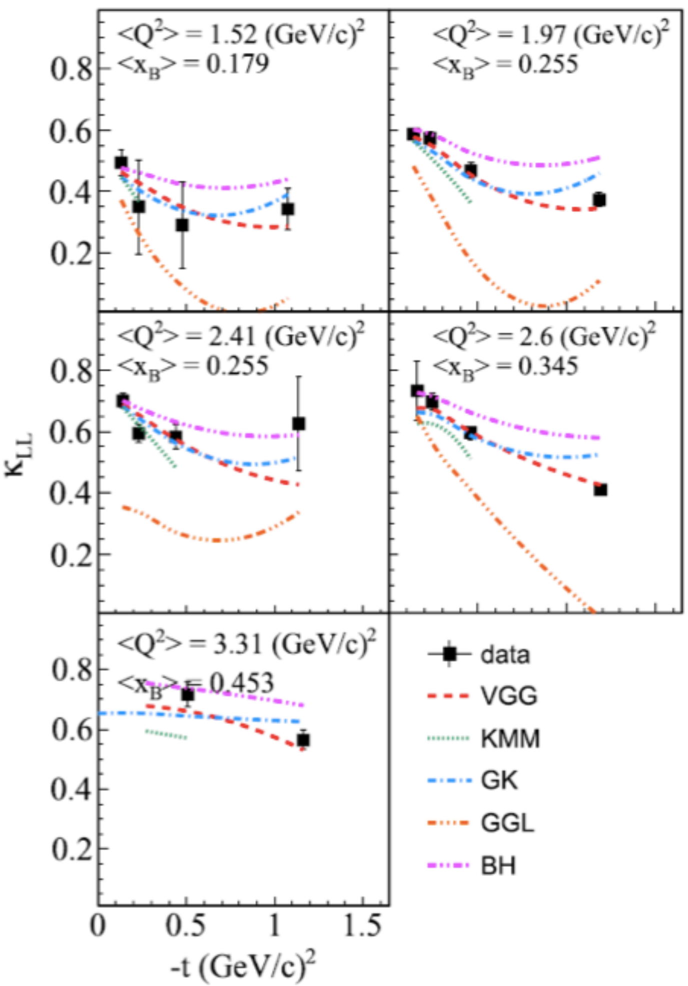

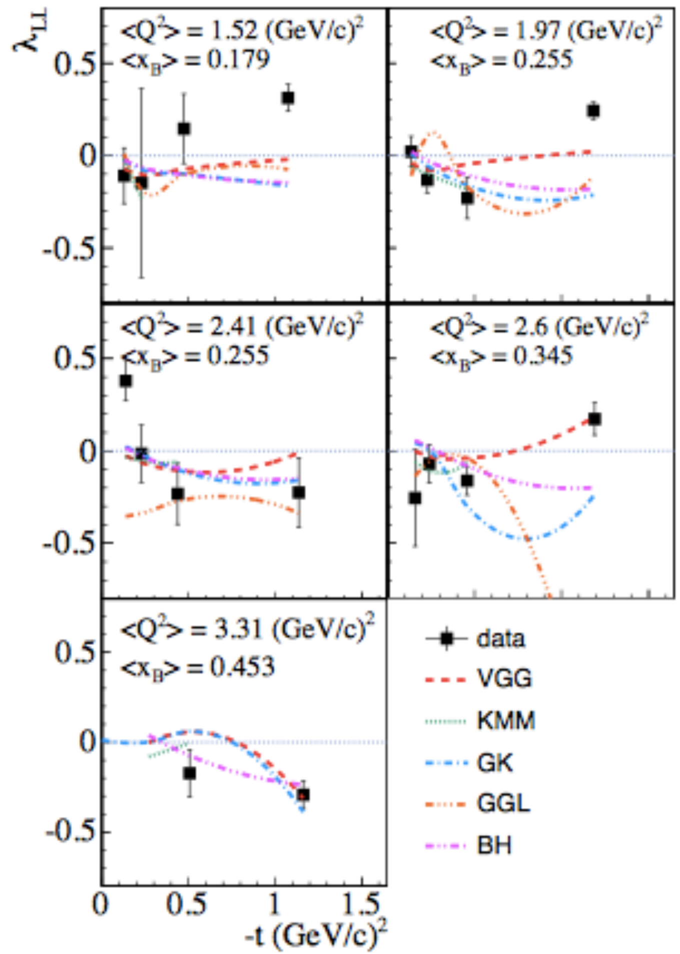

A_{LL} from fit to asymmetry:

$$\frac{\kappa_{LL} + \lambda_{LL}\cos\phi}{1 + \beta\cos\phi}$$

A_{LL} characterised by real parts of CFFs via:

$$F_1 \tilde{H} + \xi G_M \left(H + \frac{x_B}{2} E\right) + \ldots$$

* Fit parameters extracted from a simultaneous fit to BSA, TSA and DSA.
* Constant term dominates and is almost entirely BH.

E. Seder *et al* (CLAS), ***PRL* 114** (2015) 032001

S. Pisano *et al* (CLAS), ***PRD* 91** (2015) 052014

CFF extraction from three spin asymmetries at common kinematics.

Projected sensitivities to *Im(H)* CFF

$Q^2 = 2.6\ GeV^2, x_B = 0.23$ $Q^2 = 5.9\ GeV^2, x_B = 0.35$

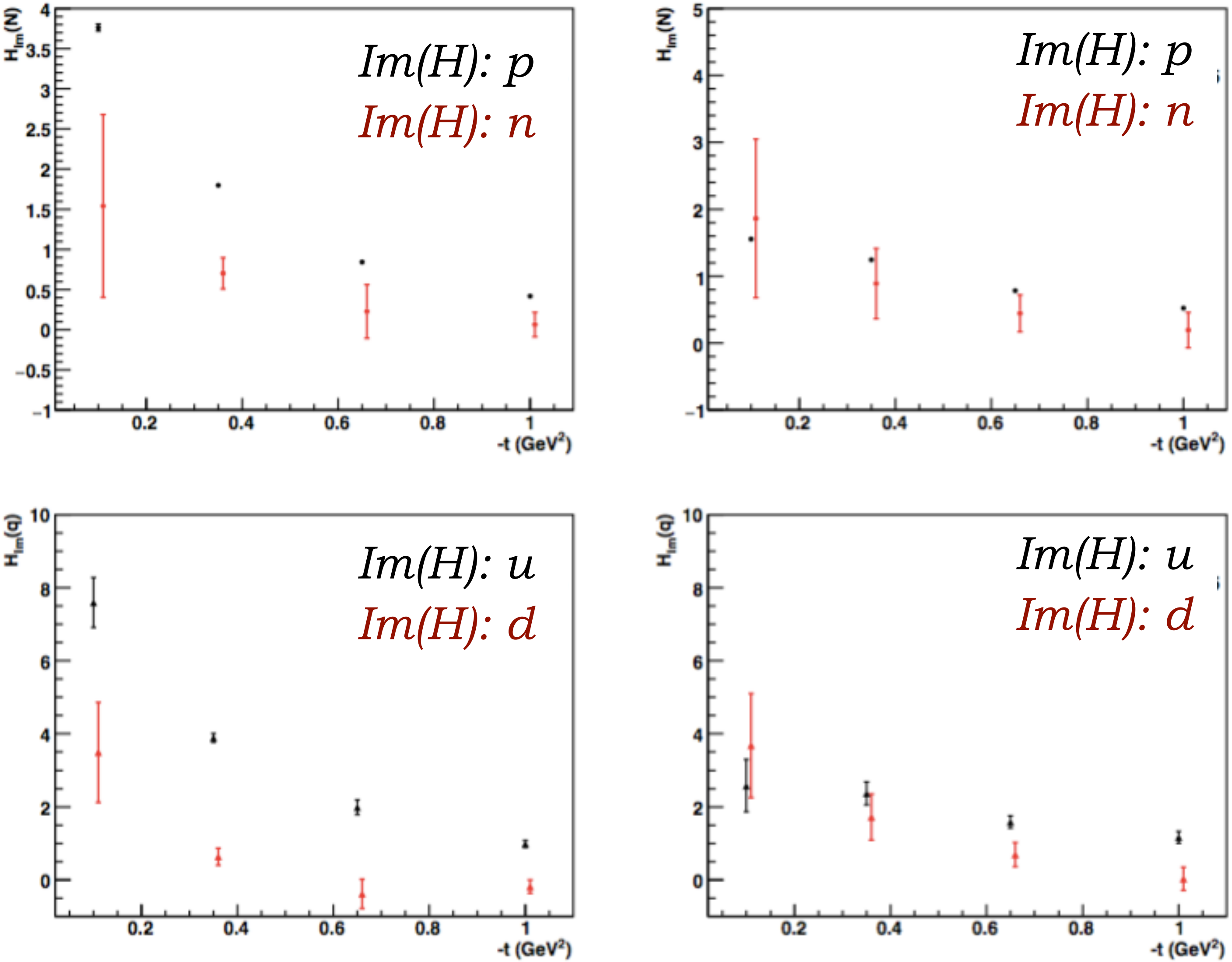

Projections for *Im(H)* neutron and proton and up and down CFFs extracted from approved CLAS12 experiments.

VGG fit (M. Guidal)

Projected sensitivities to *Im(E)* CFF

CLAS12

$Q^2 = 2.6$ GeV^2, $x_B = 0.23$ $\qquad$ $Q^2 = 5.9$ GeV^2, $x_B = 0.35$

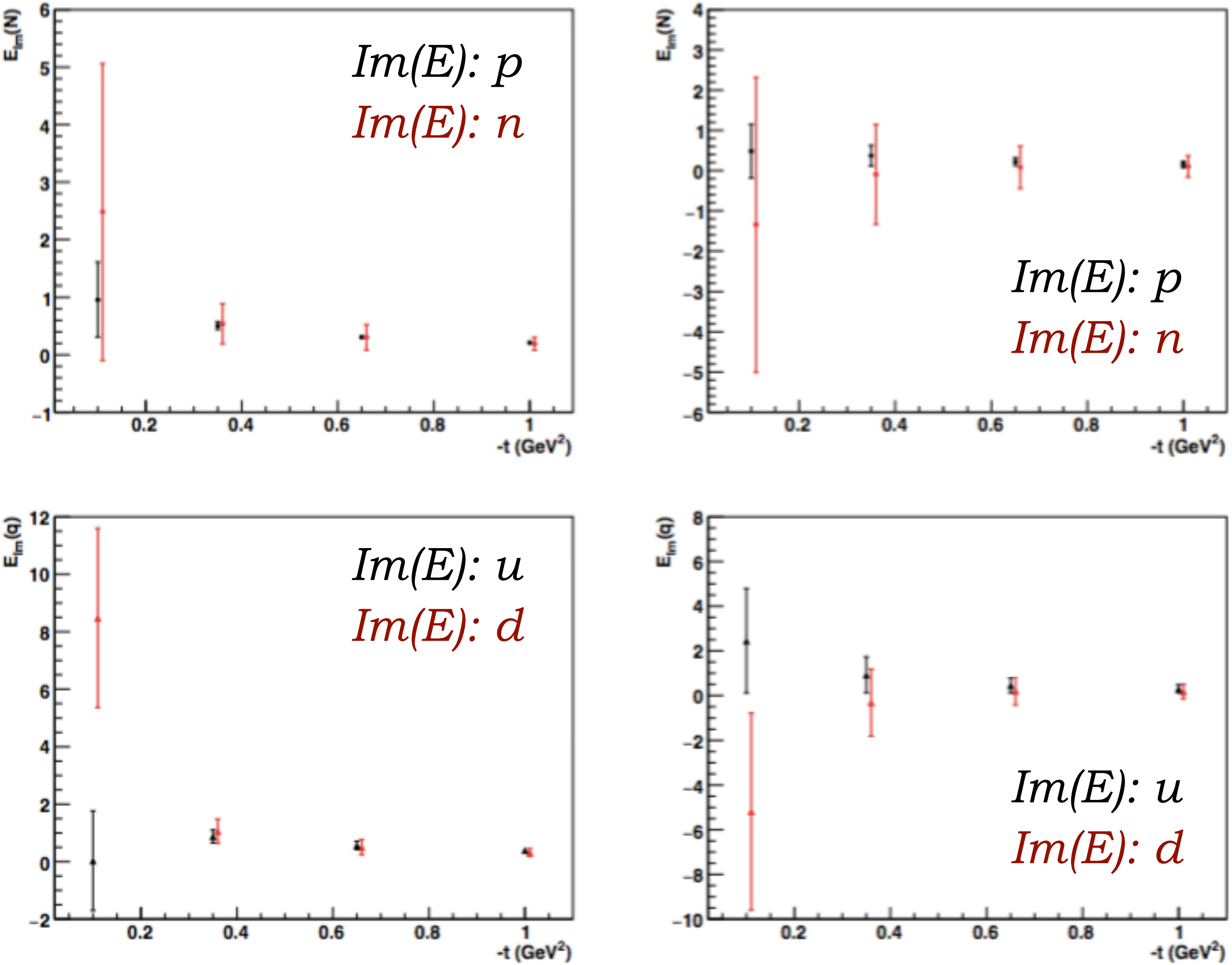

Projections for *Im(E)* neutron and proton and up and down CFFs extracted from approved and conditionally-approved CLAS12 experiments.

VGG fit (M. Guidal)

Nuclear GPDs: coherent DVCS on ^{4}He

- *^4He* is spin-0, so only one GPD at leading twist, $\mathbf{H_A}$.

$$\Re e(\mathcal{H}_A) = \mathcal{P}\int_0^1 dx[H_A(x,\xi,t) - H_A(-x,\xi,t)]\,C^+(x,\xi)$$
$$\Im m(\mathcal{H}_A) = -\pi(H_A(\xi,\xi,t) - H_A(-\xi,\xi,t))$$

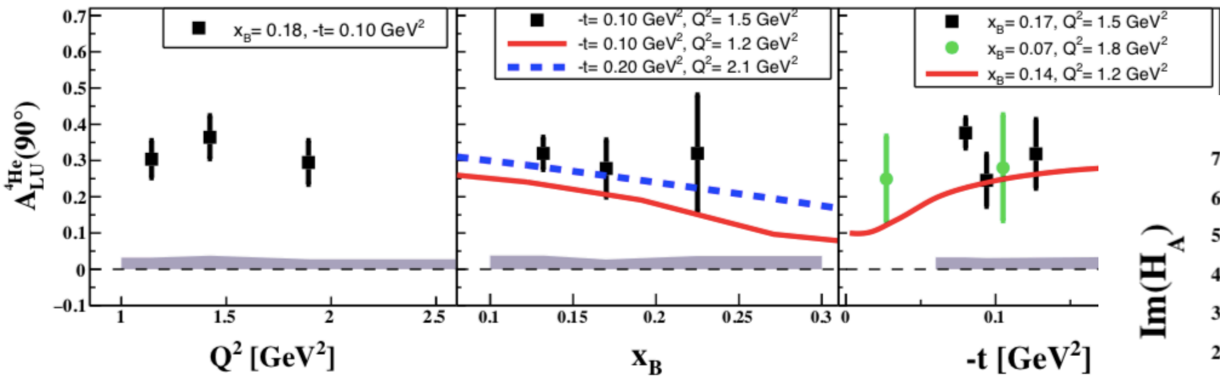

HERMES

S. Liuti, K. Taneja, PRC72, 032201 (2005)

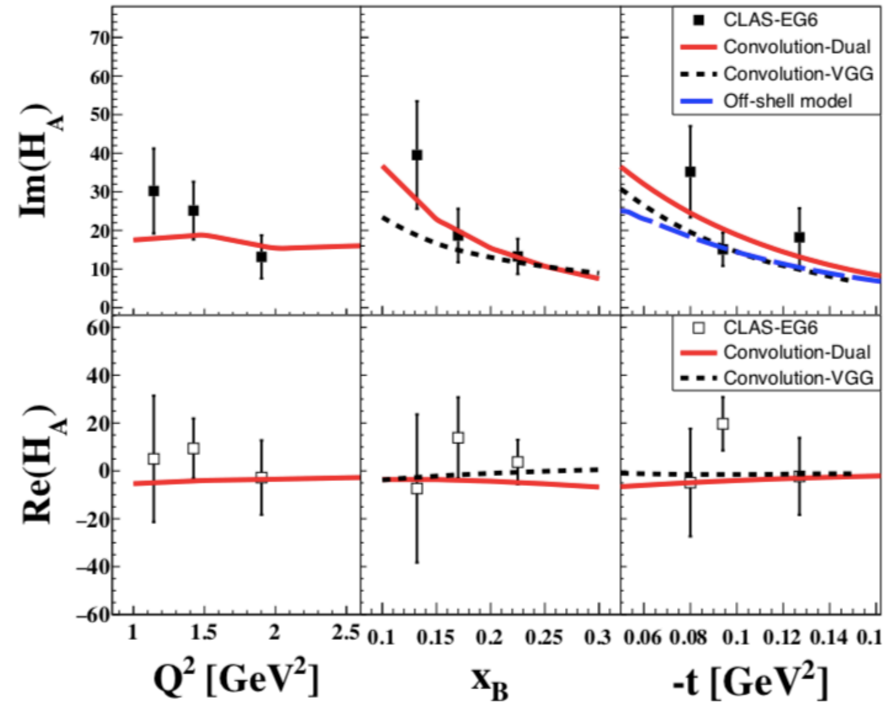

V. Guzey, PRC78, 025211 (2008)

M. Guidal *et al*, PRD72, 054013 (2005)

J. Gonzalez-Hernandez *et al*, PRC88, 065206 (2013)

- Beam spin asymmetry in coherent DVCS from *^4He*: CLAS and a radial time projection chamber (RTPC) for detection of recoiling helium, data taken in 2009.
- Paves the way for measurements at 11 GeV.

M. Hattawy *et al*, PRL 119 (2017) 202004.

Nucleon Tomography from GPDs

- At a fixed Q^2, x_B, slope of GPD with t is related, via a Fourier Transform, to the transverse spatial spread.

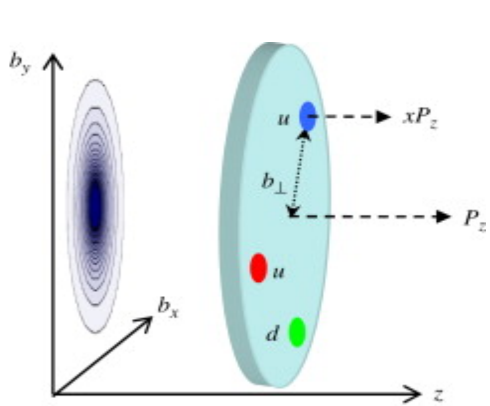

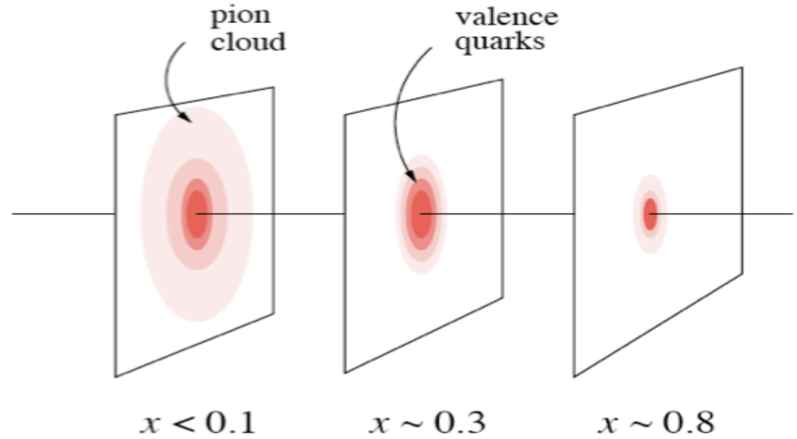

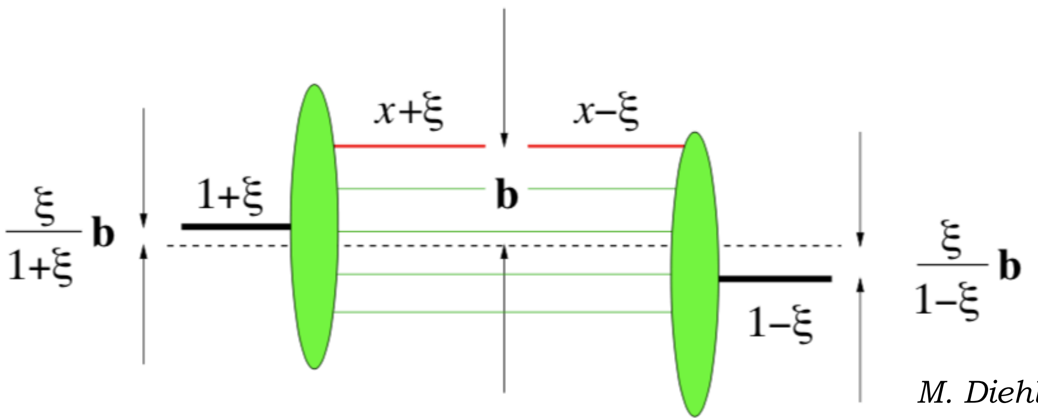

M. Diehl

Formally, the radial separation, **b**, *between the struck parton and the centre of momentum of the remaining spectators.*

- Experimentally, fit the t-dependence of structure functions or CFFs with an exponential.

eg:
$$\frac{d\sigma_U}{dt} = Ae^{Bt}$$

GPDs and nucleon spin

$$J_N = \frac{1}{2} = \frac{1}{2}\Sigma_q + L_q + J_g$$

- Ji's relation: $J^q = \frac{1}{2} - J^g = \frac{1}{2}\int_{-1}^{1} x dx \left\{ H^q(x,\xi,0) + E^q(x,\xi,0) \right\}$

Second Mellin moments of the GPDs contain information on the total angular momentum carried by quarks.

Note that the contribution from GPD *H* is given by the quark momentum, already known from PDFs:

$$2J^q = \int_0^1 \mathrm{d}x\, x[q(x) + \bar{q}(x)] + \int_{-1}^{+1} \mathrm{d}x\, x E^q(x, 0, 0)$$

Compton Form Factors in DVCS

Experimentally, DVCS amplitude is proportional to Compton Form Factors (CFFs) — sums of GPD integrals over x:

$$\int_{-1}^{1} dx F(\mp x, \xi, t) \left[\frac{1}{x - \xi + i\epsilon} \pm \frac{1}{x + \xi - i\epsilon} \right]$$

GPD

Plus sign for unpolarised GPDs, minus for polarised.

Can be decomposed into real and imaginary parts:

Cauchy's principal value integral

$$\Re\mathrm{e}\mathcal{F} = \mathcal{P} \int_{-1}^{1} dx \left[\frac{1}{x - \xi} \mp \frac{1}{x + \xi} \right] F(x, \xi, t)$$

$$\Im\mathrm{m}\mathcal{F}(\xi, t) = -\pi [F(\xi, \xi, t) \mp F(-\xi, \xi, t)]$$

* Both parts are accessible in different experimental observables

Other reactions to get at GPDs

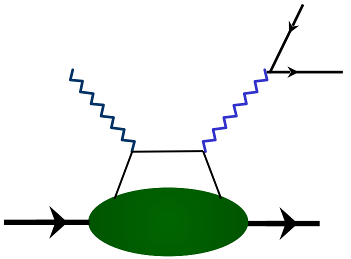

* **Time-like Compton scattering**: virtual photon is time-like. At leading order, access same integrals of GPDs. At higher orders, they differ.

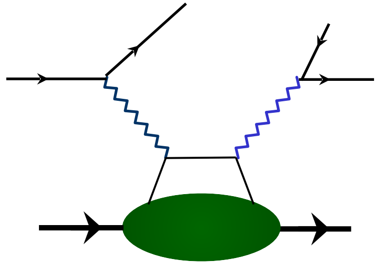

* **Double Deeply Virtual Compton scattering**: two virtual photons: the second vertex provides a second variable Q'^2. This allows direct access to x, but cross-sections are suppressed by another factor of α.

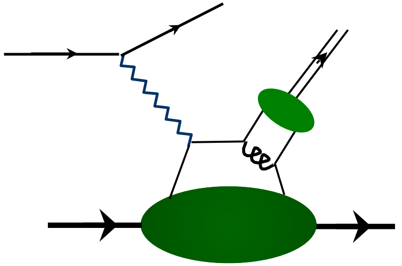

* **Deeply Virtual Meson Production**: the meson vertex provides flavour information. Amplitude now depends on GPDs and the meson Distribution Amplitudes. In light mesons, more sensitive to higher order and higher twist.

In vector mesons, gluon GPDs appear at lowest order!

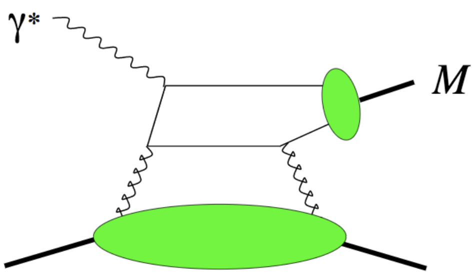

Nucleon Tomography from GPDs

* Flavour separation is possible in DVCS using different targets (proton and neutron), and in DVMP with different mesons.

For example, compare measurements of π^0 and η DVMP:

$$H_T^{\pi^0} = (e_u H_T^u - e_d H_T^d)/\sqrt{2}, \qquad H_T^{\eta} = (e_u H_T^u + e_d H_T^d)/\sqrt{6},$$

$$\bar{E}_T^{\pi^0} = (e_u \bar{E}_T^u - e_d \bar{E}_T^d)/\sqrt{2}, \qquad \bar{E}_T^{\eta} = (e_u \bar{E}_T^u + e_d \bar{E}_T^d)/\sqrt{6}.$$

Up-quark charge

(Goloskokov-Kroll model)

* Different GPDs represent different aspects of the parton distributions: EM charge, axial charge, transversity, etc….

* Sensitivity to gluon distributions through gluon GPDs.

Particularly cleanly accessible for heavier q: J/Ψ

Extracting asymmetries

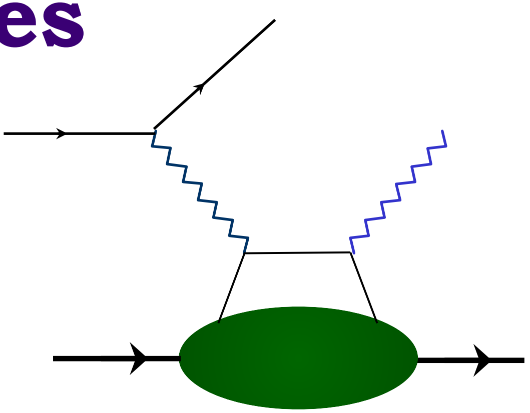

Number of DVCS/BH events for each kinematic bin:

$$N^{bt} = (1 - B^{bt}_{\pi^0}) \cdot \frac{N^{bt}_{ep\gamma}}{FC^{bt}}$$

Number of detected events in identified reaction

Polarisation state of beam, target

Background due to π^0 contamination

Normalisation by beam current (in Faraday Cup)

* Beam-spin asymmetry:

$$A_{\mathrm{LU}} = \frac{P_t^-(N^{++} - N^{-+}) + P_t^+(N^{+-} - N^{--})}{P_b(P_t^-(N^{++} + N^{-+}) + P_t^+(N^{+-} + N^{--}))}$$

Beam, target polarisation

* Target-spin asymmetry:

$$A_{\mathrm{UL}} = A^{\mathrm{lab}}_{\mathrm{UL}} + c_{A_{\mathrm{UT}}}$$

Correction for electron / virtual photon axes

$$A^{\mathrm{lab}}_{\mathrm{UL}} = \frac{N^{++} + N^{-+} - N^{+-} - N^{--}}{D_f(P_t^-(N^{++} + N^{-+}) + P_t^+(N^{+-} + N^{--}))}$$

Dilution factor due to unpolarised background

* Double-spin asymmetry:

$$A_{\mathrm{LL}} = A^{\mathrm{lab}}_{\mathrm{LL}} + c_{A_{\mathrm{LT}}}$$

$$A^{\mathrm{lab}}_{\mathrm{LL}} = \frac{N^{++} + N^{--} - N^{+-} - N^{-+}}{P_b \cdot D_f(P_t^-(N^{++} + N^{-+}) + P_t^+(N^{+-} + N^{--}))}$$

The DVCS/BH amplitude

$$\mathcal{T}^2 = |\mathcal{T}_{\mathrm{BH}}|^2 + |\mathcal{T}_{\mathrm{DVCS}}|^2 + \mathcal{I}$$

Interference term for DVCS/BH

$$|\mathcal{T}_{\mathrm{BH}}|^2 = \frac{e^6}{x_B^2 y^2 (1+\epsilon^2)^2 t\, \mathcal{P}_1(\phi)\mathcal{P}_2(\phi)} [c_0^{\mathrm{BH}} + \sum_{n=1}^{2} c_n^{\mathrm{BH}} \cos n\phi + s_1^{\mathrm{BH}} \sin \phi]$$

$$|\mathcal{T}_{\mathrm{DVCS}}|^2 = \frac{e^6}{y^2 \mathcal{Q}^2} \{c_0^{\mathrm{DVCS}} + \sum_{n=1}^{2} [c_n^{\mathrm{DVCS}} \cos n\phi + s_n^{\mathrm{DVCS}} \sin n\phi]\}$$

$$\mathcal{I} = \frac{e^6}{x_B y^3 t \mathcal{P}_1(\phi)\mathcal{P}_2(\phi)} \{c_0^{\mathcal{I}} + \sum_{n=1}^{3} [c_n^{\mathcal{I}} \cos n\phi + s_n^{\mathcal{I}} \sin n\phi]\}$$

Intermediate lepton propagators

Coefficients depending on Compton Form Factors

From asymmetries to CFFs

At leading twist, beam-spin asymmetry (BSA) can be expressed as:

$$A_{\mathrm{LU}}(\phi) \sim \frac{s^{\mathcal{I}}_{1,\mathrm{unp}} \sin\phi}{c^{\mathrm{BH}}_{0,\mathrm{unp}} + (c^{\mathrm{BH}}_{1,\mathrm{unp}} + c^{\mathcal{I}}_{1,\mathrm{unp}} + \ldots)\cos\phi \ldots}$$

higher-twist terms…

The leading coefficient is related to the imaginary part of the Compton Form Factors:

$$s^{\mathcal{I}}_{1,\mathrm{unp}} \propto \Im\mathrm{m}[F_1 \mathcal{H} + \xi(F_1 + F_2)\widetilde{\mathcal{H}} - \frac{t}{4M^2} F_2 \mathcal{E}]$$

At CLAS kinematics, this dominates

F_1, F_2: Dirac, Pauli form factors

Likewise, for the target-spin asymmetry (TSA):

$$A_{\mathrm{UL}}(\phi) \sim \frac{s^{\mathcal{I}}_{1,\mathrm{LP}} \sin\phi}{c^{\mathrm{BH}}_{0,\mathrm{unp}} + (c^{\mathrm{BH}}_{1,\mathrm{unp}} + c^{\mathcal{I}}_{1,\mathrm{unp}} + \ldots)\cos\phi + \ldots}$$

$$s_{1,\mathrm{LP}} \propto \Im\mathrm{m}[F_1 \widetilde{\mathcal{H}} + \xi(F_1 + F_2)(\mathcal{H} + \frac{x_B}{2}\mathcal{E}) - \xi(\frac{x_B}{2} F_1 + \frac{t}{4M^2} F_2)\widetilde{\mathcal{E}}]$$

At CLAS kinematics, these CFFs dominate

* Obtain coefficients from fitting the phi-dependence of the asymmetry:

$$A_i = \frac{\alpha_i \sin\phi}{1 + \beta_i \cos\phi}$$

Proton DVCS @ 11 GeV

CLAS12

Impact of CLAS12 unpolarised target proton-DVCS data on the extraction of Re(H) and Im(H).

Re(H)

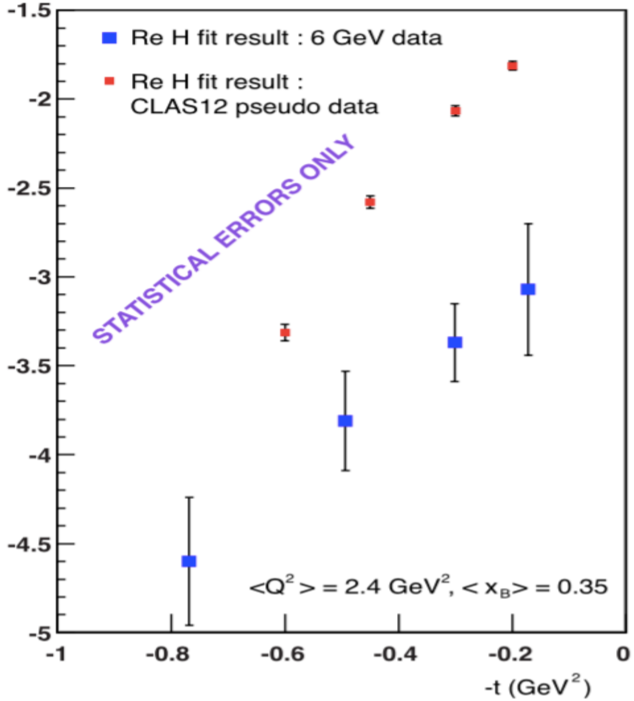

Im(H)

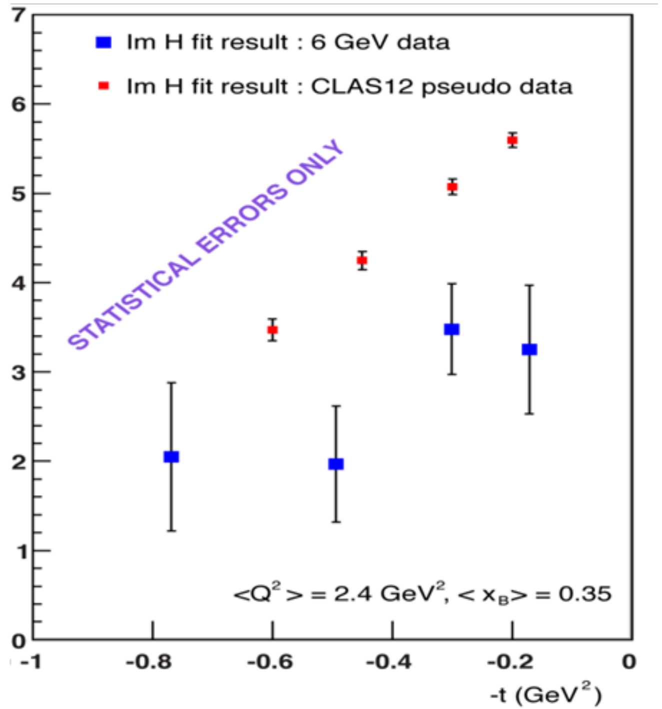

(CLAS 6 GeV extraction H. Moutarde)

DVCS @ JLab12

* Scheduled experiments to measure cross-sections and spin asymmetries with unpolarised and longitudinally polarised liquid H_2 and D_2 targets using CLAS12. → ***Im*(E$_n$), *Im*(H$_p$), *Im*($\widetilde{H}_p$), *Re*(H$_p$)**

- Dynamic Nuclear Polarisation (DNP) of target material, cooled in a *He* evaporation cryostat.
- P_{proton} = 80%,
- $P_{deuteron}$ up to 50%

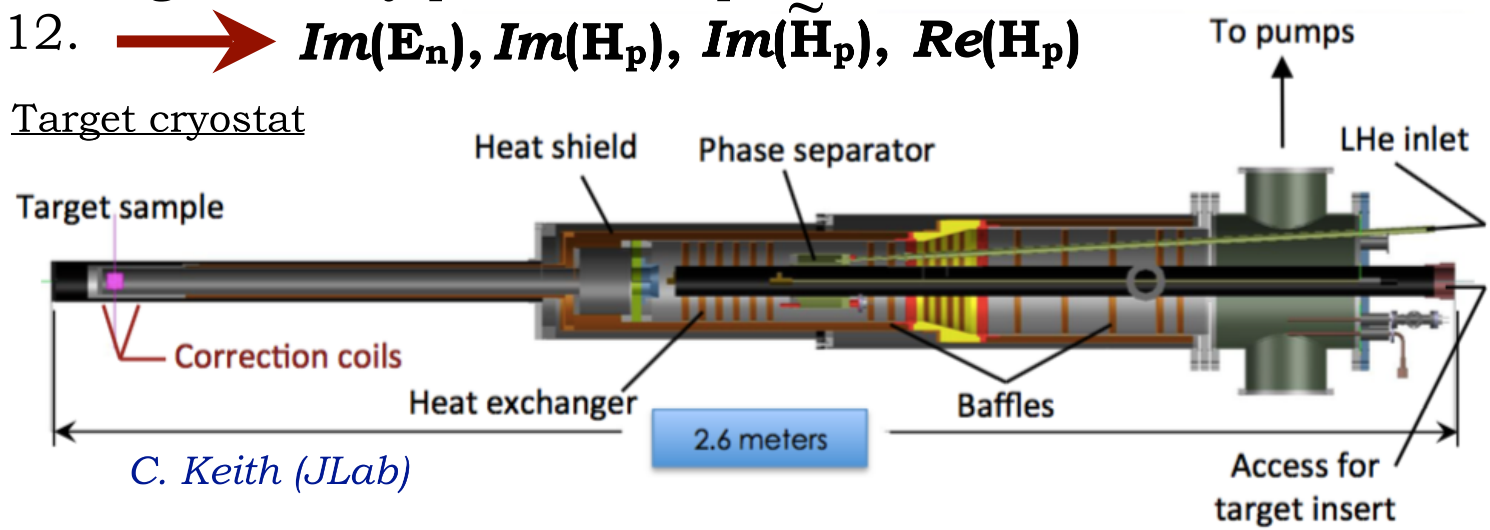

C. Keith (JLab)

* Measurements of cross-sections at 10.6, 8.8 and 6.6 GeV (allows separation of pure DVCS amplitude and the DVCS/Bethe-Heitler interference terms) in Halls A, B and C.

* Transversely-polarised target (HD) for use with electron beams is under development (Hall B). → ***Im*(E$_p$)**

* Measurement of beam-spin asymmetry in coherent DVCS from a ^4He target (CLAS12 + recoil detector ALERT): partonic structure of nuclei. → ***Im*(H$_A$)**

JLab 6 GeV era DVCS X-sections: kinematics

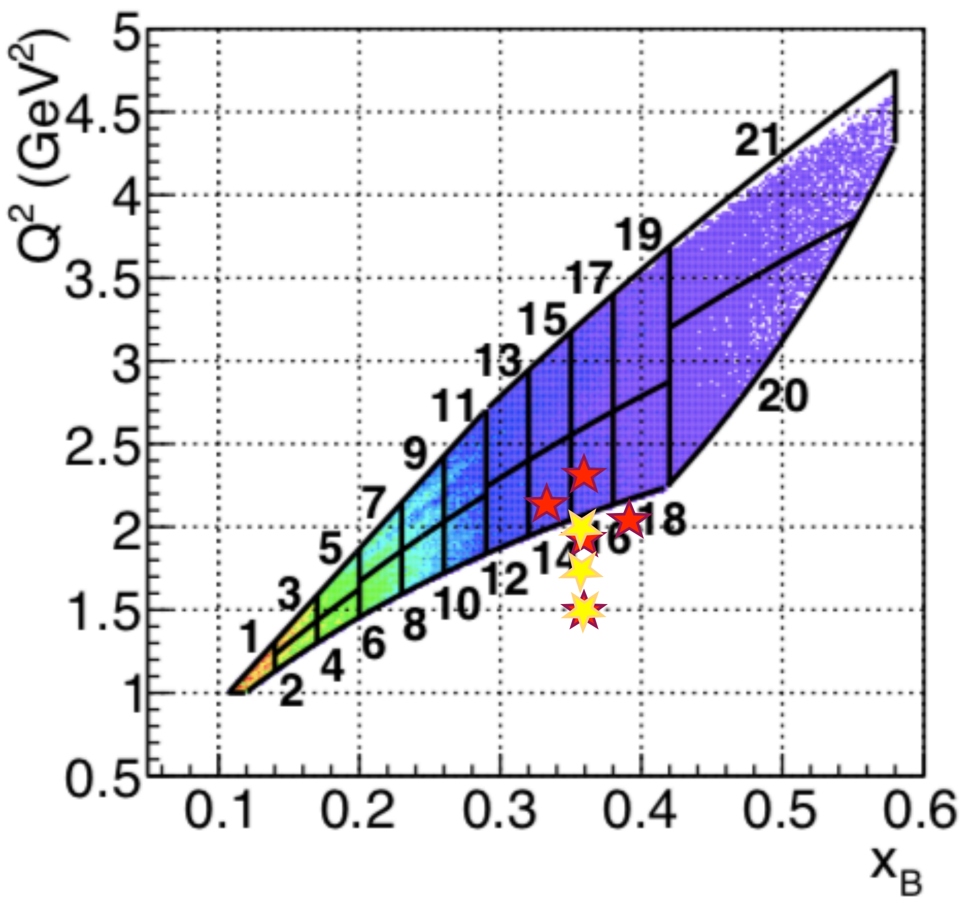

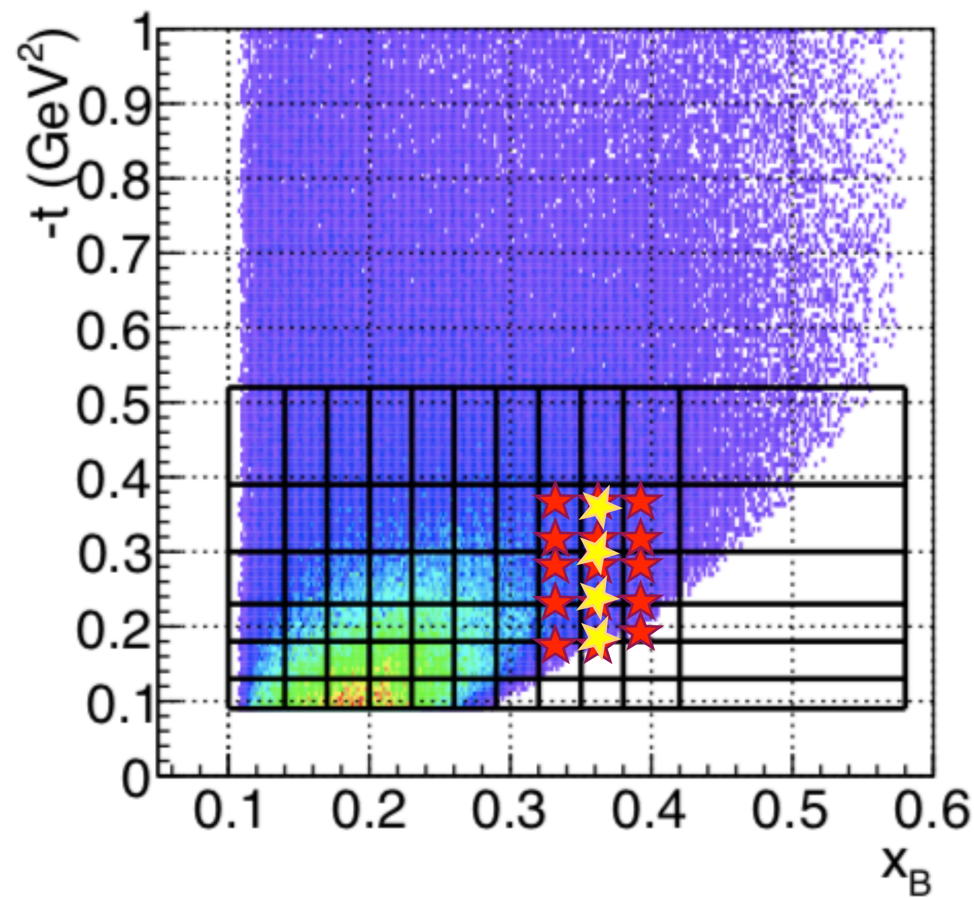

CLAS 2D distributions: H.-S. Jo *et al* (CLAS), ***PRL* 115** (2015) 212003

Hall A

★ M. Defurne *et al*, ***PRC* 92** (2015) 055202

★ M. Defurne *et al*, ***Nature Communications* 8** (2017) 1408

Proton DVCS @ 11 GeV

CLAS12

Experiment E12-06-119

F. Sabatié et al.

P_{beam} = 85%
L = 10^{35} $cm^{-2}s^{-1}$
1< Q^2 < 10 GeV^2
0.1 <x_B< 0.65
$-t_{min}$< −t < 2.5 GeV^2

Kinematics similar for all proton DVCS @ 11 GeV with CLAS12 experiments

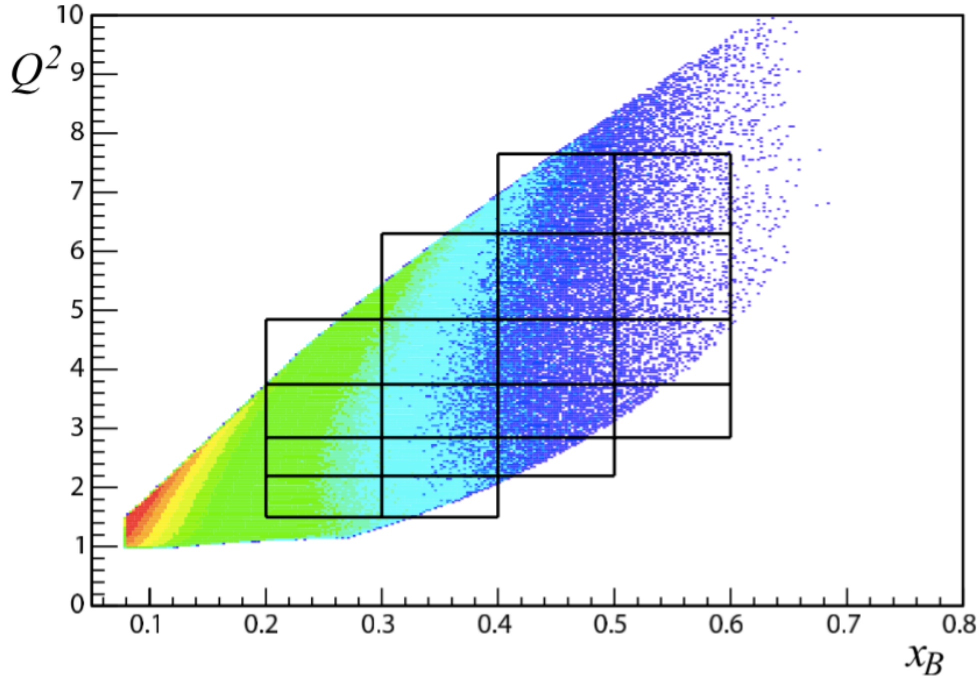

First experiment with CLAS12

Unpolarised liquid H_2 target:

- Statistical error: 1% - 10% on sinφ moments
- Systematic uncertainties: ~ 6 - 8%

Started this February!

A_{LU} characterised by imaginary parts of CFFs via:

$$F_1 H + \xi G_M \tilde{H} - \frac{t}{4M^2} E \longrightarrow Im(H_p)$$

DVCS at lower energies with CLAS12

CLAS12

Experiment E12-16-010B
F.-X. Girod et al.

Unpolarised liquid H_2 target:

- Beam energies: 6.6, 8.8 GeV
- Simultaneous fit to beam-spin and total cross-sections.

* Rosenbluth separation of interference and $|T_{DVCS}|^2$ terms in the cross-section

* Scaling tests of the extracted CFFs

* Model-dependent determination of the D-term in the Dispersion Relation between *Re* and *Im* parts of CFFs: sensitivity to Gravitational Form Factors.

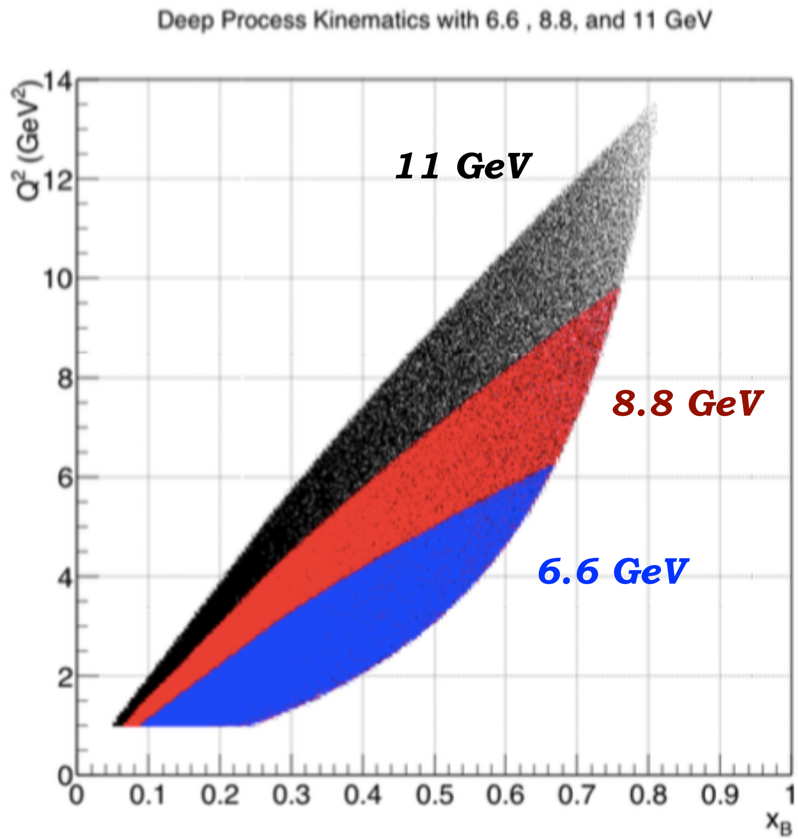

Compare with measurements from Halls A and C: cross-check model and systematic uncertainties.

DVCS at lower energies with CLAS12

Projected extraction of CFFs (red) compared to generated values (green). Three curves on the *Re(H)* show three different scenarios for the D-term.

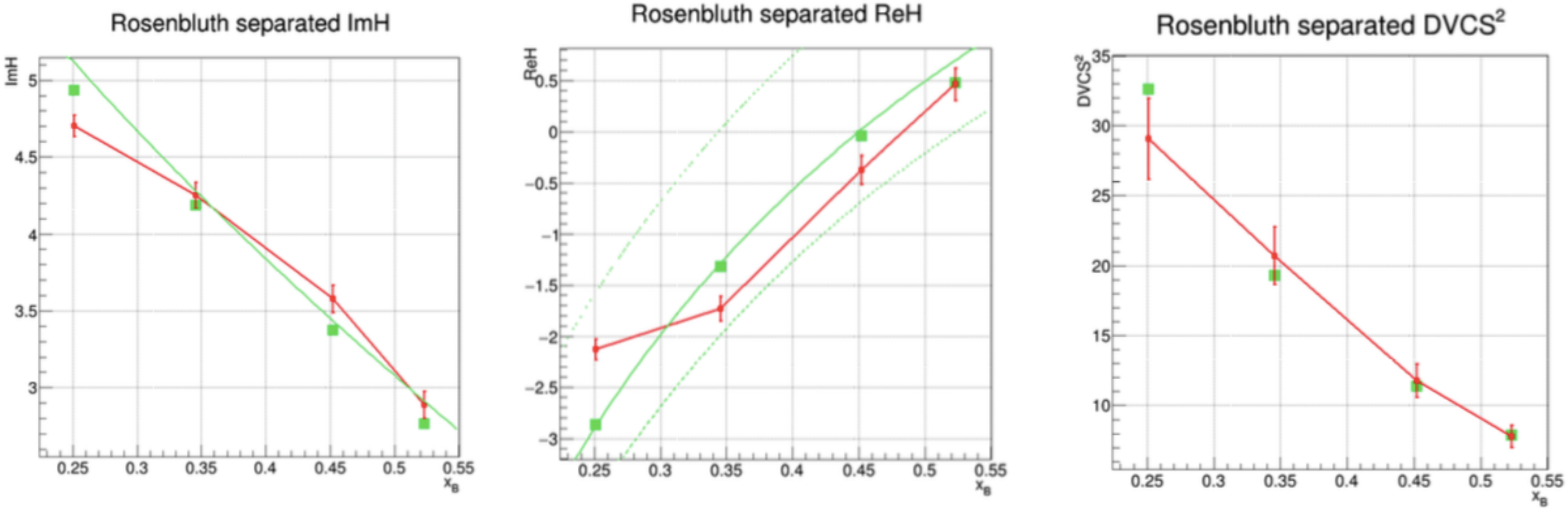

F.-X. Girod et al.

CLAS12

Neutron DVCS @ 11 GeV

Experiment E12-11-003

S. Niccolai, D. Sokhan et al.

$$\Delta\sigma_{LU} \sim \sin\phi \; \mathbf{Im}\{F_1 H + \xi(F_1+F_2)\tilde{H} - kF_2 E\}d\phi$$

Im (E$_n$) dominates.

Simulated statistical sample:

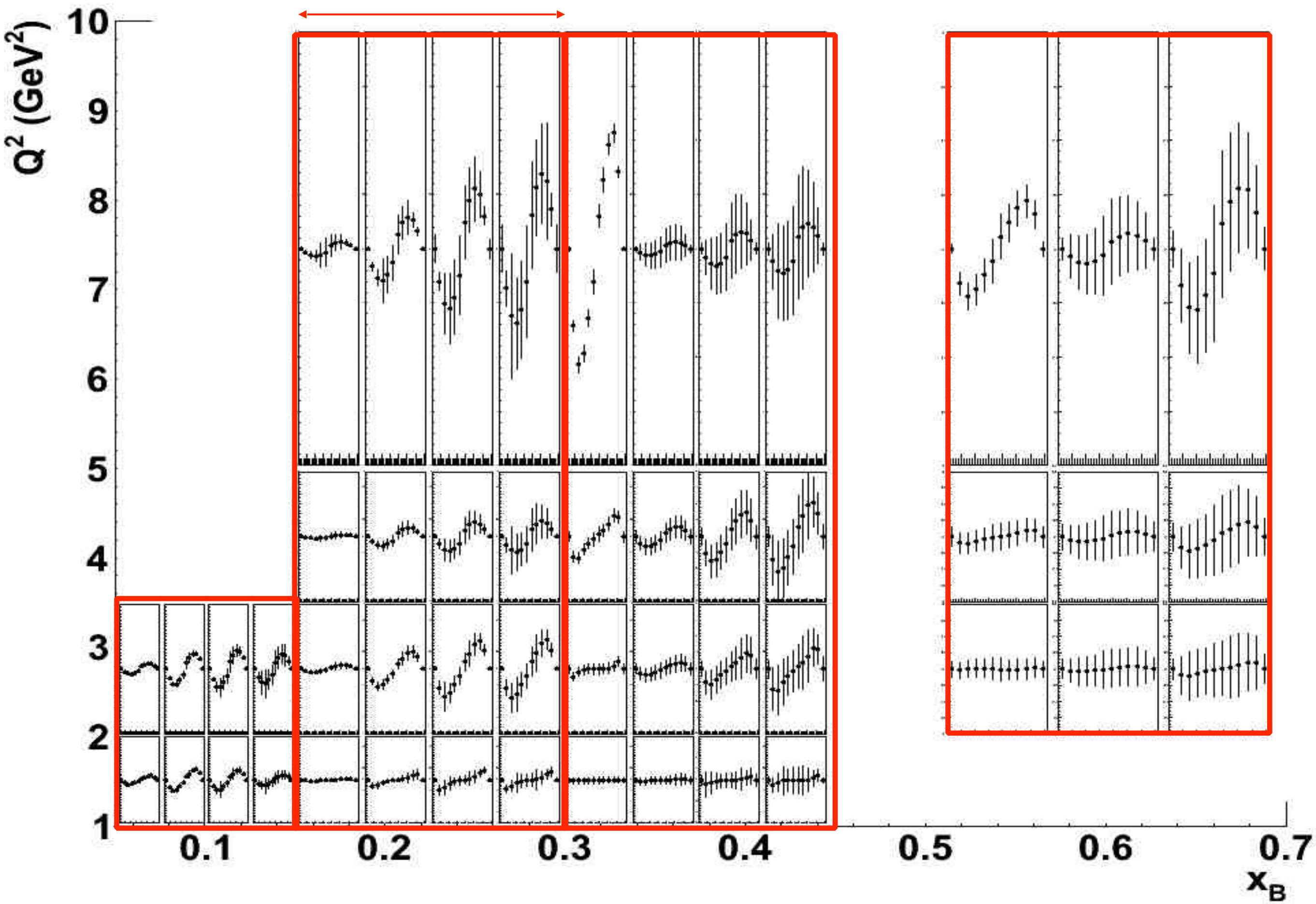

L = 10^{35} cm^{-2}s^{-1}/nucleon

$$e + d \rightarrow e' + \gamma + n + (p_s)$$

CLAS12 +

Forward Tagger +

Neutron Detector

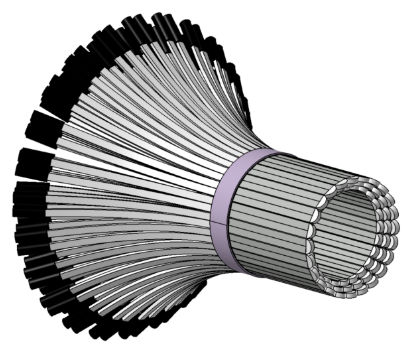

Scheduled: 2019

Neutron DVCS with a longitudinally polarised target

CLAS12

Experiment E12-06-109A.
S. Niccolai, D. Sokhan et al.

Longitudinally polarised ND_3 target:

- Dynamic Nuclear Polarisation (DNP) of target material in a cryostat shared with the NH_3 target.
- $P_{deuteron}$ up to 50%
- Systematic uncertainties: ~ 12%

A_{UL} characterised by imaginary parts of CFFs via:

$$F_1 \tilde{H} + \xi G_M (H + \frac{x_B}{2} E) - \frac{\xi t}{4M^2} F_2 \tilde{E} + \ldots$$

→ ***Im*(H$_n$)**

In combination with pDVCS, will allow flavour-separation of the H_q CFFs.

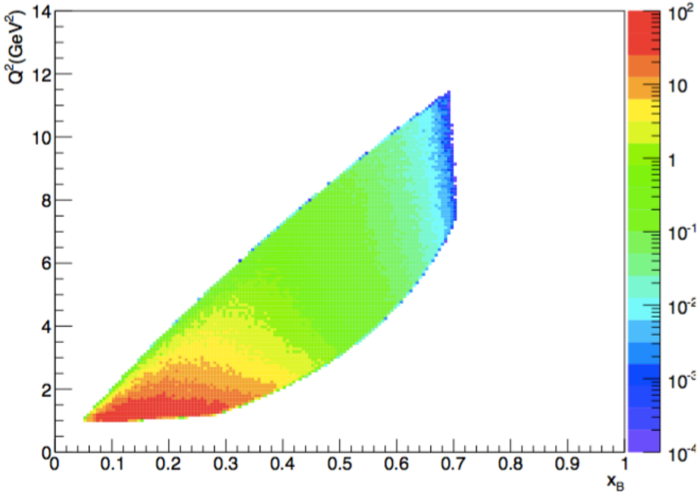

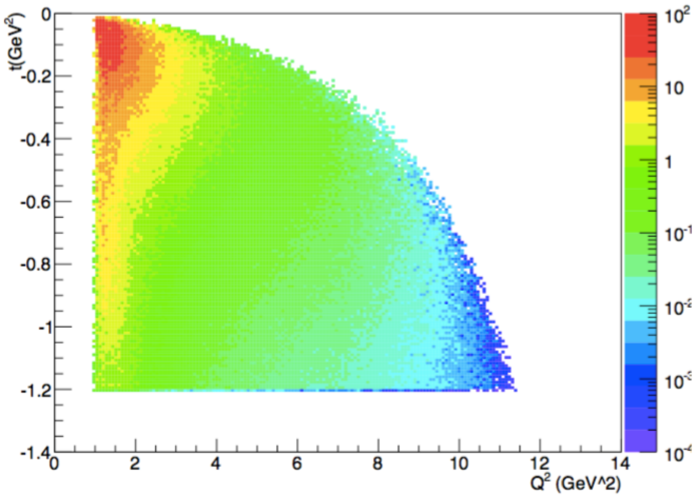

Tentative schedule: 2020

Proton DVCS with transversely polarised target at CLAS12

CLAS12

C12-12-010: with transversely polarised HD target (conditionally approved).

L. Elouardhiri et al.

$\Delta\sigma_{UT} \sim \cos\phi \, \mathrm{Im}\{k(F_2 H - F_1 E) + \ldots\} d\phi$

Sensitivity to ***Im(E)*** for the proton.

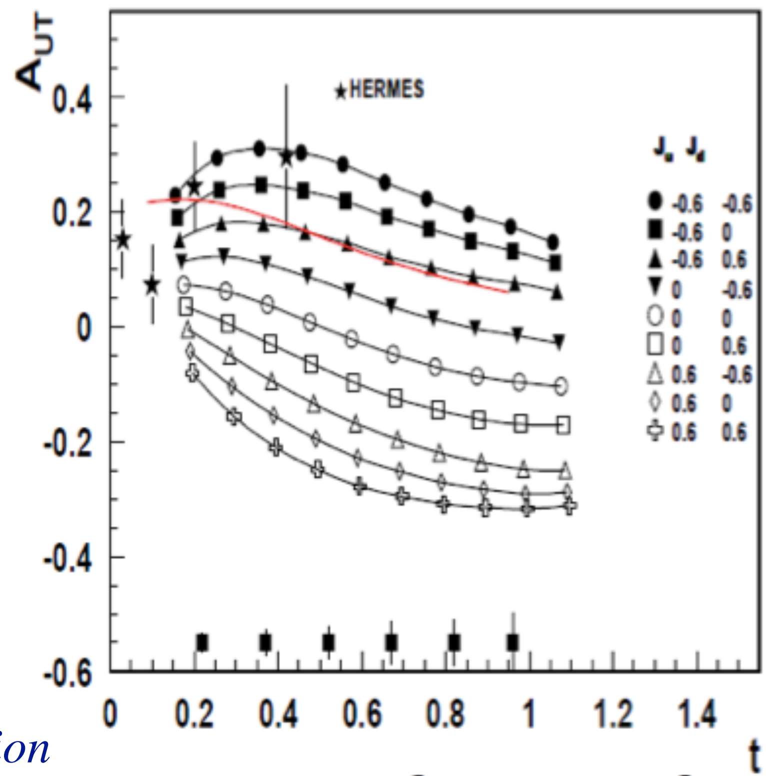

$\langle x \rangle = 0.2, \langle Q^2 \rangle = 2.5\ GeV^2$

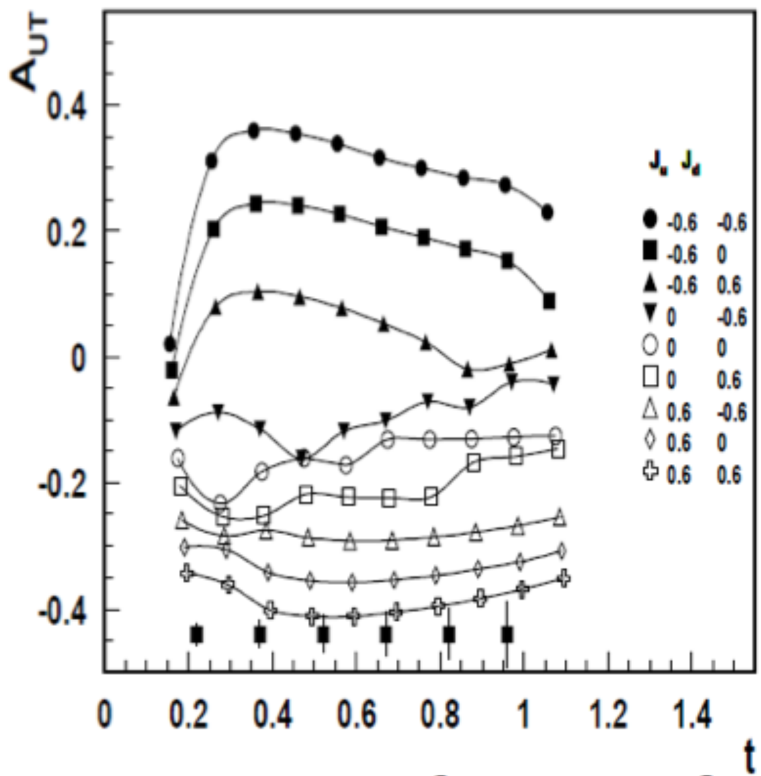

$\langle x \rangle = 0.33, \langle Q^2 \rangle = 2.5\ GeV^2$

VGG extraction (M. Guidal)

Towards nucleon tomography: local fits

Quasi model-independent extraction of CFFs based on a local fit:

- Set 8 CFFs as free parameters to fit, at each (x_B, t) point, the available observables.
- Limits imposed within +/- 5 times the VGG model predictions (Vanderhaeghen-Guichon-Guidal).
- Leading-twist DVCS amplitude parametrisation based on Double Distributions.

The best constraints in fits to CLAS data were obtained on H_{Im}.

Parametrise its dependence on t:

$$H_{Im}(\xi, t) = A(\xi)e^{B(\xi)t}$$

Relates to quark density

Inverse relation to spatial distribution

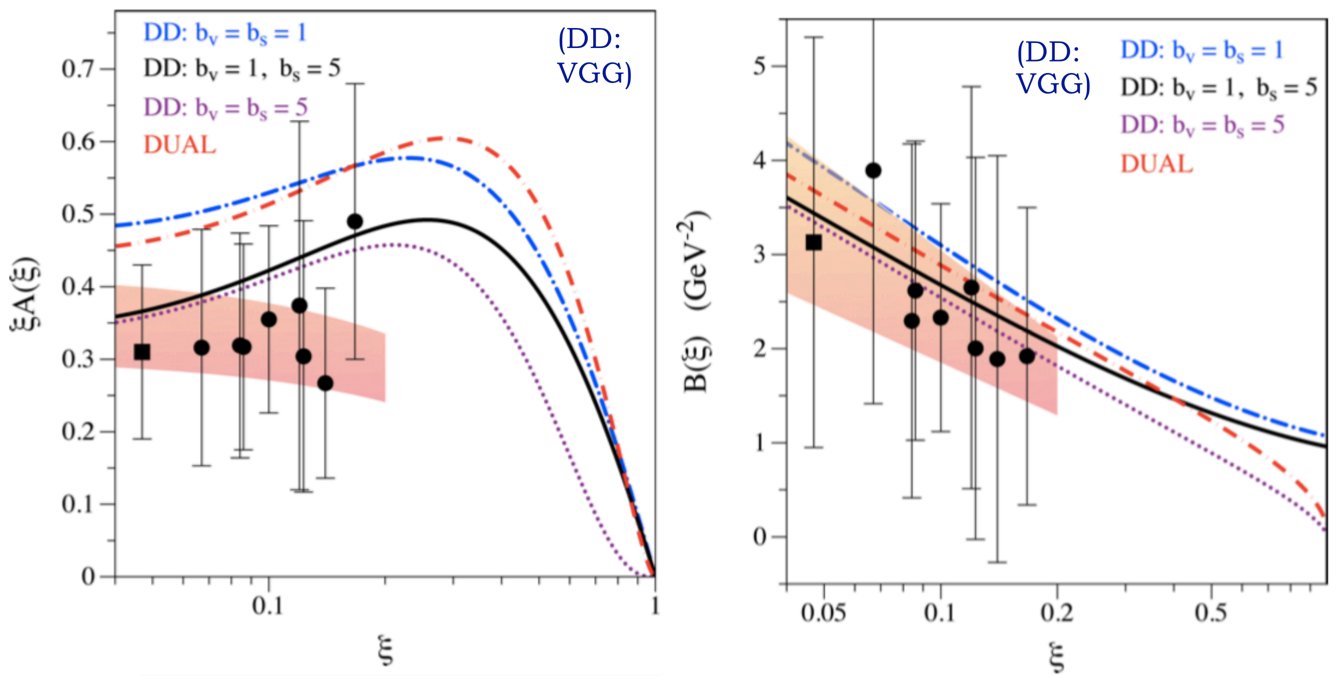

R. Dupré *et al.*, Eur. Phys. J **A 53** (2017) 171

Towards nucleon tomography: local fits

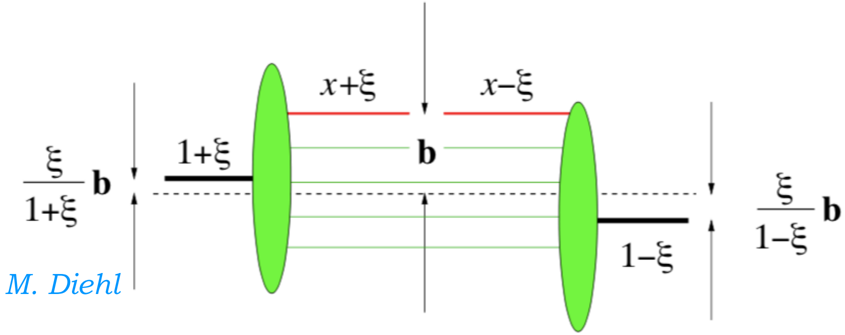

Transverse parton position interpretation only at $\xi = 0$.

Relating the impact parameter to helicity-averaged transverse distribution:

$t = \Delta^2$

$$\rho^q(x, \mathbf{b}_\perp) = \int \frac{d^2\mathbf{\Delta}_\perp}{(2\pi)^2} e^{-i\mathbf{b}_\perp \cdot \mathbf{\Delta}_\perp} H^q_-(x, 0, -\mathbf{\Delta}_\perp{}^2)$$

$$H^q_-(x, 0, t) \equiv H^q(x, 0, t) + H^q(-x, 0, t)$$

Transverse four-momentum transfer to nucleon

Assuming leading-twist and exponential dependence of GPD on t, using models to extrapolate to the zero skewness point $\xi = 0$ and assuming similar behaviour for u and d quarks there:

$$\langle b_\perp^2 \rangle^q(x) = -4 \frac{\partial}{\partial \mathbf{\Delta}_\perp^2} \ln H^q_-(x, 0, -\mathbf{\Delta}_\perp{}^2)\Big|_{\mathbf{\Delta}_\perp = 0}$$

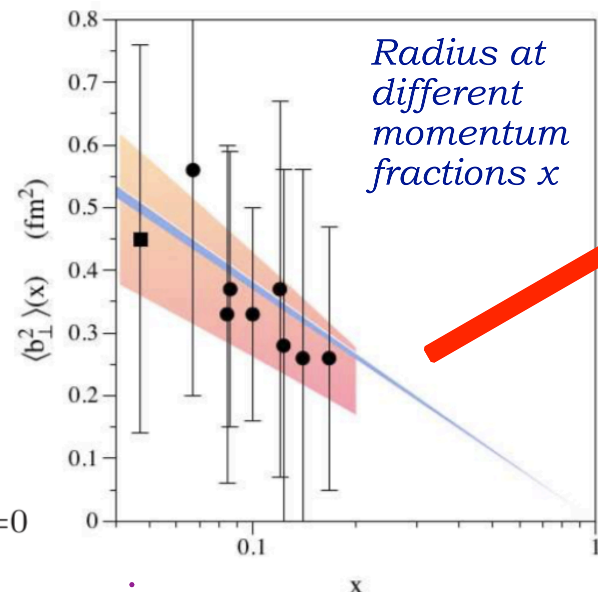

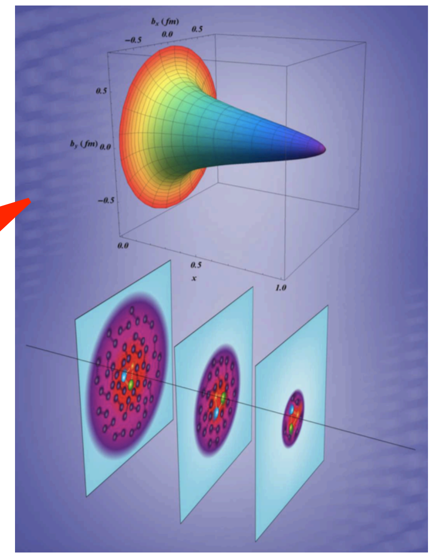

Tentative hints of 3D distributions are emerging.

We need more data from JLab @ 11 GeV!

R. Dupré *et al.*, Eur. Phys. J **A 53,** (2017) 171

Towards nucleon tomography: global fits

- PARTONS framework: global fits and neural networks to minimise model-dependence in the extraction of CFFs.

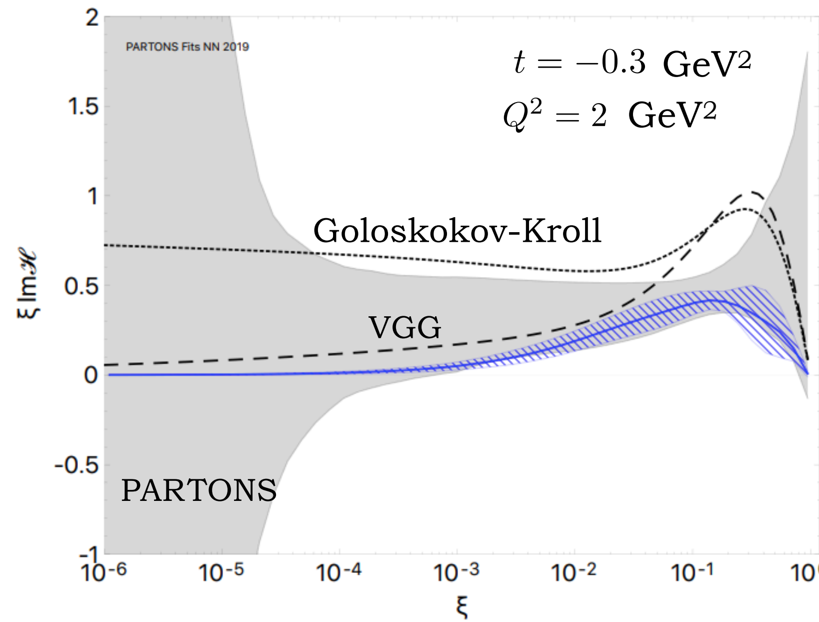

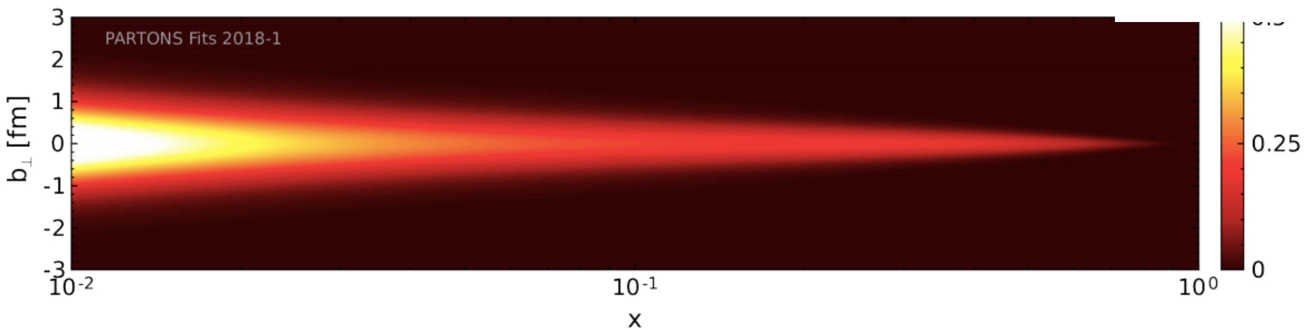

u

H. Moutarde *et al.*, Eur. Phys. J C79, 614 (2019)

Inclusion of other channels into PARTONS underway.

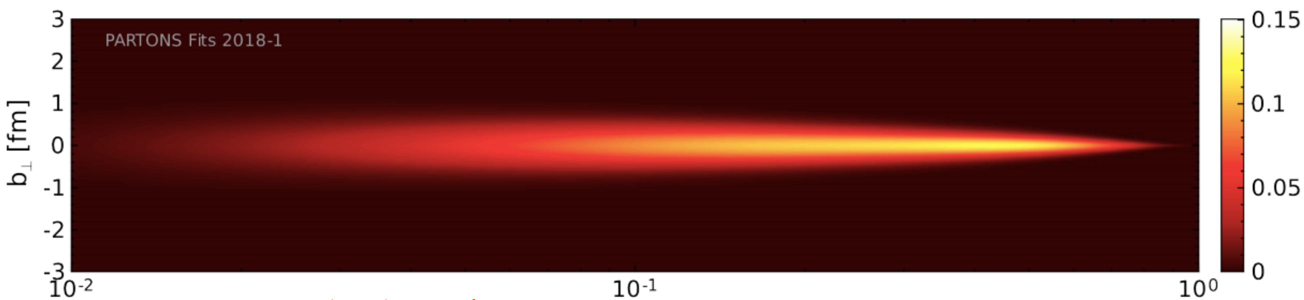

Δu_{val}

Framework in place: more data needed!

no uncertainties shown!

Image from Pawel Sznajder, IWHSS 2019